

**OPTIMISING AN AIRBORNE GAS CHROMATOGRAPH/MASS
SPECTROMETER TO MEASURE TROPOSPHERIC VOLATILE ORGANIC
COMPOUNDS**

BY

JAMIE K MINAEIAN B.Sc. (Hons)

**Submitted in accordance of the degree of Master of Science by
Research in Chemistry at the University of York**

December 2012

ABSTRACT

Work to optimise the temperature program of an airborne gas chromatography mass spectrometer was carried out in order to increase the number of analyses that can be carried out per flight. This was done by measuring the amount of time taken by the GC oven to cool from a range of final temperatures to a range of initial temperatures. In addition, experiments were carried out in order to determine how the resolution varied with changing temperature programs. This was done in order to decrease the amount of time the instrument was idle for, increasing the amount of time the instrument spent analysing tropospheric air samples.

It was found that the initial temperature had a much larger effect on chromatographic resolution than the final temperature. Increasing the initial temperature from 40 °C by 2-4 degrees yielded a cool down time much shorter than that at 40 °C, with only a slight loss of resolution.

The problem of water on the column, seen in chromatograms from the BORTAS field campaign, was also addressed, and a cold trap was developed to freeze water out of air samples.

CONTENTS

LIST OF FIGURES.....	5
LIST OF TABLES.....	9
LIST OF EQUATIONS	12
ACKNOWLEDGEMENTS.....	13
CHAPTER 1. INTRODUCTION.....	15
1.1. Motivation for this Study.....	15
1.2. Introduction to Gas Chromatography.....	16
1.3. Theoretical Plates.....	21
1.4. Changeable GC parameters	22
1.5. Mass Spectrometer.....	33
1.6. Applications.....	37
1.7. Brief Introduction To the University Of York Airborne GC/MS.....	41
1.8. Aims and objectives of this study	42
CHAPTER 2. EXPERIMENTAL	49
2.1. Introduction to the Instrument.....	49
2.2. Individual Components.....	50
2.3. Standard Operating Conditions	56
2.4. Temperature Testing.....	58
2.5. Resolution and Dead time Calculations	59
CHAPTER 3. RESULTS AND DISCUSSION.....	62
3.1. Investigating the effect of temperature programming upon peak resolution	62

CHAPTER 4. ANALYSIS OF DATA QUALITY FROM THE FIRST DEPLOYMENT OF THE INSTRUMENT	77
4.1. Introduction	77
4.2. Experimental.....	80
4.3. Results and Discussion	88
4.4. Conclusion.....	97
CHAPTER 5. CONCLUSION.....	103
CHAPTER 6. APPENDIX 1	105
CHAPTER 7. APPENDIX 2	113
LIST OF ABBREVIATIONS	119
REFERENCES.....	120

LIST OF FIGURES

Figure 1.1: Chromatograms to showing resolution values of 1 (top), 1.5 (middle), and 2 (bottom).....	24
Figure 1.2: Van Deemter plot of theoretical plate height against gas velocity for N ₂ , He and H ₂	26
Figure 1.3: Dimethyl Polysiloxane.....	28
Figure 1.4: A 2D GC plot of a monoterpene gas standard	29
Figure 1.5: Simplified schematic of a mass spectrometer, highlighting key components	36
Figure 2.1: The University of York TD-GC-MS in the aircraft rack.....	50
Figure 2.2: Section of a chromatogram of a gas standard showing a peak arising from column degradation.....	52
Figure 2.3: Photograph of the internals of the Flow Control Unit.....	53
Figure 2.4: The four position valve used to select the gas sample for analysis. Here, the valve is set to sample air.....	53
Figure 2.5: The two position valve used to add a known volume of deuterated toluene into each sample. The valve is shown here in the two positions; the sample flowing onto the TDU (left) and the injection of 5µL of deuterated toluene from the sample loop onto the TDU (right).....	54
Figure 2.6: Chromatogram of NPL monoterpene standard.....	57
Figure 3.1: A graph to show how varying the initial and final temperatures effects the time taken for the GC oven to cool down.....	65
Figure 3.2: 3D plot of initial temperature, final temperature and cool down time	65
Figure 3.3: Chromatogram of a monoterpene standard. Initial GC temperature is 40 °C	66
Figure 3.4: Chromatogram of the same monoterpene standard. Initial GC temperature is 65 °C.....	67

Figure 3.5: How resolution varies with changing initial temperatures at various final temperatures	69
Figure 3.6: How resolution varies with changing initial temperatures at various final temperatures with anomalous points removed	69
Figure 3.7: 3D plot of resolution for ethyl benzene and m- and p- xylene as a function of changing initial and final temperatures	70
Figure 3.8: Scatter plot to show the non-linear relationship between the cool down times and the resolution. Anomalous areas are highlighted.....	73
Figure 3.9: Scatter plot of cooling times against resolution with data removed	73
Figure 3.10: Scatter plot of cooling times against resolution with initial temperatures marked.....	74
Figure 3.11: First portion of cooling times against resolution graph at low cooling times ...	75
Figure 3.12: Second portion of cooling times against resolution graph at medium cooling times	75
Figure 3.13: Third portion of cooling times against resolution graph at long cooling times.	76
Figure 4.1: The structure of the Nafion monomer (Haubold, Vad, Jungbluth, & Hiller, 2001)	80
Figure 4.2: (a) Sample chromatogram from the BORTAS field campaign, showing a very noisy baseline across the entire chromatogram, but especially at retention times between 0.4 and 0.9 minutes. The noisy baseline was caused by an abundance of water on the column and (b) the extracted ion of isoprene	83
Figure 4.3: (a) sample chromatogram from the BORTAS data showing a less noisy baseline, but (b) a poor peak shape for isoprene	84
Figure 4.4: Schematic diagrams of the cold trap showing (top) the Peltier devices and power supply from a side on view, (middle) the cold trap inside the copper sheath from a bird's eye view and (bottom) a CAD image of the copper sheath.....	86

Figure 4.6: Chromatograms showing (a) a split CCl ₄ peak with a less well defined peak shape from the BORTAS field campaign (b) a CCl ₄ peak from laboratory air whilst using the cold trap to remove water.....	90
Figure 4.7: Chromatograms showing (a) toluene peak extracted from the BORTAS data, showing poor peak shape, and (b) toluene peak extracted from York laboratory air data showing a much improved peak shape	91
Figure 4.8: Showing the baselines of chromatograms taken when the Nafion dryer was included in the sample line (black) and when the cold trap was included in the sample line (blue).....	93
Figure 4.9: Mass spectrum of the major impurity peak when the Nafion dryer was added to the sample line.....	93
Figure 4.10: Assigned chromatograms of the OVOC standard through (a) the Nafion dryer, and (b) the cold trap. The software is capable of determining many more compounds when the cold trap is used.....	96
Figure 4.11: Sample chromatogram from SAMBBA, showing extracted isoprene.....	98
Figure 4.12: Sample chromatogram from SAMBBA, showing extracted methylvinyl ketone	98
Figure 4.13: Sample chromatogram from SAMBBA, showing extracted benzene	99
Figure 4.14: Sample chromatogram from SAMBBA, showing extracted toluene	99
Figure 4.15: Sample chromatogram from SAMBBA, showing extracted m- p- and o- xylene	100
Figure 4.16: Changing concentrations of isoprene, methylvinyl ketone and methacrolein during a flight.....	101
Figure 4.17: Changing concentrations of benzene, toluene, m- and p- xylene and naphthalene during a flight.....	102

LIST OF TABLES

Table 1.1: A sample of compounds detectable by the instrument, and their respective boiling points.	45
Table 2.1: Compounds and relative concentrations found in the VOC standard used to test the instrument resolution	59
Table 4.1: Compounds in the OVOC gas standard used in testing the various sample drying methods.	88
Table 6.1: Average time taken to cool down from 130 °C to a range of initial temperatures	105
Table 6.2: Average time taken to cool down from 135 °C to a range of initial temperatures	106
Table 6.3: Average time taken to cool down from 140 °C to a range of initial temperatures	106
Table 6.4: Average time taken to cool down from 145 °C to a range of initial temperatures	107
Table 6.5: Average time taken to cool down from 150 °C to a range of initial temperatures	107
Table 6.6: Average time taken to cool down from 155 °C to a range of initial temperatures	108
Table 6.7: Average time taken to cool down from 160 °C to a range of initial temperatures	108
Table 6.8: Average time taken to cool down from 165 °C to a range of initial temperatures	109
Table 6.9: Average time taken to cool down from 170 °C to a range of initial temperatures	109

Table 6.10: Average time taken to cool down from 175 °C to a range of initial temperatures	110
Table 6.11: Average time taken to cool down from 180 °C to a range of initial temperatures	110
Table 6.12: Average time taken to cool down from 185 °C to a range of initial temperatures	111
Table 6.13: Average time taken to cool down from 190 °C to a range of initial temperatures	111
Table 6.14: Average time taken to cool down from 195 °C to a range of initial temperatures	112
Table 6.15: Average time taken to cool down from 200 °C to a range of initial temperatures	112
Table 7.1: Resolution of the ethyl benzene and o- and p-xylene peaks where the initial temperature is varied and the final temperature is 130 °C.	113
Table 7.2: Resolution of the ethyl benzene and o- and p-xylene peaks where the initial temperature is varied and the final temperature is 135 °C.	113
Table 7.3: Resolution of the ethyl benzene and o- and p-xylene peaks where the initial temperature is varied and the final temperature is 140 °C.	114
Table 7.4: Resolution of the ethyl benzene and o- and p-xylene peaks where the initial temperature is varied and the final temperature is 145 °C.	114
Table 7.5: Resolution of the ethyl benzene and o- and p-xylene peaks where the initial temperature is varied and the final temperature is 150 °C.	114
Table 7.6: Resolution of the ethyl benzene and o- and p-xylene peaks where the initial temperature is varied and the final temperature is 155 °C.	115
Table 7.7: Resolution of the ethyl benzene and o- and p-xylene peaks where the initial temperature is varied and the final temperature is 160 °C.	115

Table 7.8: Resolution of the ethyl benzene and o- and p-xylene peaks where the initial temperature is varied and the final temperature is 165 °C.	116
Table 7.9: Resolution of the ethyl benzene and o- and p-xylene peaks where the initial temperature is varied and the final temperature is 170 °C.	116
Table 7.10: Resolution of the ethyl benzene and o- and p-xylene peaks where the initial temperature is varied and the final temperature is 175 °C.	116
Table 7.11: Resolution of the ethyl benzene and o- and p-xylene peaks where the initial temperature is varied and the final temperature is 180 °C.	117
Table 7.12: Resolution of the ethyl benzene and o- and p-xylene peaks where the initial temperature is varied and the final temperature is 185 °C.	117
Table 7.13: Resolution of the ethyl benzene and o- and p-xylene peaks where the initial temperature is varied and the final temperature is 190 °C.	117
Table 7.14: Resolution of the ethyl benzene and o- and p-xylene peaks where the initial temperature is varied and the final temperature is 195 °C.	118
Table 7.15: Resolution of the ethyl benzene and o- and p-xylene peaks where the initial temperature is varied and the final temperature is 200 °C.	118

LIST OF EQUATIONS

Equation 1.1	21
Equation 1.2	22
Equation 1.3	22
Equation 1.4: The Van Deemter equation	25
Equation 2.1	60
Equation 2.2	61

ACKNOWLEDGEMENTS

I would like to thank my supervisor, Professor Ally Lewis, for his guidance and encouragement, and for taking me on as both an MSc student and PhD student.

In addition, Dr. Sam Edwards for constantly reading draft after draft, Dr. Jim Hopkins and Dr. Ruth Purvis for always helping me in labs, and answering all my questions.

Many thanks also go to all in the Atmospheric Research Group- your constant humour kept me positive throughout! I hope we have many more football and pub sessions!

In addition, thanks go to all my friends who have helped me out in all manner of ways.

Finally, many thanks to Mum and Dad, without whose financial and emotional help, this thesis would not have been possible. Thanks for always being just a phone call away.

Declaration

I, the candidate, hereby declare that all work presented here is my own, except where otherwise acknowledged, and has not been submitted in full or part for any other degree.

Jamie Minaeian

CHAPTER 1. INTRODUCTION

1.1. Motivation for this Study

Volatile organic compounds (VOCs) are present throughout the atmosphere and in thousands of different chemical forms. They exist with many different functionalities and structures and as such display a wide variety of chemical and physical behaviours. For example, different VOCs can exhibit widely different mixing ratios (Atkinson, 2000; Barletta *et al.*, 2002; Seco *et al.*, 2011), reactivities (Darnall & Lloyd, 1976) and toxicities (WHO, 2000), which can affect human and animal health. Once in the atmosphere, VOCs can react with compounds such as OH radicals and ozone and their by-products interact with NO_x to form ozone (Atkinson, 2000). Larger VOCs when oxidised can contribute to organic aerosols, and some can be removed from the atmosphere by either wet or dry deposition (Hallquist, 2009).

A range of platforms are used to monitor VOCs in the atmosphere, most commonly ground-based, online monitoring stations, but also on board ships to study marine environments, and, increasingly, aircraft observations. Aircraft observations allow a wide range of different environments to be studied in a short period, and allow sampling of regions that otherwise might be too remote to access. Aircraft observations allow monitoring of VOCs in places such as forested areas (Yokelson *et al.*, 2007), urban environments (Karl *et al.*, 2009), and tropospheric marine environments (Kormann *et al.*, 2003). This study investigates the parameters of an airborne GC/MS used to identify tropospheric VOCs.

A range of analytical techniques can be used to measure VOCs, including optical methods and proton transfer reaction-mass spectrometry (PTRMS), but the most common technique is thermal desorption and gas chromatography (GC). This can be coupled to a wide range of detectors with differing sensitivities towards particular families of compounds, tailoring the

instrument to specific analytes. GC can produce reliable, repeatable data for even the most complex of mixtures. The principles behind gas chromatography involve the partition of a gaseous mobile phase passing an immobile stationary phase, within a narrow column. Separation of a sample is acquired through different compounds having differing affinities with a stationary phase (Fowles, 1995).

1.2. Introduction to Gas Chromatography

Gas chromatography (GC) is the separation of compounds in a gaseous flow of eluent. In order to perform GC, the compounds for analysis must be sufficiently volatile to exist within the column as a vapour within the operating temperatures applied to that column. In essence a mixture of compounds passes through a column containing a stationary phase. As compounds move through the column they go through a series of partitions between the mobile gaseous phase and the stationary phase. Different compounds within the mixture interact to different extents with the stationary phase, which can be a solid or liquid coating on a solid substrate, typically fused silica. As a consequence, individual compounds leave the column (elute) at different times to one another. This is referred to as the retention time- the amount of time the column retains the analytes, as compared to the time taken for a completely unretained compound to pass through the column. After eluting from the column, compounds pass into a detector to determine the amount of material present. Many types of detectors are currently used for GC analysis, such as Flame Ionisation Detection, Photon Ionisation Detection and Mass Spectrometry. Conditions such as stationary phase, column length, temperature and pressure can all be varied to produce different selectivity, retention times and different degrees of separation.

1.2.1. A History of GC Development

The invention of GC is generally accredited to James and Martin in 1952 (James & Martin, 1952). They described the use of a gas-liquid partition to separate small quantities of fatty acids, and they followed this work by separating bases in the same year (James & Martin, 1952). To carry out the separation, they reported using nitrogen gas as the mobile phase with silicon oil/stearic acid bound to diatomaceous earth as the stationary phase. The stationary phase consisted of a liquid bound to a solid support, whilst the mobile phase was gaseous. Hence, the process was referred to as Gas-Liquid chromatography. One of the greatest challenges for early GC was the separation of petroleum, which then was beginning to challenge coal as a fuel source (Smolková-Keulemansová, 2000). Thanks to its use in a wide variety of chemical applications such as biochemistry (Lipsky & Landowne, 1960), food and flavour chemistry, and reaction kinetics, GC was rapidly adopted as a key analytical technique (Knox, 1955). It has been reported that by 1960, over 200 papers describing the use of GC had been published (Bartle & Myers, 2002).

Early GC columns differ from the capillary columns used most frequently today. The very first GC system separated a mixture of fatty acids using what would now be described as a packed column. Typical packed columns were 1-5 m long with an internal diameter of 1-5 mm (Bartle & Myers, 2002) and were filled with particles of silica, onto which the stationary phase is bound. Advances in manufacturing techniques have reduced packed column dimensions. Currently they have internal diameters that are typically less than 1 mm. Packed columns are no longer widely used because they have more limited resolving power. This is due to the non-uniform interior of the column, which leads to non-uniform passage of molecules along the column, which causes a loss of chromatographic resolution. The packed nature of the column causes a pressure drop along the column due to the resistance to gas flow which limits length to approximately 5 m. This places an upper limit

on resolution. Though they have largely been superseded by capillary columns, today's packed columns are used for separating simple mixtures containing few compounds.

In 1956, Martin, (Martin, et al., 1957), and independently, Golay in 1957 (Golay, 1958) described the use of a new type of column- the capillary column. In contrast to the packed column, the stationary phase is bound to the inside wall of the column. The stationary phase can either bind straight to the wall as a thin film, or be bound to a porous layer on the inner wall. Capillary columns were a significant improvement on packed columns. Paths taken by molecules in a packed column can vary significantly, whereas in open tubular capillary columns, the path is much more uniform, and molecules will have a more uniform interaction with the stationary phase. A more uniform interaction with the stationary phase leads to greater separation efficiency and narrower peaks, improving overall resolution. In addition, capillary columns are more effective at lower temperatures than packed columns as molecules within the column meet less resistance. The capillary column can give a better separation in the same amount of time due to improved resolution. According to Bartle & Myers, capillary columns can yield results up to 10 times faster than packed columns (Bartle & Myers, 2002) as capillary columns can separate more compounds per unit time than packed columns. However, due to the much smaller dimensions of capillary columns (and therefore the amount of stationary phase), the capacity of capillary columns is much lower (<100 ng). Capillary columns are much easier to overload. This is not necessarily a drawback as only a small amount of sample is required to produce a reasonable separation. The main drawback of using a small amount of sample is that a more sensitive detector must be used.

Prior to 1960, columns were manufactured from a variety of materials. However, the advantage of glass (i.e. inertness), was quickly recognised. In 1960, Desty *et al* described a device that was capable of manufacturing large amounts of coiled glass capillaries (Desty,

Haresnape, & Whyman, 1960). By 1973, glass was the most widely used material in column manufacture, with many reports demonstrating its advantages (German, Pfaffenberger, Thenot, Horning, & Horning, 1973).

Whilst glass columns were an improvement on materials used previously, they were by no means ideal. Highly polar compounds had a high affinity with the exposed glass present due to manufacturing flaws, meaning that often, compounds were lost to the column. The columns were also extremely fragile.

In 1979, Dandaneau and Zerenner introduced capillary columns made of fused silica that were flexible, inexpensive, and chemically inert (Dandaneau & Zerenner, 1979). Externally, the fused silica was treated with a protective polyimide layer making the column flexible and strong, whilst internally, a wide variety of stationary phases could be used. This new design of column could be used to separate almost any mixture with a high success rate. Further progress was achieved by Lee *et al* in the 1980's to determine the physical properties of the stationary phase. In doing so, they were able to create a fused silica column with a uniform, thermally and chemically stable stationary phase. The silica contained reactive hydroxyl groups that could be deactivated by silylation. Once the reactive groups on the stationary phase have been deactivated, the stationary phase can easily be tailored to meet specific criteria depending on the nature of the analyte. Early stationary phases were generally large hydrocarbons such as oils and greases. They have largely been replaced by polysiloxanes with large pendant groups attached. For example, for separating VOCs, a stationary phase of 5% diphenyl/95% dimethyl polysiloxane can be used to give a significant amount of separation. Capillary columns are the most widely used columns today. Typical capillary columns have internal diameters of ~0.1 mm to 0.5 mm and film thicknesses of ~0.1 µm to 1 µm. Column lengths can vary between 5 m and 100 m.

The stationary phase type and thickness is essentially the main tool for changing sensitivity and resolution for a particular analyte. To help quantify the separating power of any given column, Golay introduced the concept of 'theoretical plates' in 1958 (Golay & Desty, 1958). Theoretical plates are a way of viewing the separation power of a particular column. The higher the number of theoretical plates, the higher the separation power, and therefore the resolution of a column. That is, the more plates a column has, the more resolved peaks could be stacked side by side next to one another. The number of theoretical plates is dependent on the dimensions of the column, such as the inner diameter (i.d.), the film thickness (d.f.) and the length of the column. A full description on theoretical plates is given in section 1.3.

The original method of detecting analytes eluted from the column was by an automated titration system (Bartle & Myers, 2002). In 1954, this was changed to a katharometer, after its invention by Ray (Ray, 1954). A katharometer operates by detecting a change in temperature of a filament, by measuring its electrical resistance. After the invention of the open tubular capillary column, the katharometer was no longer used as it wasn't sensitive enough to detect the small volumes of analytes eluting from the new columns. Alternative methods of detection were needed. Separately, Harley *et al* and McWilliam and Dewar both proposed using a flame ionisation detector (FID) as the method of detection in 1958 (Harley, Nel, & Pretorius, 1958; McWilliam & Dewar, 1958). Now, many different types of detectors are used, such as FID's, photoionisation detector (PID) and mass spectrometry (see section 1.5 for more on detectors).

Whilst the appearance of a modern GC is vastly different to that of the original, the principles remain almost identical. Capillary columns can produce a much higher level of resolution, meaning modern columns can separate compounds much faster, giving a shorter analysis time. Modern GC instruments are heated during the analysis to increase

the rate at which compounds elute. At higher temperatures, analytes spend less time interacting with the stationary phase, decreasing retention times, particularly of the less volatile compounds in the analyte. The temperature program is one of many GC parameters that can be changed to alter, for example, analysis time and compound resolution.

1.3. Theoretical Plates

Theoretical plates are a way of explaining separation in chromatography. The separation is also referred to in terms of column efficiency. The efficiency of a column directly affects the resolution of eluting analytes. Theoretical plates are based on the mathematics of distillation columns. The number of theoretical plates, N , describes the number of sites where analytes can theoretically bind to the stationary phase. This can also be described as locations where an equilibrium between compounds in the stationary and mobile phase has been reached. The number of plates is not the only parameter in calculating column efficiency and hence resolution. The height of theoretical plates (HETP) also plays a part. Using the distillation column analogy, a lower plate height means that more plates are present along a length, L . Equation 1.1 shows how these parameters are related.

$$N = \frac{L}{HETP} \quad \text{Equation 1.1}$$

In addition, the number of theoretical plates can be obtained from chromatograms by expressing N with regards to the width of a peak at half height.

$$N = 5.54 \left(\frac{t_R}{W_{1/2}} \right)^2 \quad \text{Equation 1.2}$$

Where $W_{1/2}$ is the peak width at half height,

t_R is the retention time of a particular analyte.

The equation for resolution includes the number of theoretical plates as well as parameters for capacity and selectivity. The capacity factor describes the rate of migration of analytes along a column, taking into account the capacity of the stationary phase. Selectivity is given by the ratio of the capacity factors of two closely eluting peaks. The overall resolution equation therefore is shown in Equation 1.3. Each constituent of the resolution is labelled

$$R_s = \frac{\sqrt{N}}{4} \left(\frac{\alpha - 1}{\alpha} \right) \left(\frac{k'}{1 + k'} \right)^2 \quad \text{Equation 1.3}$$

Where R_s is the resolution,

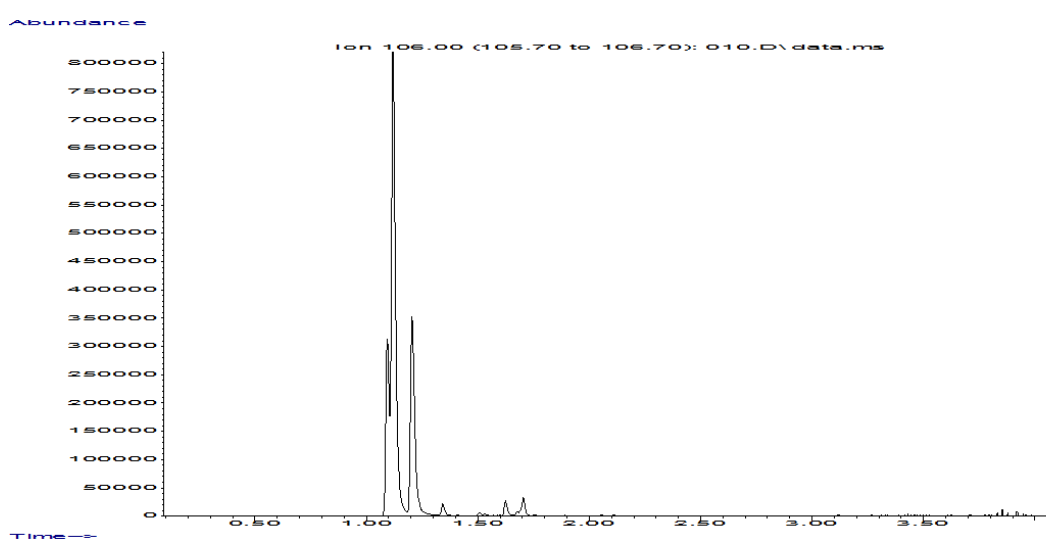
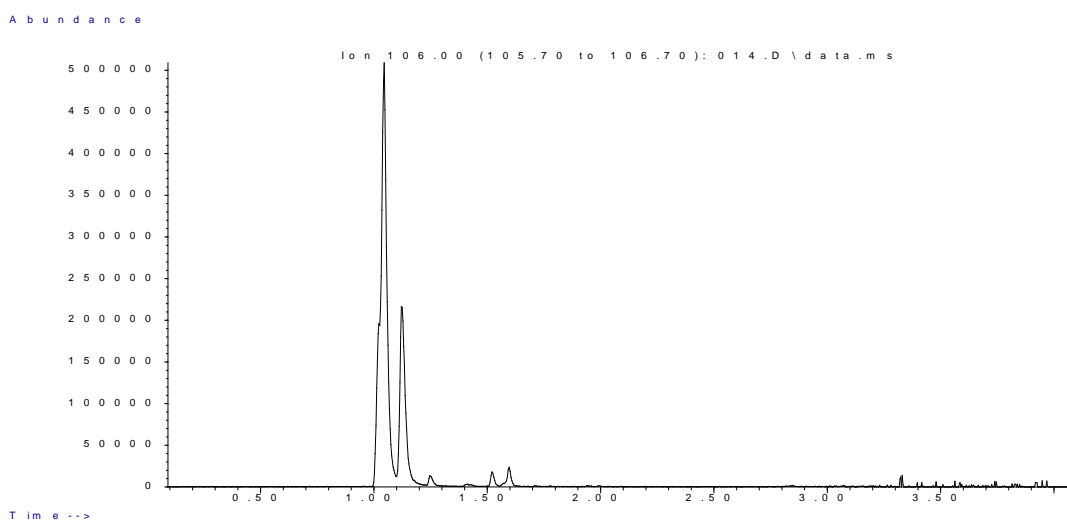
α is the selectivity factor

k is the capacity factor.

1.4. Changeable GC parameters

Changes in GC parameters can have a large effect on the resulting chromatograms. In general, parameters such as the temperature program or column length are changed to optimise the analysis by either improving resolution or decreasing the analysis time. If two peaks are resolved to a resolution value of >1.5 , they could be regarded as being over-resolved and this implies the analysis time could be reduced. Figure 1.1 shows how

resolution values of 1, 1.5 and 2 appear on chromatograms. They show ethyl benzene and *m*- and *p*- xylene, taken from a total ion count chromatogram by extracting ions of mass 106. Matisová & Dömötöröová proposed a list of changeable GC parameters that affect the amount of time taken to run a GC analysis (Matisová & Dömötöröová, 2003) In order to decrease the time of a GC analysis, one of these parameters must be chosen and altered with care, so as not to reduce resolution to below an acceptable level. The parameters listed below are discussed to determine their effectiveness at shortening the analysis time, and hence the best parameters to alter in order to achieve the shortest analysis time.



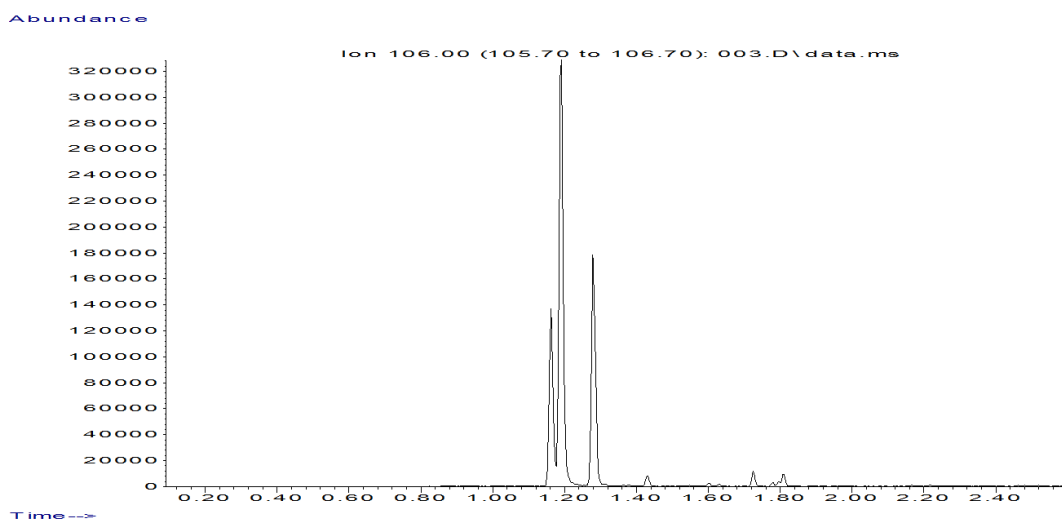


Figure 1.1: Chromatograms to showing resolution values of 1 (top), 1.5 (middle), and 2 (bottom).

1.4.1. Column Length

A shorter column length leads to a shorter GC analysis time at constant pressure. A shorter column also means of course fewer total theoretical plates, giving fewer opportunities for analytes to interact with the stationary phase. A shorter column reduces the overall analysis time, as well as decreasing the chromatographic resolution.

1.4.2. Carrier Gas Velocity/Inlet Pressure

The carrier gas velocity can be varied in modern instruments using electronic pressure controllers (EPC) at the column inlet. EPCs allow the pressure to be adjusted rapidly to ensure fixed or variable flow. An increase in carrier gas velocity would decrease the time needed for analysis. Compounds in the column are affected by the carrier gas when they are not interacting with the stationary phase (i.e. they are in the mobile phase). If the speed of the carrier gas is increased, compounds will travel further per unit of time when they are out of the stationary phase. This will decrease the amount of time taken for compounds to elute from the column, and decrease the overall analysis time.

There are however, negatives associated with increasing the carrier gas velocity. An increase in carrier gas velocity can reduce resolution since fewer opportunities exist for interactions with the stationary phase.

Carrier gas velocity and inlet pressure are linked to the height equivalent to a theoretical plate (HETP) by the Van Deemter equation. The Van Deemter equation is a method of describing the resolving power of a chromatography column. It is shown in Equation 1.1

Equation 1.4: The Van Deemter equation

$$HETP = A + \frac{B}{u} + C \cdot u \quad \text{Equation 1.4}$$

The equation takes into account the Eddy-diffusion parameter, A, the diffusion coefficient, B, the resistance to mass transfer coefficient, C, and the linear velocity, u .

1.4.3. Carrier Gas

The choice of carrier gases is important in terms of the speed of each GC analysis. Lighter gases have a higher optimum velocity. Figure 1.2 shows a Van Deemter plot for nitrogen, helium and hydrogen. Whilst nitrogen gives the lowest height of theoretical plate (HETP), the optimum velocity is much slower than for hydrogen and helium at ~10 cm/sec). A lower height of theoretical plates gives a higher number of theoretical plates, which in turn, gives better resolution. Hydrogen and helium give much flatter curves, indicating that they give a wider range of optimum velocities at close to optimum theoretical plate heights. Hydrogen produces the lowest and flattest curve; however, due to the explosive nature of using hydrogen, helium is most widely used as a carrier gas. It is also very difficult to couple

hydrogen gas to mass spectrometry, since the gas is much more difficult to remove using turbomolecular pumps.

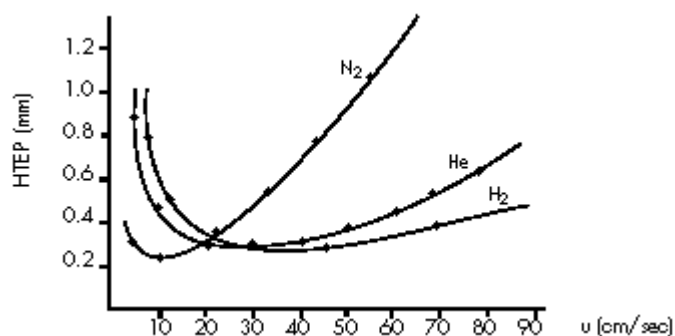


Figure 1.2: Van Deemter plot of theoretical plate height against gas velocity for N_2 , He and H_2

The Van Deemter equation is given in Equation 1.4, above. The diffusion parameters can affect the HETP. For instance, if the diffusion coefficient, B , is too high, compounds will diffuse down the column (i.e. they will not interact with the stationary phase as much), and so peaks will broaden.

1.4.4. Inner Column Diameter

Reducing the inner column diameter at constant carrier gas flow increases the pressure drop across the column. An increase in pressure favours analytes bound to the stationary phase as the equilibrium lies towards the solid phase. Therefore, a higher resolution will be acquired in a shorter time. According to Blumberg and Klee's definitions for fast chromatography, an increase in resolving power means an increase in analysis speed.

A narrow column has less capacity for analytes than a slightly wider column, assuming all other parameters (such as film thickness) remain the same. This reduction is extremely reducing by a power factor of $5/2$. It is therefore easier to overload a narrow column.

Overloading columns can cause peak tailing, which decreases resolution and changes retention time. In addition, the increased pressure needed at the head of the column make working with other GC components difficult, for example, maintaining a good seal with a syringe injection port, or enabling coupling to a thermal desorption unit. Most GC have an upper working limit of around 100 psi carrier gas, which is sufficient for columns as narrow as 100 μm , but not much narrower.

1.4.5. Film Thickness

Decreasing the film thickness reduces the amount of stationary phase in the column and further limits interactions with analytes. Therefore, the effect of reducing the film thickness on the overall resolution is two-fold. Firstly, with a reduction in the amount of stationary phase comes the corresponding loss of sites at which compounds can bind to. Compounds would then spend less time in contact with the stationary phase meaning closely eluting compounds could now be eluting together, causing a loss of resolution. Too much stationary phase is also deleterious to the quality of separation. With very thick films, analytes spend a large amount of time in the stationary phase and mass transfer within the phase causes band broadening and wider peaks. For measurement of VOCs film thicknesses tend to the upper end used in GC analyses.

1.4.6. Selective Stationary Phase

A suitable stationary phase must be chosen for each type of analyte. Analytes interact differently with different stationary phases. Depending on the types of compounds in a sample, different types of stationary phases may yield better results. Generally, stationary

phases contain a compromise material that can provide some resolution of low, moderate, and high polarity analytes (Abraham, Poole, & Poole, 1999). Where originally, silicon oil bound to a solid backbone was used as the stationary phase, now polymeric compounds such as poly (ethylene glycol) and functionalised polysiloxanes are used (Poole, Li, Kiridena, & Koziol, 2000). Polysiloxanes contain many polar regions, and versatile side groups can be designed to give the column both polar and apolar sites. Figure 1.3 shows the structure of dimethyl polysiloxane, which is a commonly used stationary phase for analysis of VOCs.

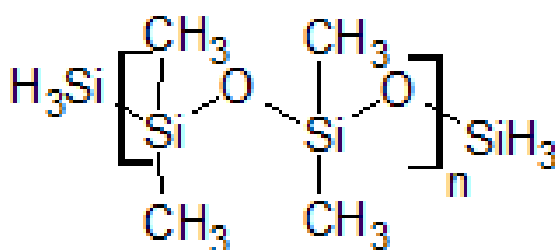


Figure 1.3: Dimethyl Polysiloxane

1.4.7. Column Length

A shorter column length leads to a shorter GC analysis time at constant pressure. A shorter column also means of course fewer total theoretical plates, giving fewer opportunities for analytes to interact with the stationary phase. A shorter column reduces the overall analysis time, as well as decreasing the chromatographic resolution.

to elute very quickly, whilst the other may take some time to elute from the column.

1.4.8. Two-Dimensional GC

Two-dimensional gas chromatography is a relatively new branch of gas chromatography (Simmons & Snyder, 1958). In essence, two columns with distinctly different separation

properties are coupled together using a modulator. In general, the first (primary) column is used to separate peaks based on their volatilities, whilst the second (secondary) column separates compounds based on their polarity. The purpose of the modulator is to collect the eluent from the primary column and periodically inject it onto the secondary column. The modulator is typically set to inject onto the second column once every 5-10 seconds. The resulting chromatogram looks very different to those acquired from one-dimensional chromatography. Figure 1.4 shows a chromatogram produced from a two dimensional GC analysis. Two dimensional GC is deemed a faster method than one dimensional GC. Even though GCxGC takes more time, it is capable of resolving considerably more peaks per unit of time. In accordance with Blumberg and Klee's definitions of fast chromatography, the power to resolve 10 peaks in 10 seconds might be referred to as very fast GC whereas the power to resolve just 2 peaks in 10 seconds is referred to as fast GC. Of course, these parameters also take into account the peak width. Peak width might be better determined by using a highly sensitive detector. Therefore, the separation and resolution power of GCxGC is much higher than that of standard 1-D GC.

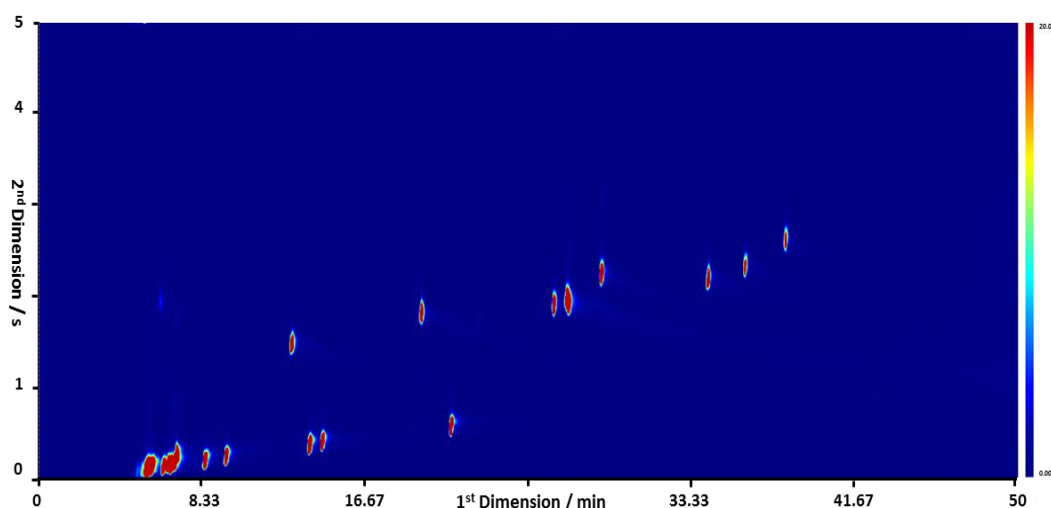


Figure 1.4: A 2D GC plot of a monoterpene gas standard

1.4.9. Backflushing

Backflushing is a technique that involves reversing the flow of the carrier gas at the end of each run. Once at the end of the GC analysis, the carrier gas is sent back along the column to the inlet. The principle of backflushing is that any retained compounds or impurities are expelled through the inlet. This therefore saves time as the column requires less baking out.

1.4.10. Turbulent Flow Conditions

Axial turbulence across the column can help speed up a GC analysis. Because of the axial flow, friction within the column is increased so compounds in the analyte have more time to interact more with the stationary phase. This larger interaction leads to a greater separation of compounds. Theoretically, the height of theoretical plates is decreased and the number of plates is increased. This means that the optimum carrier gas velocity is greater, speeding up the analysis. It is not always possible to carry out an analysis with turbulent flow through the column since pressures and flow rates required are high. Commercial GC instruments are not always compatible with this option.

1.4.11. Column Temperature

Relatively few GC analyses use an isothermal temperature throughout the analysis cycle, although they do have several practical advantages over a temperature programmed analysis. In the context of this work, as the column temperature remains constant throughout the run, the GC 'equilibration time' before the start of the next analysis is eliminated. The equilibration time is defined as the amount of time taken for the GC to return to its initial state ready for the next analysis from its final state of the previous

analysis. In temperature programmed GC, this can take up to several minutes as the GC oven must cool down, usually from over 100 °C – 200 °C to less than 50 °C. It has been calculated that, theoretically, the intrinsic efficiency is higher in isothermal GC for a single peak (Blumberg & Klee, 2001). Efficiency in chromatography is defined as the measure of dispersion of an analyte as it travels through the instrument. It is proportional to the number of theoretical plates. If a column contains more theoretical plates, it will have a higher efficiency (see equations 1.1- 1.4 above).

The drawbacks of using isothermal GC are that it takes longer to perform each analysis, particularly when carrying out a separation on complex mixtures, and that peak broadening for lower volatile compounds can become extreme. Klee and Blumberg calculated that theoretically, whilst an isothermal GC analysis can yield a 25% increase on efficiency, it can take up to 1000x longer to complete the analysis (Blumberg & Klee, 2001). The choice of temperature for an isothermal analysis must be carefully considered. Compounds in a given mixture will likely be of different volatilities. Therefore, an isothermal temperature in between the volatilities of two compounds will cause one compound to elute very quickly, whilst the other may take some time to elute from the column.

1.4.12. Higher Initial Temperature

The initial temperature of a GC temperature program can be increased to decrease the analysis time. The gain of increasing the initial temperature is two-fold. Firstly, compounds will initially move faster through the column due to the higher temperature and therefore reduce the amount of interactions with the stationary phase. Secondly, the analysis time is shortened as the oven takes less time to cool to a higher initial temperature, which decreases the GC equilibration time.

Because compounds spend less time in the column, resolution may be affected, as compounds will spend less time interacting with the stationary phase. Compounds entering the column are collected on the head of the column, as they are moving from the heated injector port, onto the cooler column. This refocusing ensures that compounds are separated only on their affinity with the stationary phase. A higher initial temperature would decrease the amount of refocusing. This is because the initial temperature affects the amount of refocusing on the head of the column, once compounds are injected. A low initial temperature increases the amount of refocusing, meaning peaks will be sharper. A higher initial temperature leads to less refocusing, and hence peaks broaden, particularly for early eluting compounds.

1.4.13. *Faster Temperature Programming (Ramp Rate)*

A faster ramp rate leads to a faster GC analysis. The GC oven under fast ramping conditions take less time to heat the column from the initial temperature to the final temperature. Faster ramp rates can however lead to a decrease in resolution, as the analyte will elute from the column in a shorter amount of time leaving less time for separation. A ramp rate for a GC oven requires a higher power consumption when compared to a resistively heated column. A fast ramp rate for a GC oven may be as fast as 40 °C/min. However, the upper limit on the speed of a resistively heated column ramp rate is regulated only by the loss of resolution observed.

1.5. Mass Spectrometer

Detector selection is very important in gas chromatography. The detector employed will depend on the type of analyte, sensitivity and, for this particular application, transportability. The amount of information needed about an analyte is also important to consider. For instance, if the analyte is a mixture of known compounds, the structural information obtained from mass spectrometry fragmentation might not be necessary. Many different detectors can be used in conjunction with gas chromatography, and only a few are described here.

Different detectors are more sensitive to specific compounds. Flame Ionization Detection (FID) and Photoionization detection (PID) are widely used in gas chromatography as they are small, relatively cheap and are highly sensitive. Flame ionization detection is highly sensitive towards all hydrocarbons and is close to a 'universal' detector. Flame ionization detectors operate by using a hydrogen-air flame to ionize compounds. Ions are then accelerated by a potential difference maintained across the length of the detector. When the ions collide with the negative electrode a current is generated that is proportional to the concentration of the organic compound eluting from the column. This current can be detected using a picoammeter. Hydrocarbons are easily ionized in the flame and the FID is very sensitive towards organic compounds. However, FID is a destructive detection method, meaning compounds cannot be recovered after detection and the FID gives no information of structure or chemical composition.

Photoionization detection operates on a similar principle but instead relies on UV light to ionize compounds. Photoionization detectors can only detect compounds that have ionization energies less than that produced by the UV light. In addition, sensitivity is lost in environments that have a large water vapour concentration, due to the ability of water to

remove or supply electrons to ionized compounds. However, photoionization detection is a non-destructive detection method, and therefore can be used in-line with other detectors. Unlike FID, the sensitivity of PIDs is variable. Organic compounds with double bonds are much more easily ionised by the UV light.

Mass spectrometry as a detection method gives the most amount of information about analytes. This is because each individual compound gives its own unique fragmentation pattern. Mass spectrometry is among the most sensitive of GC detectors. By changing the ion source between electron ionisation (producing many positively charged fragments) and chemical ionisation (producing few positively charged fragments), the mass spectrometer can be altered to aid specificity and be sensitive towards many compounds. However, due to their size and power requirements, mass spectrometers are not always suitable for fieldwork. They require a powerful vacuum pump in order to create an environment where ion lifetimes are sufficiently long to allow them to be detected, making them less transportable.

When coupled to a GC instrument, mass spectrometry is a highly sensitive, versatile detector. Ionisation methods can be changed to give specific or universal selectivity. Due to recent developments reducing size and cost, they are widely used in many industries. Mass spectrometers have three main, critical components: the ion source, the mass analyser and the detector.

There are many ways to ionise analytes for mass spectral analysis. Electron ionisation is a hard ionisation method that is most widely used. Compounds are ionised by electrons emitted from a heated filament. The electrons collide with analytes causing them to lose an electron, leaving them positively charged. The interaction with an electron results in an excess of energy being imparted onto the molecule. If the imparted energy is greater than that of the bond dissociation energy, bonds within the compound break. This leaves a

neutral species and a positive species. It is the positive species that is then accelerated towards the detector. A more energetic collision results in more molecular fragmentation. Many fragments are produced for each analyte which gives considerable structural information about the compound.

Proton transfer reaction (PTR) is another type of ionisation method. Instead of using electrons to ionise analytes, PTR makes use of a chemical reagent such as H_3O^+ . A proton is transferred from protonated water to the analytes, causing them to be positively charged. However, this only occurs if the proton affinity of the analyte is greater than that of water. Small alkanes and compounds such as acetone cannot be ionised in this way. This is a much softer chemical ionisation technique as much less energy is transferred in the process. This means that less fragmentation occurs, making obtained spectra easier to interpret since the molecular ion is typically intact.

After ionisation, the ions formed are accelerated and measured for their individual charge and mass properties. This is usually done by an electromagnetic field. Quadrupole mass spectrometry makes use of four charged rods to steer ions of a particular mass and charge towards a detector. The four rods are held parallel to each other in an orientation that creates a hyperbolic field and a voltage is applied across them. Adjacent rods have equal and opposite charges. Ions are accelerated down the length of the rods, and due to the strength of the electromagnetic field, they begin to oscillate. The size of the oscillations depends on the ions' mass to charge ratio (m/z) and the intensity of the electromagnetic field. The electromagnetic field produced by the rods can be altered rapidly to allow ions of specific mass to charge ratios to pass through to the other side.

Time of flight (TOF) is another type of mass analyser for mass spectrometry. Ions are accelerated towards a reflectron that is kept under an electric field of known strength. The reflectron deflects the ions towards the detector. The time taken for ions to reach the

detector is dependent on the amount of kinetic energy they have. Heavy, weakly charged ions will take a longer path to the detector compared to small, highly charged ions. The strength of the reflectron electric field can be altered to analyse different ions.

The detector is the final critical part of the mass spectrometer. Having passed through the mass analyser, individual ions need detection and counting. This is achieved typically using either an electron multiplier or a photomultiplier. Ions leaving the mass analyser are directed into a cone-like chamber that is held at a known negative voltage. Ions impacting upon the side of the chamber cause an electron to be emitted. The emitted electron collides with the chamber elsewhere causing a cascade of electrons moving down the cone. This release of electrons results in a current that can be amplified and measured.

Photomultiplier detector (PMD) operates on a similar principle to ECDs. Ions strike an electron rich plate, causing an electron to be released. The electron strikes the side of the chamber, and a cascade of photons is initiated, rather than a cascade of electrons. The photons released are detected by a highly sensitive light detector.

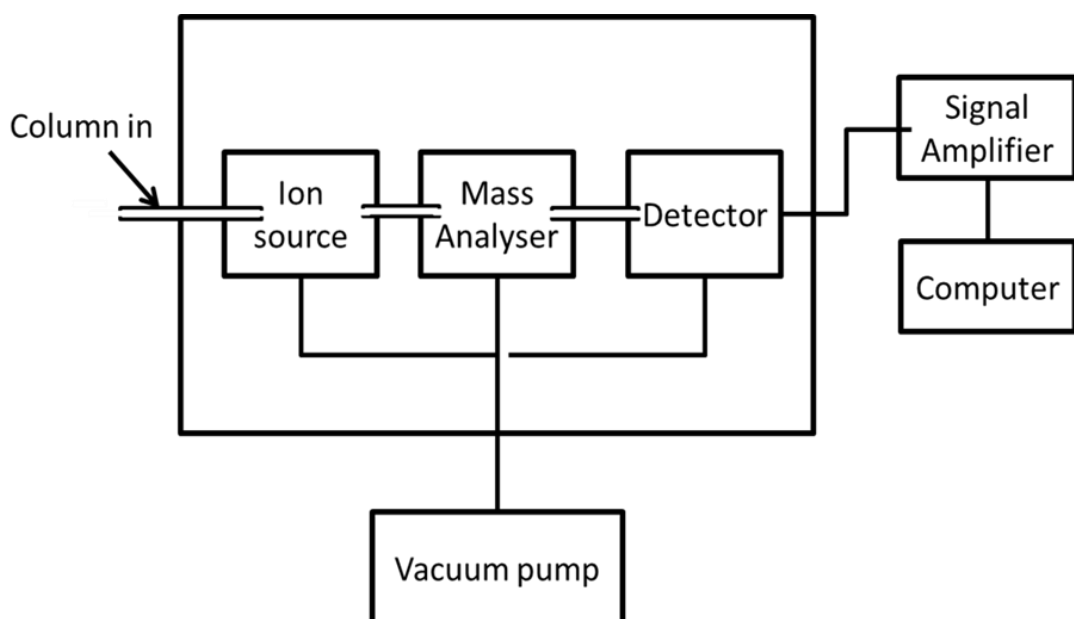


Figure 1.5: Simplified schematic of a mass spectrometer, highlighting key components

1.6. Applications

Gas chromatography-mass spectrometry is widely used in the field of environmental and atmospheric science. This is due, in part, to the relatively low costs, the versatility of the GC column and the detector for measurements of a range of important trace organic species. They are reasonably transportable and can be placed *in situ* and left running or can be taken on field campaigns to analyse the chemical composition of particular geographic regions. Many atmospheric field campaigns have taken place globally in the past that have used GC/MS, generally to analyse volatile organic compounds (VOCs) and halocarbons. Halocarbons are known to have a deleterious effect on stratospheric ozone (Montzka, Butler, & Myers, 1996). For example, campaigns have taken place in urban and industrial areas (Ribes *et al.*, 2007), above open ocean, in and around the Arctic (Wang, Fingas, & Sergy, 1995), as well as over forests (Graham, 2002). Data collected is used to improve or validate global models and monitor air quality.

Chlorofluorocarbons (CFCs) are also detectable by gas chromatography-mass spectrometry. O'Doherty *et al* reported increased levels of hydrochlorofluorocarbons (HCFCs) and hydrofluorocarbons (HFC) using atmospheric observatories in Mace Head, Ireland, and Cape Grim, Tasmania (O'Doherty, 2004). They analysed data from these two observatories between 1998 and 2002 to establish trends in HCFC and HFC concentrations. They reported the use of a thermal desorption-gas chromatography-mass spectrometer to analyse compounds to a very high degree of precision. The instrument was run every 2 hours, alternating between a gas standard and air, giving 6 measurements per day for the 4 years. An increase in concentrations was found from the results. They estimated that mole fractions increased at rates of 3.4 ± 0.4 ppt/year for HCFC-134a, 1.6 ± 0.1 ppt/year for HCFC-141b, 1.1 ± 0.1 ppt/year for HCFC-142b and 6.0 ± 0.4 ppt/year for HCFC-22. It is important to note that HFC-134a (1,1,1,2-tetrafluoroethane) is the only compound that

was seen to rise at an increasing rate during this time frame. HFC-134a was widely used as a refrigerant for domestic refrigerators and in automobile air conditioning units. However, as of 2011 its use was banned by the EU due to its environmental impact (Parliament Council of the European Union, 2006). The data collected by the two GC/MS instruments was integrated into the NAME dispersion model to determine average emissions over Europe, whilst a 12-box atmospheric model was used to determine global emissions estimates. In addition, measurements of HCFCs and CFCs have been used to produce the evolution of tropospheric chlorine loading. An extrapolation of the constant rates of increase of HCFCs between 1999 and 2001 indicates that “these increases will be offset in the future by declines in other tropospheric loading gases” (O’Doherty, 2004). Therefore tropospheric chlorine loading will slowly decrease in the future.

VOCs are of particular importance in the lower atmosphere where along with NO_x and CO , they can act as a precursor to ozone in the troposphere. Tropospheric ozone is a pollutant as it can contribute to the greenhouse effect and is highly toxic, affecting the respiratory system in humans (Dewulf & Van Langenhove, 1999). It forms a major part of photochemical smog, the mechanisms of formation first being identified in the 1970s and leading to a Nobel Prize in Chemistry for Crutzen, Molina and Rowland (Crutzen, 1971; Molina & Rowland, 1974). Ozone is formed from VOCs and NO_x by reactions 1-5. Initially, VOCs react with OH in the presence of oxygen to yield RO_2 (Krupa & Manning, 1988). The photooxidation of VOCs yields hydroperoxy (HO_2) and alkylperoxy (RO_2) radicals that react with NO.





NO reacts with both HO₂ and RO₂ to form nitrogen dioxide, which then undergoes photo-dissociation at wavelengths less than 420nm to yield NO and an oxygen atom that binds to O₂ to give ozone.

On global scales isoprene and monoterpenes from biogenic sources are by far the largest global source of VOCs (Guenther, Hewitt, & Erickson, 1995). VOCs in urban environments are often formed due to incomplete combustion and from the evaporation of fuels. In any given location, sources can be a mix: anthropogenic (for instance, petrol in cars, industrial processes, domestic solvent) or natural (leaf and plant emissions, forest fires, oceanic). Urban environments typically have a higher total concentration of VOCs due to local sources of anthropogenic emissions. For example Investigations into urban VOC emissions were carried out between March 2006 and February 2007 in the industrial town of Tarragona, southern Spain (Ras, Marcé, & Borrull, 2009). The region was chosen due to its large amount of industrial activity. Samples were taken at seven sites throughout the city on a monthly basis. Four of these sites were located within the city, all with medium to high levels of road traffic and traffic jams, except for one, which was located in an area where traffic was restricted. Two more sites were located in an industrial complex near a large shipping port to the south of the city, but at a reasonable distance from roads. A further site was located to the north of the city, in close proximity to an oil refinery.

GC/MS was used to analyse air samples at all these sites. After calibration of the instrument, the instrument sampled air at each of the sites on a monthly basis with reportedly good reproducibility. In total, forty two compounds were detected and quantified in the urban and industrial areas. Out of the forty two compounds, the most

abundant were *i*-pentane and toluene with concentrations between 15.2 and 202.1 $\mu\text{g m}^{-3}$, and 1.6 and 150.6 $\mu\text{g m}^{-3}$ respectively. Xylenes were also observed in high concentrations in the urban sites. This provides some evidence that urban environments are heavily influenced by road traffic, which could lead to elevated levels of ozone in these areas. Another example is that described by Lee *et al* in 2006. They reported elevated levels of VOCs, ozone, and other photochemical by-products as a direct result of a heatwave in Europe during August 2003. An increase in sunlight, and elevated temperatures lead to an increase in ozone production, that has been attributed to an abnormal number of deaths reported at the time (Lee *et al.*, 2006).

Another source of VOCs are phytoplankton in the oceans (Yassaa & Williams, 2005). The release of monoterpenes from South Atlantic phytoplankton was investigated and quantified using GC/MS. Nine monoterpenes were identified, with maximum levels of total monoterpenes at 100 – 200 pptv which was found when sampling involved crossing a phytoplankton

A further application of GC/MS is in the measurement and analysis of organic aerosols. Graham *et al* describe how a GC/MS was used to monitor aerosols during the CLAIRE field work campaign in Balbina, Amazonia, Brazil (Graham, 2003). The purpose of the study was to examine the concentrations and nature of organic aerosol in the atmosphere over the Amazon rainforest, as few previous studies had investigated this. The two main objectives of the study were to determine the diurnal variation in composition and concentrations of organic aerosols, and to investigate the formation of secondary organic aerosols (SOA) via photooxidation.

1.7. Brief Introduction To the University Of York Airborne GC/MS

The instrument used throughout this project is a commercial Agilent GC/MS, with both custom built and commercial parts used to ensure the set-up is fully automated. See chapter 2 for a full breakdown of the individual components. The instrument is fitted into a rack that can be loaded onto a BAe 146-301 aircraft. From here, the instrument can be flown around an area of interest to take samples of air and analyse them *in situ*. There were several challenges in developing such an instrument, due to the regulations of the aircraft, and the logistics of mounting it. Several parameters had to be taken into account such as safety, weight, size, reliability, stability and consistency of reporting. In order to mount the instrument onto the aircraft, a custom built rack was provided (Avalon Aero, UK). This immediately placed an upper limit on size. As such, the GC used was an Agilent 6850, selected due to its smaller footprint when compared with other GC instruments. In addition, to fit with rack weight limits for safety, the total instrument package had to be designed to be under a certain weight. In its current configuration, the entire instrument and rack weighs 200 kg. The mass spectrometer is bolted to the bottom plate of the rack using anti-rattle washers, and rubber washers are in between the base plate and the rack. This is to reduce vibrations within the instrument, which could cause internal disruption to the functioning of the instrument. A Markes TT 24-7 thermal desorption unit (TDU) was used to trap VOCs, ready for injection onto the column. The traps used contained Tenax, which reportedly has a large affinity for VOCs. (Brown & Purnell, 1979; MacLeod & Ames, 1986) The TDU contains two traps for constant sampling. When one trap is injecting onto the GC column and cooling down, the other is collecting the next sample. This provides a high number of samples per flight. This setup was used in the BORTAS field campaign in August 2011, prior to this research. This was the first test of the aircraft instrument. This campaign focussed on the composition and distribution of biomass burning products and

their effects on ozone flux over the boreal forest fires in North East Canada and the North West Atlantic Ocean. Several papers on the composition of VOCs in these areas are currently in preparation.

1.8. Aims and objectives of this study

The number of analyses that can be run per flight is crucial. The aircraft typically flies at 100 m/s; 200 knts, meaning that the faster samples can be analysed, the greater the spatial resolution that can be attained by the instrument. The cost of running the aircraft is very high and there is a strong imperative to obtain the highest data coverage possible in each research mission. The first deployment of the instrument on the BAe 146-301 aircraft was as part of the BORTAS field campaign across the North Atlantic. Further details are given in chapter 4. During the campaign, it became apparent that substantial amounts of time were being wasted whilst the GC oven was cooling down. Indeed, the oven cool down period was the longest single element of the analytical cycle. The thermal desorption traps had finished sampling and were waiting for the GC to return to its initial state. However, the GC oven was taking a significant amount of time to return to the initial temperature. As the instrument is located on an aircraft with a set flight plan, any time the instrument is idle results in a loss of measurements, decreasing spatial resolution. Ideally as many measurements as possible should be taken whilst in the air. The objective here is to reduce the lag time to improve sampling rate, without compromising on resolution, beyond that which is necessary.

Therefore, one or more of the GC parameters listed in earlier sections needed to be altered, in order to maximise the number of samples analysed per flight by minimising the

amount of time the GC is idle for. Each of the parameters will be considered in turn and an analysis will be made on the most appropriate parameter to change.

Column length affects the separation, and therefore resolution of analytes as described above. Resolution is linked to column length by equations 1.1-1.4 above. The square root relationship between resolution and the number of theoretical plates is of particular importance. Practically, it means that any change in the length of the column only has a moderate effect on the overall resolution. In addition, if the length of the column is increased, the time of the GC analysis will increase. Therefore, any changes to the column length will only have a modest impact on the time of the analysis, and the subsequent resolution. The Rtx-5 10 meter column currently in the instrument has produced results that show acceptable degrees of resolution.

The carrier gas velocity cannot be altered due to the use of a thermal desorption unit (TDU). The TDU requires a certain flow rate to be able to move compounds efficiently and in a narrow band from the trap, along the transfer line to the head of the column. This is regulated by a mass flow controller within the TDU, which is already set to the optimum flow. Too high a flow and the early peaks become smeared and the MS vacuum is degraded. Too low, and the time for analysis increases and again, early peaks have poor peak shape. In practice there was very little optimisation that could be performed around this parameter.

A linear temperature program is used for this particular instrument and application. For the BORTAS field campaign, the temperature in the GC oven was increased from 40 °C to 130 °C. An isothermal temperature cannot be used in this application due to the range of analyte volatilities. The instrument is set up to measure middle weight monoterpenes and other VOCs. Table 1.1: A sample of compounds detectable by the instrument, and their

respective boiling points. Table 1.1 shows the wide variety of boiling points possessed by compounds in the atmosphere.

Table 1.1: A sample of compounds detectable by the instrument, and their respective boiling points.

Compound	Boiling points (°C)	Identifier Ion 1	Identifier Ion 2
Isoprene	35	67	
Hexane	69	57	
Methacrolein	69	41	70
Benzene	80	78	
Acetophenone	80	77	105
Cyclohexane	81	56	84
Methyl Vinyl Ketone	81	55	70
Methylcyclohexane	100	83	98
Toluene	110	91	
Ethyl Benzene	136	91	106
3, 3, 4-trimethyl Hexane	138	57	71
<i>m</i> - and <i>p</i> - xylene	139	91	106
<i>o</i> - xylene	145	91	106
1-methylethyl Benzene	155	105	
Alpha Pinene	156	93	
1-methylpropyl Benzene	173	45	86
Limonene	178	68	93
Carbon Tetrachloride	190	117	
Naphthalene	218	128	

Changing the film thickness can dramatically affect the separation of compounds within the column. In addition, decreasing the film thickness to increase the speed of analysis would not yield a significant change in analysis time.

The stationary phase selectivity has relatively limited scope for manipulation in VOC analysis. The chosen stationary phase (5 % diphenyl / 95 % dimethyl polysiloxane) reportedly has a high affinity with VOCs and monoterpenes (Davies, 1990). Therefore, modifying the stationary phase further may have some effects on resolution and selectivity, but not necessarily on the overall speed of analysis.

The use of a two dimensional GC instrument has been suggested. However, due to aircraft restrictions, modifying the current system would not be practical in the confines of this project. The mass spectrometer would still need to be present, as retention times of compounds of interest are not always known, however the scan rate of the MS is relatively slow compared to the demands of GCxGC. At best, the MS used here can scan around 10 Hz, well below the data rate needed for fast GCxGC, which is around 50 Hz.

The current column configurations do not allow for a backflushing program to be introduced, however, there is some scope for time reduction, notably in reducing the top temperature required to back out the heaviest VOCs. However, VOC analysis is essentially self-limiting in terms of higher boiling point compounds. They have to exist in the gas phase to get in to the column, which by default means they eluate quite readily. Backflushing is primarily of use when high boiling point material enter the column via split/splitless or on column injection.

The current carrier gas used is helium. Hydrogen would be more ideal from a GC perspective, but due to its explosive nature, it cannot be used onboard the aircraft. It is also very difficult to pump in MS systems and leads to higher MS operating pressures, decreasing sensitivity. The carrier gas is also used in this instrument to purge the TDU traps, so a small amount of hydrogen will be leaking into the cabin. Therefore helium is favoured. It has a lower theoretical plate height value at faster velocities than that of nitrogen.

Because of the use of the mass spectrometer, there is already a vacuum present at the column outlet. This means that compounds will move towards the end of the column faster, decreasing the analysis time.

It was concluded that the temperature program was the optimum parameter to change. Temperature can have a large effect on gas chromatography. In particular, the initial

temperature affects peak shape in obtained chromatograms. A low initial temperature means that analytes are refocused on the head of the column after moving down the transfer line. The transfer line is kept at a high temperature (~150 °C), in contrast to the column which is kept at a comparatively lower temperature (~40 °C). Compounds moving from the transfer line to the column will immediately slow down and refocus. This provides sharper peaks as the only factor affecting separation will be the compounds affinity with the stationary phase.

If the column temperature was higher, less refocusing would occur. Compounds entering the column would slow down to a lesser extent, meaning that velocity through the transfer line would also play a part in separation. This would lead to a Maxwell-Boltzmann type distribution where most molecules of a particular compound would have a similar range of velocities; however, a significant proportion would have velocities above or below the mean range. Therefore peak tailing increases, which can lead to closely eluting compounds to elute together.

So, whilst a higher initial temperature decreases the overall analysis time, a loss in resolution may also be observed due to less refocusing on the head of the column. The impact of varying the initial temperature will be investigated in this study to find an optimum temperature where the time taken to cool down is reduced, but where an acceptable level of resolution is still gained from the system.

Another factor in the temperature program is that of the rate of heating. A faster heating rate reduces the amount of time taken for the GC oven to reach the final temperature. However, a loss of resolution is also seen, as compounds spend less time interacting with the stationary phase. In addition the power consumption increases as the ramp rate increases, and such high demands on the power cannot necessarily be met by the aircraft.

Therefore, ramp rate will not be investigated due to the nature of the location of the instrument.

The final changeable temperature parameter is the final temperature. A higher final temperature extends the run time of the GC. Compounds with a high affinity with the stationary phase and a low volatility take much more time to elute, so a higher final temperature will allow this to happen in less time. This will also be investigated, to determine any benefits.

This study will investigate the effects of changing the initial and final temperatures of the GC temperature program on chromatographic resolution. The possible changeable parameters have been considered, and it can be concluded that the initial and final temperatures will have the largest effect on the GC idle time.

CHAPTER 2. EXPERIMENTAL

2.1. Introduction to the Instrument

The instrument used throughout this project is an Agilent 6850/5975c GC/MS, coupled to a Markes TT 24-7 thermal desorption unit. It is installed in a rack that can be fitted onto a modified BAe-146-301 aircraft where it can be used to take *in situ* measurements of atmospheric VOCs. The aircraft flies at a speed of 230.156 mph (200 knots), at altitudes of between 15 m (50 ft) to 10 km (35000 ft). Flying ranges vary, and are dependent on weight etc., but typical ranges are approximately 4-6 hours. When on the aircraft, the instrument is used to analyse lower and mid-layer tropospheric air samples. The data acquired can be used stand-alone or entered into box models, regional models or global model of the atmosphere for the purposes of understanding atmospheric processes and making predictions about how the atmosphere is changing. The main function of the GC/MS described here, is to analyse the chemical types and quantities of VOCs in the atmosphere which have molecular weights between 45 amu and 220 amu. The method and setup described here is that was used on the BORTAS field campaign (Purvis *et al*, manuscript in preparation). Figure 2.1 is a photograph of the instrument with the constituent parts labelled. The instrument comprises both commercial and custom built devices. The principle parts are: a custom built rack, power distribution box, uninterrupted power supply (UPS) (Alpha Technologies, USA), laptop PC, flow control box, thermal desorption unit (TDU) and the GC/MS itself. Power to the GC/MS, TDU, flow control valves etc. is supplied by the custom-built power distribution box, with the UPS to provide power to the instrument during power change over as the aircraft's electrical supply switches between engine and ground power. All components in the instrument are automated and controlled using the

laptop PC. As far as well practicable, 1/8 inch stainless steel tubing was used as this was preferred over PTFE tubing due to previous studies showing how PTFE and other polymeric tubing can introduce impurities and remove compounds from the sample line. These were connected together throughout the instrument using 1/8 inch Swagelok (Swagelok, UK).

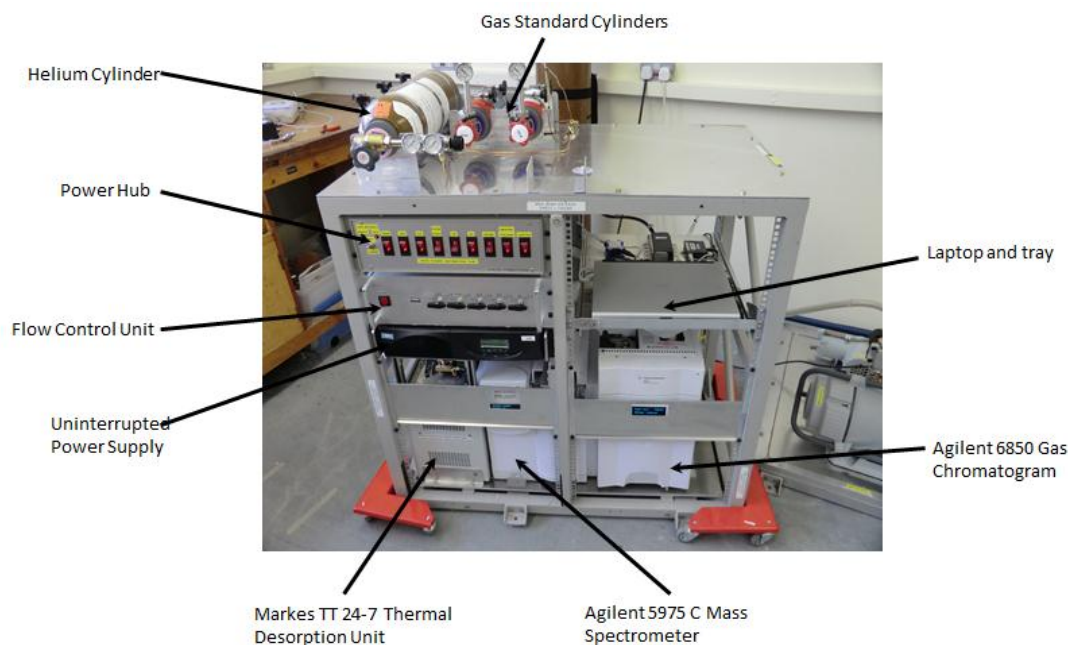


Figure 2.1: The University of York TD-GC-MS in the aircraft rack

2.2. Individual Components

2.2.1. Flow Control Unit

On-board the aircraft, the air samples are drawn from outside the aircraft via a rear-facing window mounted inlet made of 3/8" stainless steel. Air is compressed using an all stainless steel double headed bellows pump (XDS 10, Edwards, UK), which then feeds the pressurized sample (regulated to around 1 atm pressure via a pressure relief valve) into the custom built flow control box. On the ground, the method of introducing samples to the instrument depends on the nature of the sample. If a gas is compressed, for instance in a cylinder, no

pump is needed. For analysing ambient or laboratory air, a small sucking pump can be added to the thermal desorption unit outlet. A small subsample is directed to an online VOC monitor (AeroQual, New Zealand) to determine the overall quantities of VOCs in a sample. The VOC monitor contains a PID to ionise organic compounds and gives a reading in parts per million (ppm).

Inside the flow control box, the sample passes through a dryer to remove the majority of water in ambient air, as water vapour can have a detrimental effect on the GC/MS. It can increase column bleed and interferes with the stationary phase, causing peaks to widen, and therefore resolution to decrease. It affects the response of the MS and can make early parts of the chromatogram impossible to utilise for quantitative measurement. The sample dryer developed in chapter 4 of this thesis employs the Peltier cooling effect to freeze water out of the sample. The dryer cools a glass cold finger to approximately -16° (exact temperatures depend on ambient conditions) and water vapour freezes when it comes into contact with the glass surface. The dried air sample is directed then into two software-controlled rotary valves (VICI, UK). The first of these valves changes between one of four sample inlet positions, depending on the gas sample to be analysed as shown in Figure 2.4. This valve controls which sample is directed towards the GC/MS for analysis. The sample can be air, zero air, a deuterated toluene standard or a calibration gas standard. Zero air (BOC, UK) is used to test whether impurities are being introduced to the column from any upstream parts of the instrument. The zero air contains less than 1 ppm of hydrocarbons. As the instrument is highly sensitive towards hydrocarbons, a further hydrocarbon scrubber (RMSH-2, Agilent, UK) is fitted to the cylinder to remove any remaining VOCs. No compounds should be detected in the zero air chromatograms, and in general this is the case. There are, however some small peaks which contain silane groups which arise from column degradation. Figure 2.2 shows a sample chromatogram, highlighting the peak representing column degradation. The deuterated toluene and calibration standard are

used to track the run to run sensitivity of the mass spectrometer and to calibrate its response for a range of compounds for quantitative analysis.

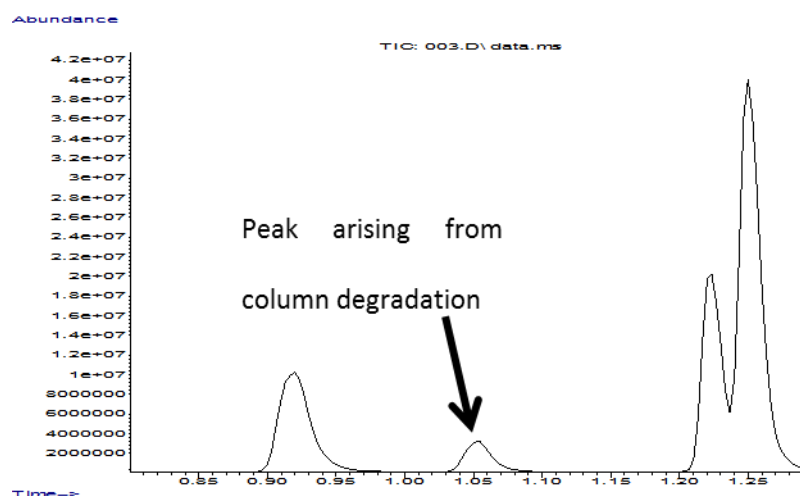


Figure 2.2: Section of a chromatogram of a gas standard showing a peak arising from column degradation

The second valve is a two position valve, which is used to inject a known volume (5 μL) of deuterated toluene into each sample (Figure 2.5). This is carried out by filling a 5 μL sample loop with the deuterated toluene, then changing the position of the valves once for each sample to introduce this gas in to the air sample stream. The toluene is injected onto the thermal desorption unit along with the sample. Injecting a known volume of deuterated toluene into every sample allows peak intensities from all chromatograms to be accurately compared for peak for quantitation.

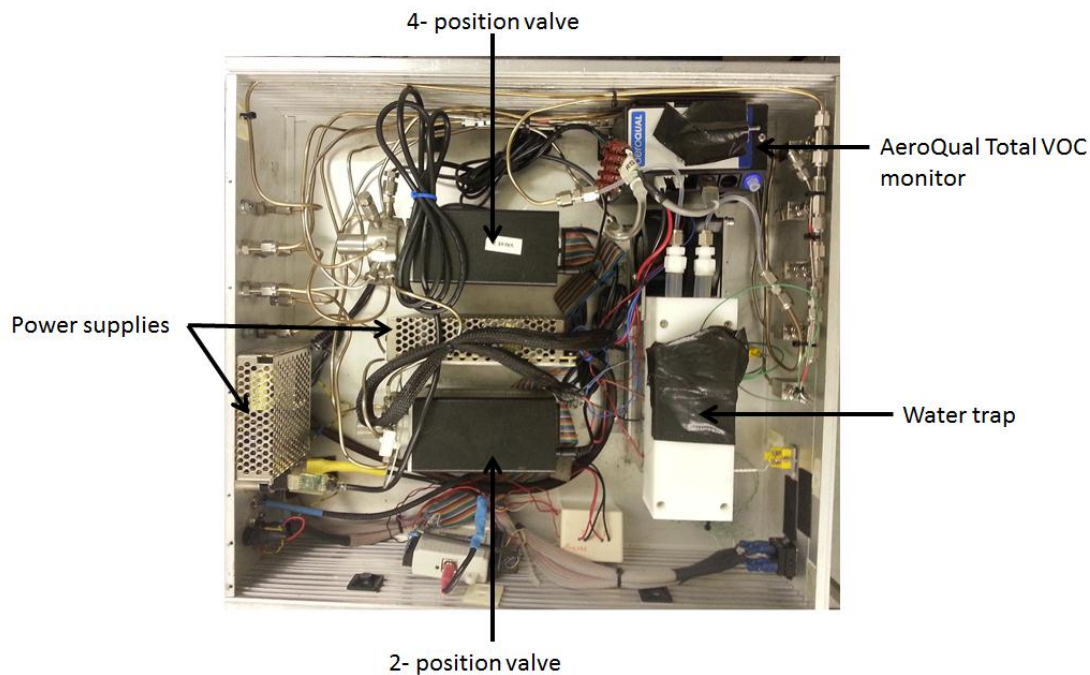


Figure 2.3: Photograph of the internals of the Flow Control Unit

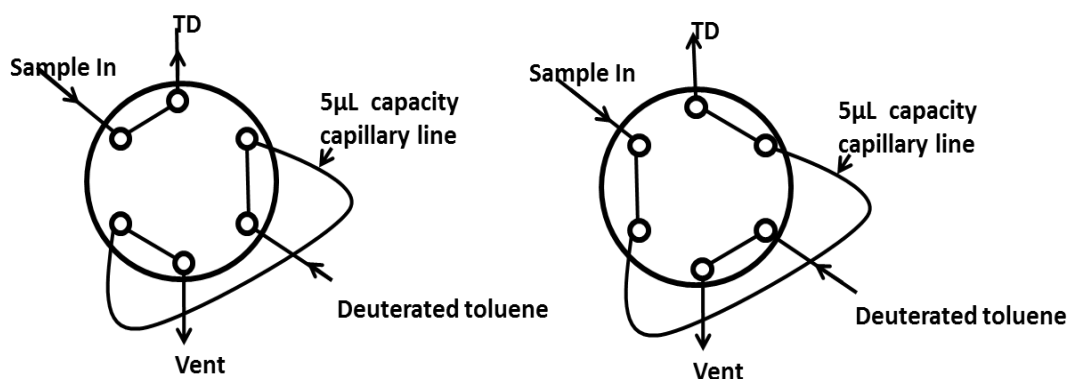


Figure 2.4: The two position valve used to add a known volume of deuterated toluene into each sample. The valve is shown here in the two positions; the sample flowing onto the TDU (left) and the injection of 5µL of deuterated toluene from the sample loop onto the TDU (right).

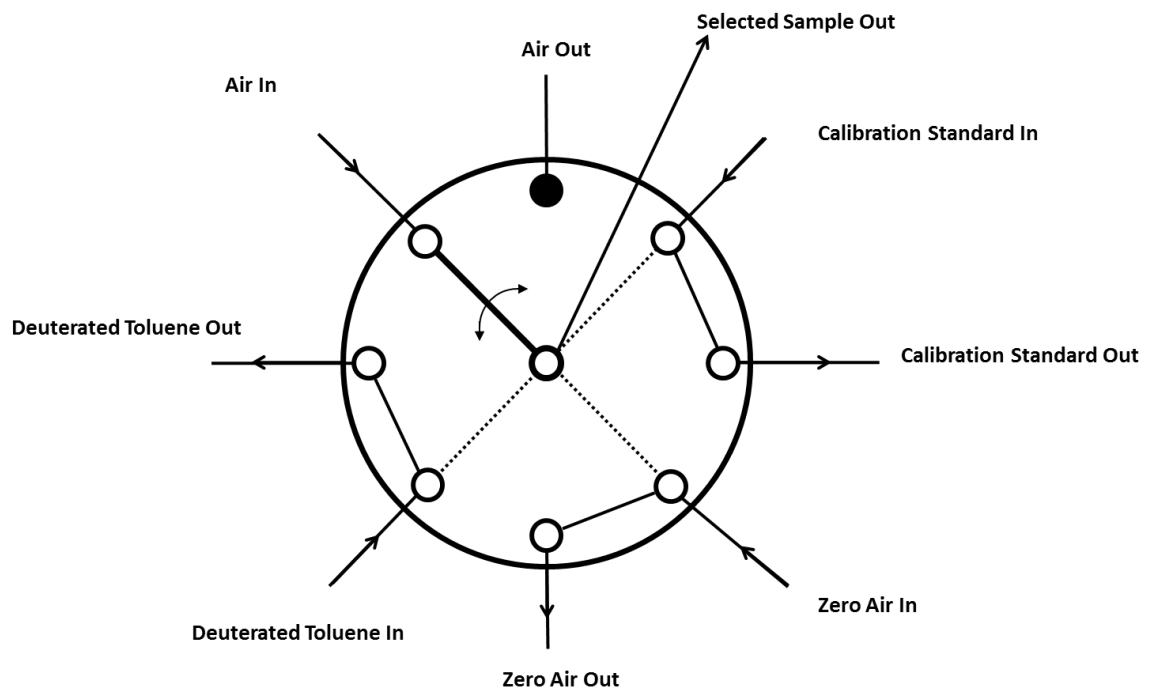


Figure 2.5: The four position valve used to select the gas sample for analysis. Here, the valve is set to sample air.

2.2.2. Thermal Desorption Unit

After passing through the valves, the air sample is directed into the TDU (Markes, UK; TT24-7). The TDU has two Tenax traps (Restek, UK) onto which compounds of interest are adsorbed. Tenax is used in the traps as it has a high affinity for VOCs (Brown & Purnell, 1979; MacLeod & Ames, 1986). Whilst collecting the sample, the traps are usually cooled to 10°C. After sample collection, the traps are rapidly heated to 230°C to desorb VOCs from the adsorbent. The desorbed sample flows into a transfer line, heated to 150 °C, and onto the GC column. The rapid increase in temperature of the trap during desorption ensures that adsorbed compounds desorb from the trap very quickly giving a rapid injection time. In addition, the transfer line is kept at a higher temperature than the front of the GC column. The heated compounds reach the cooler GC column and slow down, reducing the injection time further. A rapid injection time is preferable as it decreases peak tailing, improving resolution. Essentially, the best possible peak width of compounds that will elute from the end of the column is the width of the injection band that they are introduced in. In this instrument, narrow bore GC columns are used and so a split ratio of 6.25:1 is used. This allows for a high flow of carrier through the traps which provides the injection band width, but sacrifices some sensitivity as some sample is vented to waste. Whilst one trap is firing onto the GC and subsequently cooling down, a sample is collected on the other trap, enabling the system to maintain a 100% sampling duty cycle

2.2.3. Gas Chromatograph

The GC used in this study is an Agilent 6850. This is a top loading commercial GC oven, chosen in this case because of the smaller footprint when compared to most oven GCs. The heated transfer line directs samples from the TDU onto the GC column. Once on the column (Restek, UK)(Rtx-5 10 meter x 0.188 mm ID x 0.4 µm stationary phase column, with

5% diphenyl/95% dimethyl polysiloxane stationary phase) analytes are carried by helium carrier gas at a flow rate of 1.6 mL/min. The helium used is of very high purity and is passed through a hydrocarbon and moisture scrubber before interaction with the sample to ensure no impurities are introduced by the helium system.

2.2.4. Mass Spectrometer Analysis and Detection

The Agilent 5975C mass spectrometer employs electron ionisation and a quadrupole triple axis analyser to select the ions based on their mass to charge ratio (m/z). The detector is an electron multiplier. This mass spectrometer is used because of its relatively low cost, the speed at which the quadrupole can analyse ions, and its compatibility with the GC. When analysing samples, the mass spectrometer is set to detect ions with mass greater than m/z 44.

2.3. Standard Operating Conditions

During the BORTAS field campaign, a standard set of parameters was employed which were used throughout this project except when otherwise stated. The thermal desorption unit was set to trap at 10°C, and desorb at 230°C. These temperatures were chosen as the compounds of interest adsorb onto Tenax at 10°C, and 230°C is sufficiently high to desorb the compounds of interest in this study. Each trap was set to sample 300 mL/min for 3.5 minutes giving a sample volume of 1050 mL. A split flow of 10 mL/min was also used whilst sampling to maintain a narrow injection band width and reduce peak tailing and concomitant loss of resolution. The small internal volume of capillary columns means that large samples have large injection volumes leading to broader peaks. The external transfer line linking the TDU to the GC was heated to 150°C. The temperature program for the GC

oven was as follows: the initial temperature was set to 40°C, and ramped to 130°C at a 40°/min. The internal transfer line linking the GC with the mass spectrometer was heated to 150°C. The helium flow rate was set at 1.6 mL/min giving an inlet pressure of 15 psi at 40 °C. The mass spectrometer was set to analyse compounds with molecular weights between 45 amu and 250 amu. The mass spectrometer source and quadrupole temperatures were set to 230 °C and 150 °C respectively. Data was collected from the mass spectrometer at a rate of 0.1 Hz, with the EM voltage set at 2000 eV.

It is widely acknowledged that, whilst a high starting temperature increases the speed of analysis (as the GC oven does not need to cool down as much) it can also lead to a decrease in resolution. This project aims to establish a compromise between the loss of resolution resulting from a higher initial temperature and the speed at which the GC oven cools down, when the starting temperature is raised. What is the optimum initial temperature that allows for rapid cool down, but ensures an acceptable level of resolution? In addition the time taken for the GC oven to cool down at the end of a run is of interest, as it follows that the TDU should be sampling for as long as the GC/MS is idle, for maximum sample volume. A chromatogram of a gas standard containing many monoterpenes (NPL, UK) is shown in Figure 2.6.

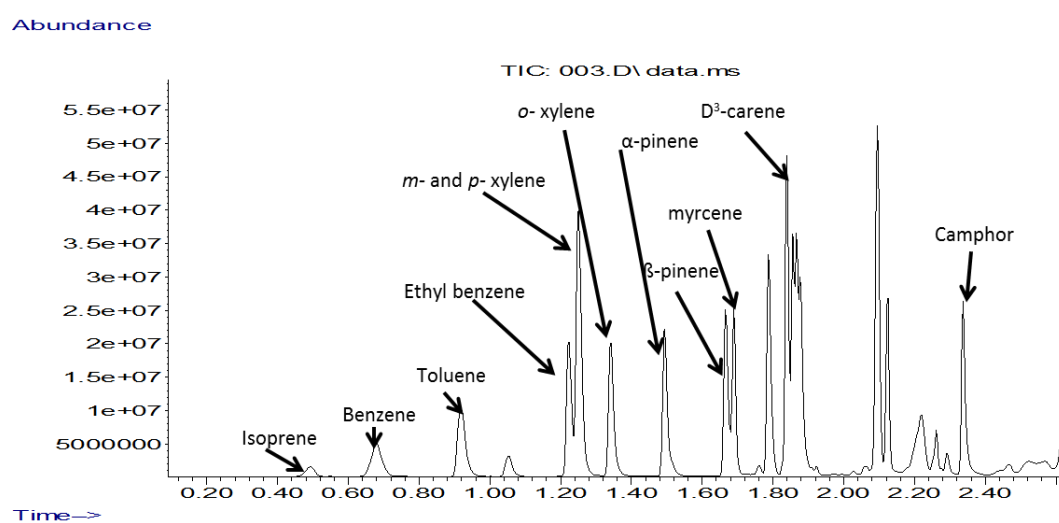


Figure 2.6: Chromatogram of NPL monoterpene standard

2.4. Temperature Testing

Experiments to determine an optimum GC temperature program were carried out on the University of York airborne GC/MS instrument described above. The first stage in optimising the temperature program was to determine the time taken for the GC oven to cool down from and to a range of temperatures. The measurement of the cooling times was acquired so a profile of cool down times could be generated and analysed for the purpose of finding a balance between a fast analysis and an acceptable level of resolution. The temperature program for the instrument was changed using the software. A stopwatch was started as soon as the new temperature program was implemented. All cooling measurements were repeated, and an average of the two times was plotted on a 3D plot using Igor Pro. A 3D plot was used as the initial column temperature was plotted against the resolution number and the time taken to cool down.

In order to determine an optimum temperature program, the chromatographic resolution obtained from each temperature range was analysed and compared to the results from the cooling plot. These tests were carried out using a gas standard of monoterpenes (NPL, UK) (see

Table 2.1). The standard was analysed at all temperature ranges to determine their viability. Feasibility of a given temperature range would be indicated by an acceptable compromise between the resolution against the time taken for the GC oven cooled down. The main focus of the resolution analysis was the shape of the ethyl benzene and *m*- and *p*-xylene peaks and the separation between them. This is because these compounds are very similar in structure and therefore, have similar retention times. The difference in the retention times will decrease as the initial temperature is increased. The separation and resolution of these two peaks was therefore ideal as an indicator of overall chromatographic resolution for all temperature ranges. In addition, the changes in

retention times and the shapes of peaks of other compounds were also noted in the interest of qualitative analysis. Chromatograms and Results are shown in chapter 3.

Table 2.1: Compounds and relative concentrations found in the VOC standard used to test the instrument resolution

Compound	Concentration (ppmv)
isoprene	4.82 ± 0.14
benzene	4.73 ± 0.14
toluene	4.68 ± 0.14
ethyl benzene	4.94 ± 0.15
<i>m</i> -xylene	5.03 ± 0.15
<i>p</i> -xylene	5.09 ± 0.15
<i>o</i> -xylene	5.02 ± 0.15
acetone	4.84 ± 0.48
(+/-) α -pinene	4.83 ± 0.24
(+/-) β -pinene	4.92 ± 0.25
myrocene	5.28 ± 0.26
Δ 3-carene	6.19 ± 0.31
limonene	4.89 ± 0.24
<i>p</i> -cymene	5.69 ± 0.28
<i>cis</i> -ocimene	4.89 ± 0.24
1,8-cineole	4.30 ± 0.21
camphor	4.87 ± 0.73

2.5. Resolution and Dead time Calculations

The resolution of the ethyl benzene and *m*-xylene and *p*-xylene peaks was calculated using Equation 2.1 shown below. The calculation takes into account both the separation of the peaks at their maximum height and the shapes of the peaks by measuring the peak width at half height, to produce an accurate representation of their resolution. Peaks that can be completely resolved down to the baseline yield a resolution value of 1.5. A value higher

than this means two peaks are completely separated (i.e. baseline resolved). Lower values indicate that peaks are co-eluting to some degree, although they may still be separated to a degree detectable by the software. The two peaks may still be clearly visible as unique compounds even though they may be partially overlapping.

$$R_s = 2 \times \frac{(T_{r2} - T_{r1})}{(W_2 + W_1)} \quad \text{Equation 2.1}$$

The instrument dead time (T_0) is needed to calculate the retention time of a peak, T_r . The dead time is the time it takes compounds completely unretained by the column to pass from the inlet to the mass spectrometer and detector. To calculate the retention time of a peak, the dead time must be subtracted from the overall retention time as shown in Equation 2.1. To determine the dead time, a practical method and a computational method were used. For the practical method, laboratory air was analysed using the process described above, except for the addition of the deuterated toluene as this was not necessary. In addition, the mass spectrometer settings were changed to permit the analysis of ions with a m/z greater than 9 rather than the usual lower limit of m/z 44. Airborne compounds such as methane, nitrogen and oxygen were then analysed by the mass spectrometer. Methane is barely retained and nitrogen and oxygen completely unretained by the GC column stationary phase and as such have a retention time approximately equal to the dead time. The time taken for the methane, nitrogen and oxygen to pass through the column was used to estimate the dead time of the instrument. This was found to be 19 seconds (0.31 minutes).

The computational method for determining T_0 employed the use of the Agilent Instrument Utilities calculator. Column parameters and conditions such as inlet pressure are entered in and the dead time is calculated by the software. The software calculated a time of 10.2 seconds (0.17 minutes). The calculated and observed values show a difference of nine

seconds. This difference exists for several reasons. Firstly, a drop in column pressure is observed when the TDU trap begins firing onto the GC column. The presence of this pressure drop is associated with valves within the TDU turning, thus opening volumes that the helium flow must fill before compounds start to move towards the column. The trap has a much larger capacity than the capillary lines feeding the helium into it. This capacity must be filled by the helium that is flowing at a rate of 1.6 mLmin⁻¹, so may take several seconds to fill. Secondly, the time taken for compounds to move along the transfer line and into the GC column is not accounted for. Throughout this study, the observed time of 19 seconds will be used as the dead time in resolution calculations.

$$T_{rx} = T_x - T_0 \quad \text{Equation 2.2}$$

CHAPTER 3. RESULTS AND DISCUSSION

3.1. Investigating the effect of temperature programming upon peak resolution

This study investigated the effect of varying the initial and final temperatures of a GC temperature program on the resulting chromatographic resolution. Experiments were undertaken to determine the time taken for the GC oven to cool down from and to a range of initial and final temperatures, followed by collecting chromatographic resolution data at all these temperature programs.

Firstly, experiments quantifying the time taken for the GC oven to reach the initial temperature were carried out. This was performed by varying the initial and final temperatures of the GC run. The initial temperature was varied between 40 °C and 65 °C. The amount of time taken to cool down from the maximum temperature to the starting temperature was recorded for a range of initial temperatures (40 – 65 °C) and a range of final temperatures (130 – 200 °C). From this the full cycle time and hence measurement frequency of the instrument could be calculated. Initially the experiments were conducted in triplicate for each start and end temperature and an average of the three times were taken. However, it was observed early on that in general, the times were consistent to within \pm 2-3 seconds. Therefore, for the majority of the data collected, only duplicate experiments were performed and averaged. Only the average values have been included here.

Figure 3.1 shows the amount of time taken for each temperature program to cool to the initial temperature. As expected, the larger the difference between the initial and final

temperature, the slower the oven took to cool down. Therefore, the temperature program that took the longest to cool down time was that with an initial temperature of 40 °C and a final temperature of 200 °C. Significant differences in the cooling times were observed across the range of temperature programs. To cool from 200 °C to 40 °C took 194.7 seconds, whilst cooling from 130 °C to 65 °C took only 54.9 seconds. Therefore the latter cools down 3.5 times faster than the former. In addition, as the temperature program from 65 °C to 130 °C takes 2.6 minutes (at a ramp rate of 40 °C/min and total hold time of 1 minute), the instrument is idle for 35 % of the total run time. A 40 °C to 200 °C temperature program takes 5 minutes to complete (using the above ramp rates and hold times). Therefore the instrument is idle for 64.9 % of the total run time.

The cooling times for all the temperature programs were then collated and the data is shown in Appendix 1. The final temperature was kept constant so the relationship between the initial temperature and the time taken to cool to that temperature can be seen. All the curves appear to follow the same uniformly shaped curve, except for some fluctuations which can be associated to ambient laboratory conditions. As the GC oven uses ambient air to cool, the temperature within the laboratory has a large effect on the speed at which the oven cools down. If the temperature in the laboratory is high, the GC oven will take longer to cool down. This could explain the slight lack of uniformity in the shapes of the cooling curves since the laboratory was not temperature controlled.

In addition, the cooling times were also plotted on a 3D contour plot using Igor Pro (Figure 3.2). Initially, cooling times were measured, varying the initial temperature between 40 °C and 65 °C with 2-3 degree intervals.

However, once the data was analysed, a more in depth investigation of the cooling times when the initial temperature was between 40 °C and 52 °C was required. Therefore, the temperature intervals in this section were decreased to 1 degree. As expected, smaller gaps

in the temperature program lead to shorter cool down times. Several bands can be seen across the plot. Rather than a merging of cooling times, this indicates that at higher initial temperatures, less time is taken to cool down from the corresponding final temperatures, to the extent that it appears to be the initial temperature that is the limiting factor in the cool down times.

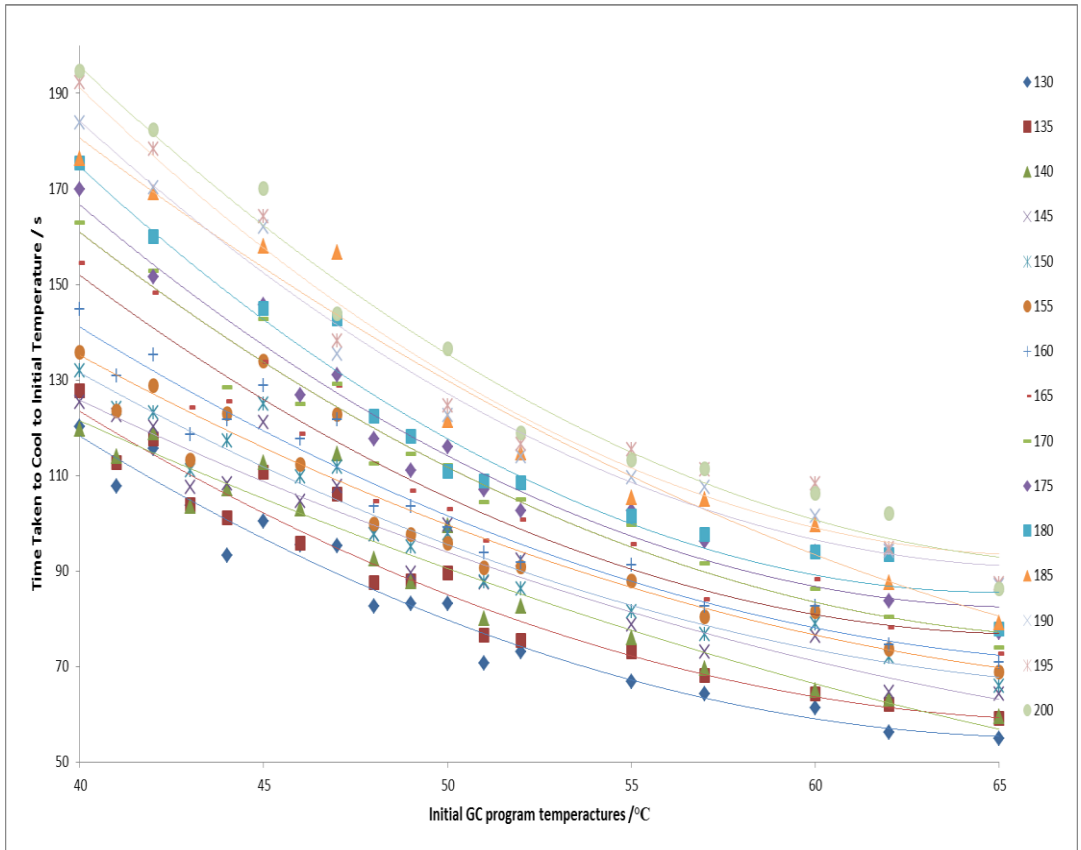


Figure 3.1: A graph to show how varying the initial and final temperatures effects the time taken for the GC oven to cool down

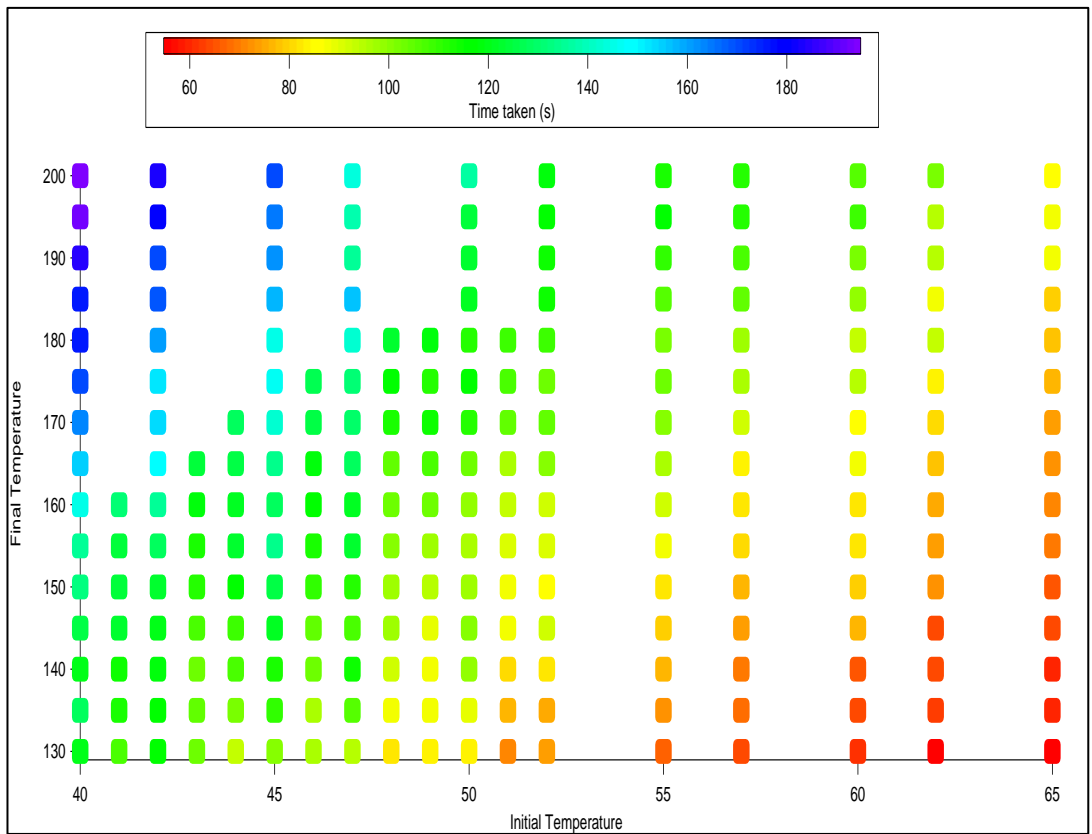


Figure 3.2: 3D plot of initial temperature, final temperature and cool down time

However, as mentioned in previous chapters, the amount of time taken for the oven to cool down is not the only factor in determining which temperature program to use. A higher initial GC oven temperature also leads to a loss of chromatographic resolution. To investigate this further, a gas standard containing monoterpenes was analysed across the temperature program range. Figure 3.3 and Figure 3.4 show how the chromatographic resolution changes when raising the initial temperature from 40 °C to 60 °C. The main point of focus is on the complete loss of resolution between the ethyl benzene peak and the combined meta- and para- xylene peak. In Figure 3.3, two sharp peaks can clearly be seen between retention times 1.2 mins and 1.3 mins. However, in Figure 3.4, the three compounds have such similar retention times that it is not possible to quantify them, either using software, or even qualitatively by eye. The compounds are represented by the peak at retention time 0.9 mins.

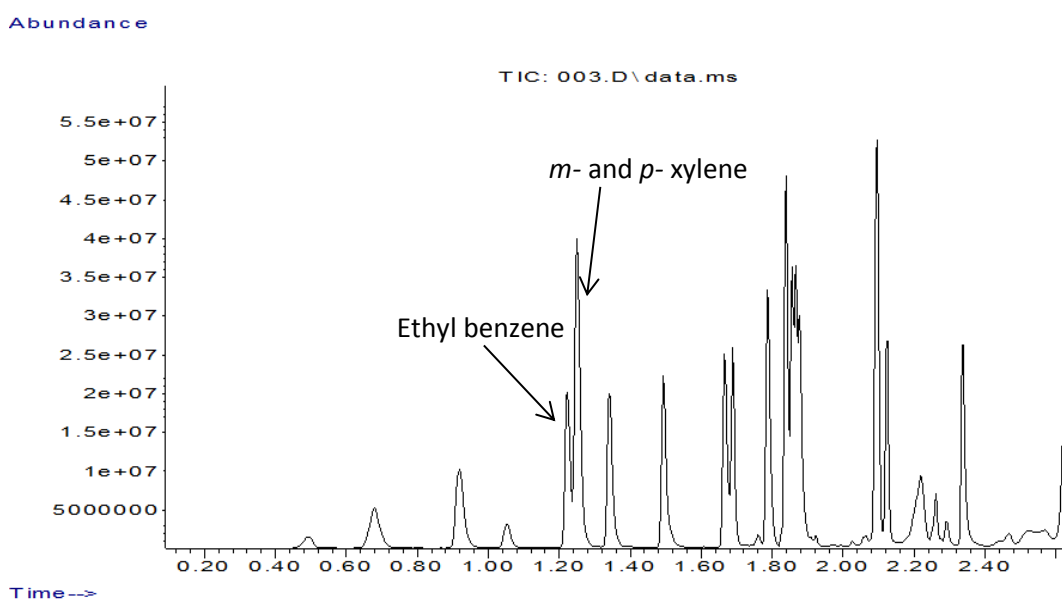


Figure 3.3: Chromatogram of a monoterpene standard. Initial GC temperature is 40 °C

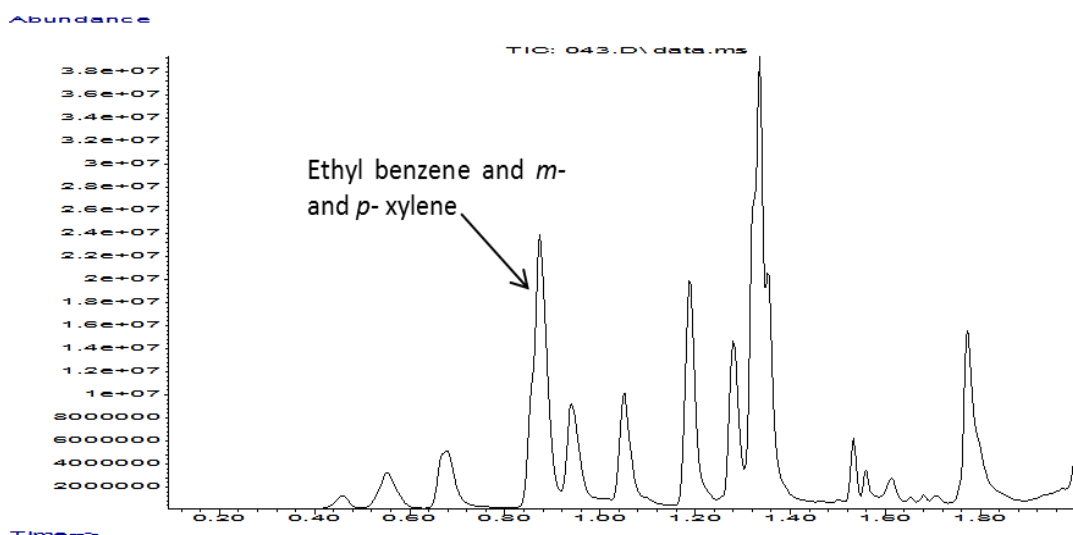


Figure 3.4: Chromatogram of the same monoterpene standard. Initial GC temperature is 65 °C

In addition to this, all the peaks in the chromatograms have moved closer together, reducing overall resolution. Therefore, a compromise must be found between the temperature programs giving the fastest cool down time, and the temperature programs giving an acceptable level of chromatographic resolution.

The resolutions of the ethyl benzene and the combined *m*- and *p*- xylene peaks were calculated for GC runs across the range of temperature programs. The calculation method is shown in chapter 2. The resolution takes into account a peaks' retention time and width, thus giving an accurate description of the overlap between two closely eluting peaks. A retention value of 1.5 or higher is considered to be completely baseline resolved. A resolution value below 1.5 indicates that two peaks are co eluting to a certain degree. The tabulated resolution data is shown in appendix 2.

At higher initial temperatures, some of the resolution values show a spike, particularly when the final temperature is also at the upper end of the scale. This is not consistent with the resolution expected at these temperatures. On closer examination of the

chromatograms, it is apparent that these high values are not indicative of the separation between the ethyl benzene and *m*- and *p*- xylene peaks. Rather, the three compounds are co-eluting so closely that the software cannot identify 2 peaks. Therefore the value that is given by the software is the resolution between the combined ethyl benzene-*m*- and *p*- xylene peak and the next peak in the chromatogram (*o*-xylene). This is baseline resolved, giving a resolution value higher than 1.5. This is shown in Figure 3.5 where the resolution number rapidly rises above usual values at higher initial temperatures.

Instances of this occurring are shown several times when the final temperature was 175 °C, 180 °C, 190 °C, 195 °C and 200 °C. From the graph, the slow decline in resolution with increasing initial temperatures can be observed. It has been determined that these data points are problematic, and therefore should be removed to avoid skewing results and conclusions from this work.

The resolution data was also plotted on a 3d plot using Igor Pro (Figure 3.7). If an acceptable level of resolution is close to 1.5, then immediately many of the temperature programs can be seen to be inadequate in terms of resolution. Therefore, the number of viable temperature programs can be narrowed down.

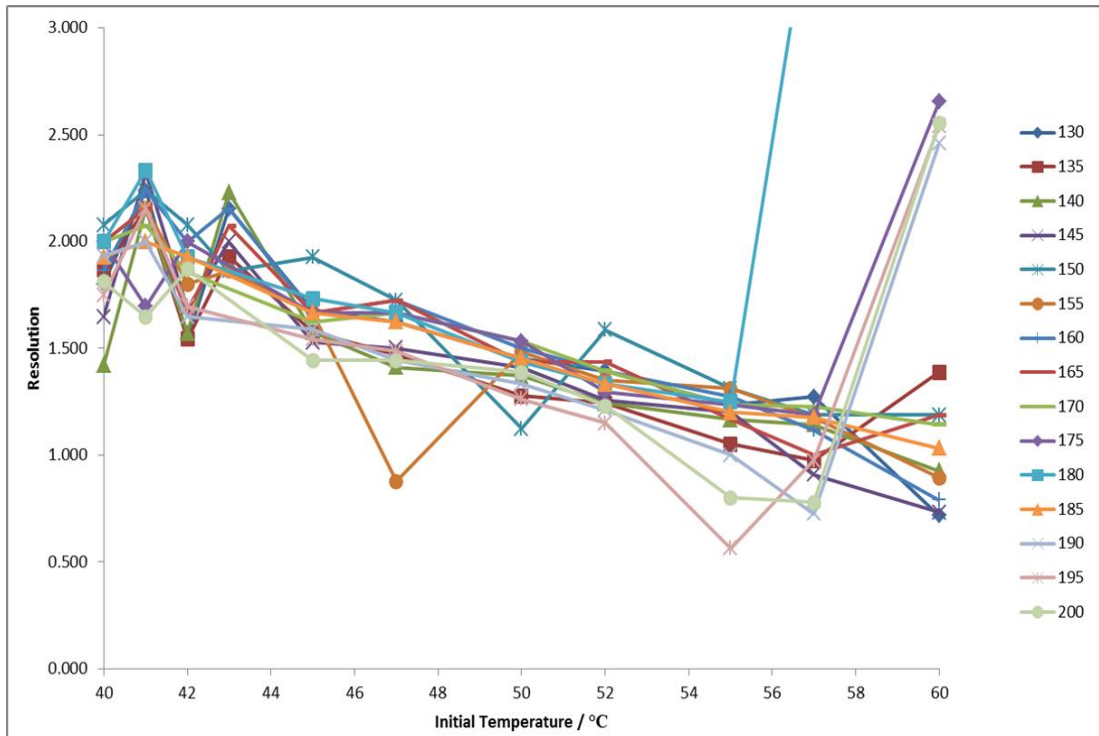


Figure 3.5: How resolution varies with changing initial temperatures at various final temperatures

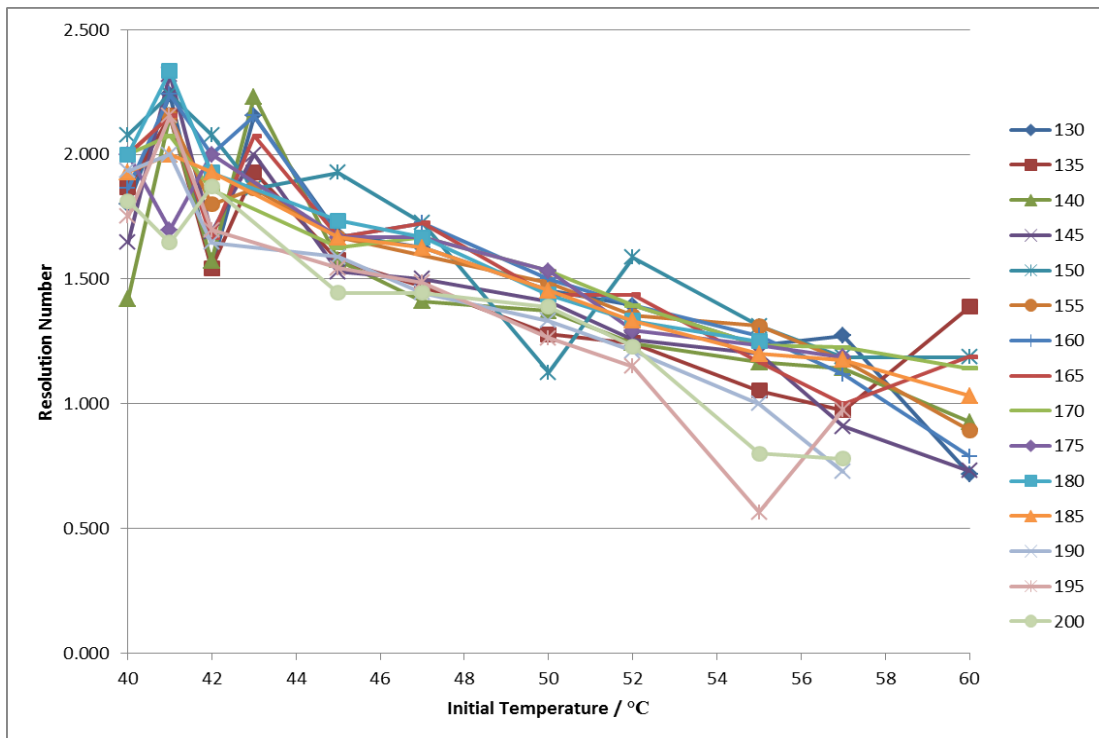


Figure 3.6: How resolution varies with changing initial temperatures at various final temperatures with anomalous points removed

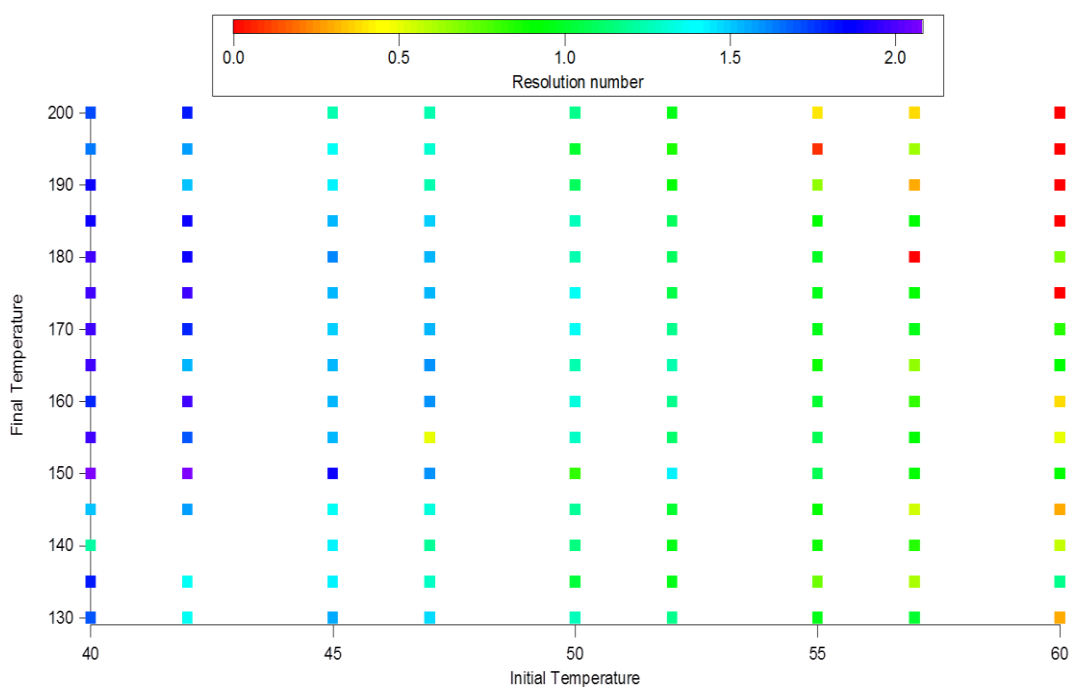


Figure 3.7: 3D plot of resolution for ethyl benzene and m- and p- xylene as a function of changing initial and final temperatures

The two sets of data were then compared to determine the optimum temperature program to use, that yields the shortest equilibration time with the acceptable $R = 1.5$ chromatographic resolution. Figure 3.8 shows the cool down times against the corresponding resolution. On analysing the graph, two distinct regions can be seen that lie further from the line of best fit than the other points (ringed). This is due to the unstable ambient temperature in the laboratory whilst carrying out the cooling tests. Therefore, at higher ambient temperatures, it will take the GC oven longer to cool down, whilst at lower ambient temperatures it will take less time to cool down. Ambient temperatures on-board the aircraft can vary even more than laboratory ambient temperatures. Temperatures on the aircraft can be as high as $35\text{ }^{\circ}\text{C}$. The ringed area below the line of best fit shows data that was taken at higher than average ambient temperature. Therefore it took the GC oven longer to cool down whilst these data points were being collected. If they were collected at an ambient temperature that was closer to the average, they would shift along the x-axis to

the left, giving a shorter cool down time. Conversely the ringed area above the best fit line shows data points that were collected when the ambient temperature was lower than average. The GC oven took less time to cool down. If the data points were collected at an ambient temperature that was closer to average, these points would shift along the x-axis to the right, giving a longer cool down time. This implies that although the ambient temperature heavily affects the cool down time, the relationship between resolution and cool down time is constant at constant ambient temperature

However, as the ambient laboratory temperature was not recorded for the period of the cooling tests, the magnitude of the shift cannot be quantified. Therefore, it follows that for the purpose of the analysis, these data points will be excluded, in order to calculate the optimum temperature program. Figure 3.9 shows the data with these areas removed, and as such, the R-squared value of the best fit line improves from 0.0943 to 0.5921, indicating that the data now lie closer to the best fit line.

By analysing the graph, it can be determined that with a smaller temperature difference, a faster cooling rate is achieved; however the chromatographic resolution is offset. With a larger temperature difference, better chromatographic resolution is observed, but with a slower cooling rate.

The curved nature of the graph indicates that at high initial temperatures a low resolution number and a short cool down time are observed. As the initial temperature is lowered, the resolution number increases to >1.5, and the cool down time increases correspondingly. However, a maximum in resolution number is observed at approximately 2, regardless of the initial temperature. Lowering the initial temperature to below 40 °C does not yield greater resolution, although does result in an increasing cool down time. The resolution is shown to plateau at greater cool down times i.e. beyond a particular limit, there is no improvement in resolution resulting from increasing the cool down time. To investigate this

further the time vs. resolution plot was divided into three separate sections showing significant changes in the relationship. This is shown by Figure 3.11, Figure 3.12 and Figure 3.13. Whilst this is a very crude approximation of behaviour, it enables us to locate the start point of the plateau and hence identify the fastest cool down time corresponding to the best resolution. A linear trend line was added to each graph to determine the gradient of each section. The gradients of the three graphs are 0.0086, 0.0069 and -0.0002 respectively, indicating the levelling out of the resolution at lower initial temperatures.

The focus lies in the second portion of the graph, where resolution is greater than that shown in the first portion (i.e. ≥ 1.5), but the time taken to cool down is less than that shown in the third portion of the graph. As the trend line begins to plateau, several data points lie above the line, indicating a high level of resolution, with shorter cooling periods. A comparison of these data with Figure 3.10 shows that these points are representative of temperature programs where the initial temperature is between 42 and 45 °C. These initial temperatures yield a high level of chromatographic resolution, with a shorter cooling period when compared with initial temperatures of 40 °C and 41 °C. It can therefore be deduced that the lower the initial temperature the slower the rate of cooling. This can be negated by raising the temperature by a few degrees, and so shortening the GC oven cool down time by up to 40 seconds.

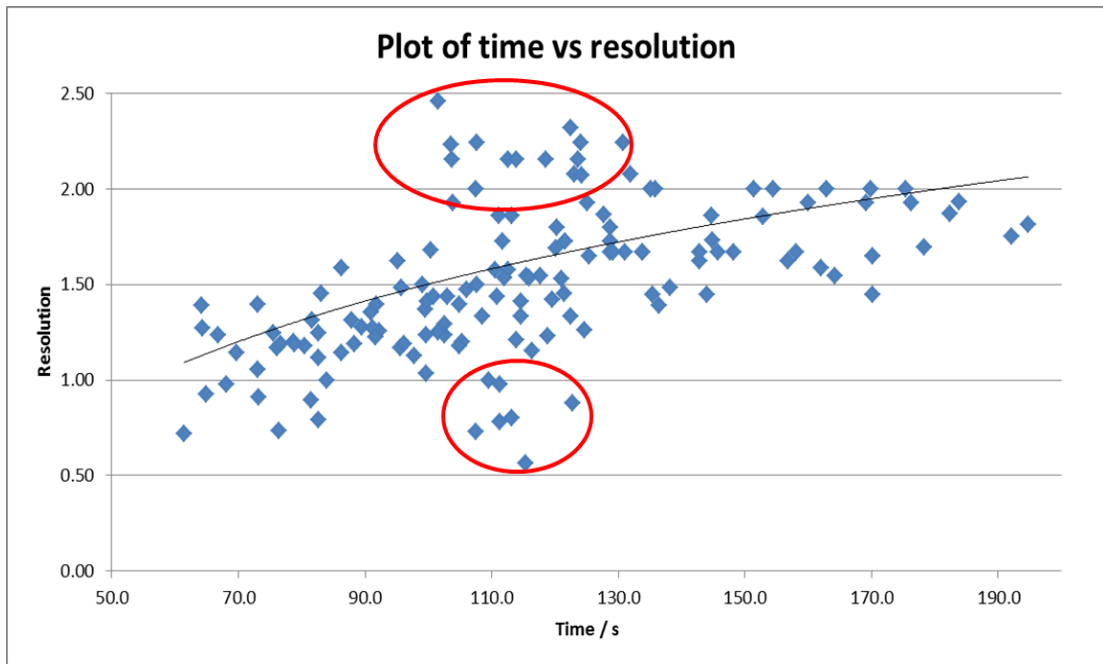


Figure 3.8: Scatter plot to show the non-linear relationship between the cool down times and the resolution. Anomalous areas are highlighted

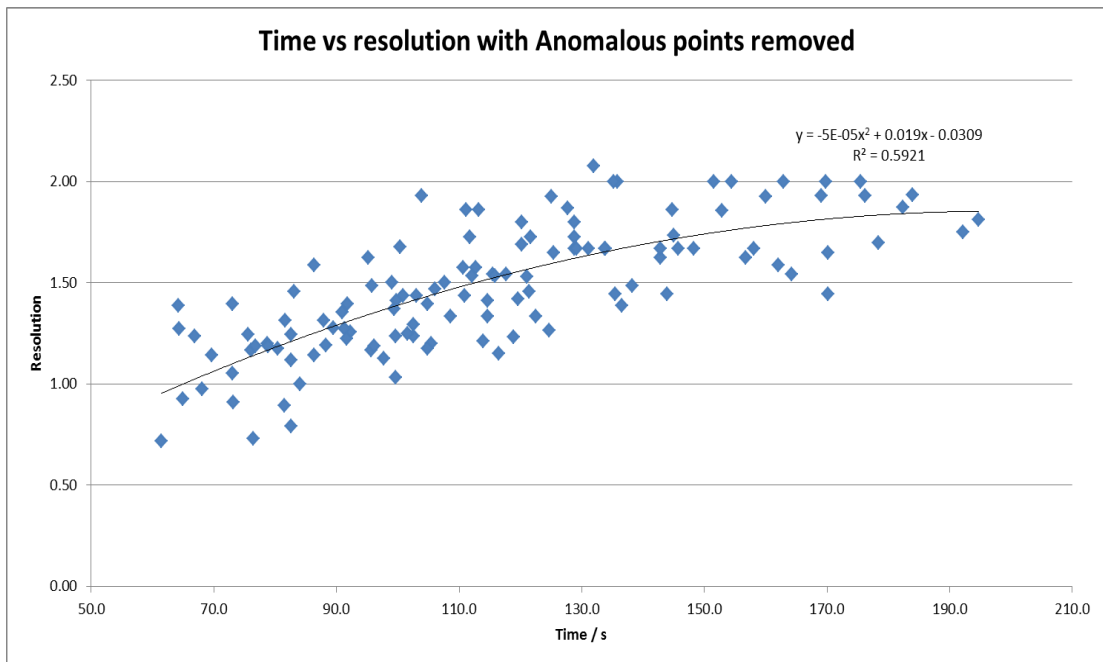


Figure 3.9: Scatter plot of cooling times against resolution with data removed

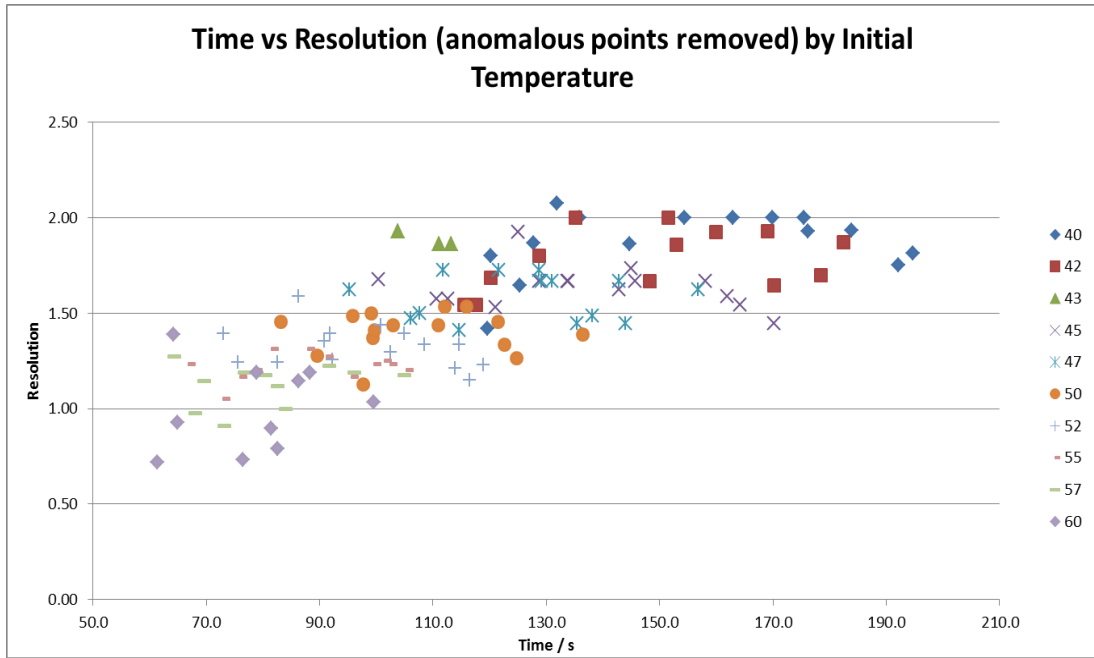


Figure 3.10: Scatter plot of cooling times against resolution with initial temperatures marked.

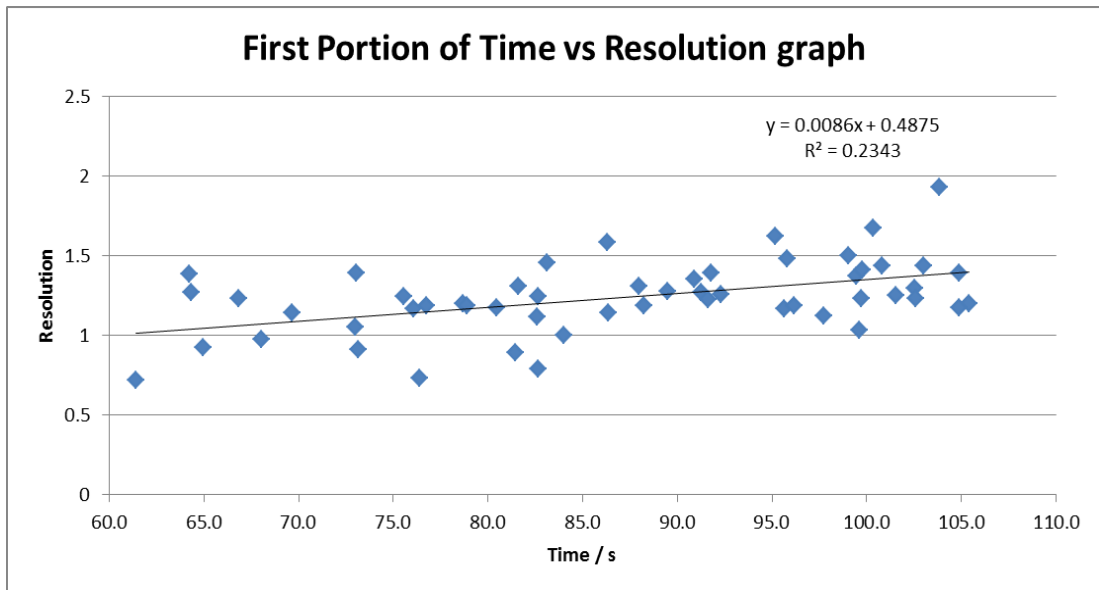


Figure 3.11: First portion of cooling times against resolution graph at low cooling times

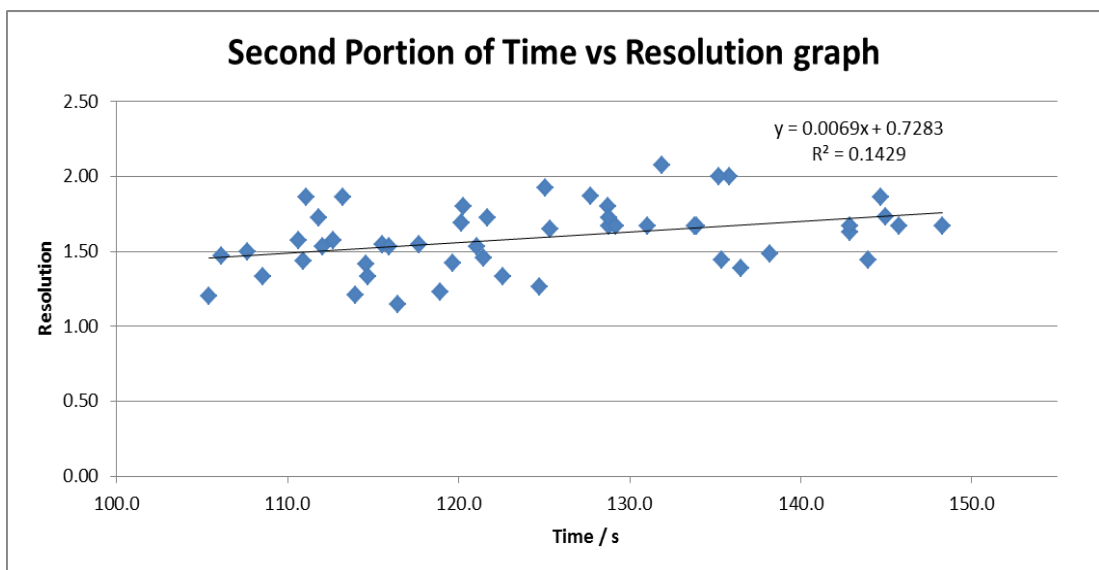


Figure 3.12: Second portion of cooling times against resolution graph at medium cooling times

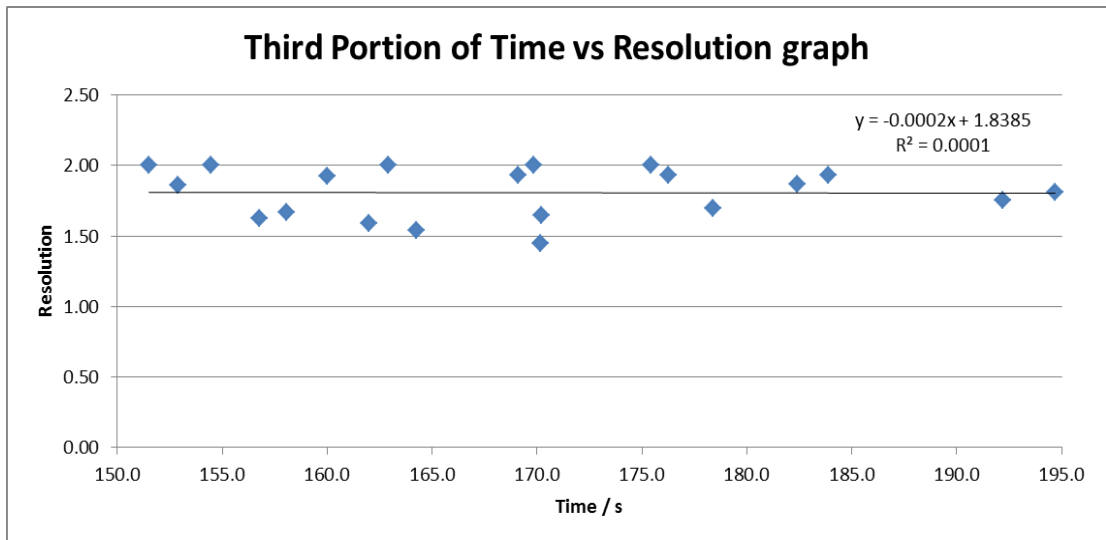


Figure 3.13: Third portion of cooling times against resolution graph at long cooling times.

CHAPTER 4. ANALYSIS OF DATA QUALITY FROM THE FIRST DEPLOYMENT OF THE INSTRUMENT

The instrument was first deployed in August 2011, on the BORTAS field campaign, investigating the effects of forest fires over the North Atlantic Ocean. In particular, this involved many high altitude flights. However, it was quickly noticed that water vapour entering the column was having a detrimental effect on the column when flying at low levels with high temperatures and humidity. Some data was lost because of water both on the TDU traps, and entering the GC column and degrading MS performance. Here follows an investigation into these effects, and the endeavours that were made to rectify the problem.

4.1. Introduction

Contaminants in chromatography can severely affect the way a column performs. Capillary columns are highly sensitive and therefore are particularly susceptible to contaminants (Marvin, 1998). The main impacts they can have upon chromatographic parameters are: loss of resolution, shifts in retention times, irregular peak shapes and a noisy or irregular baseline (Kitson, 1996). As Marvin defined in 'GC/MS: A Practical Users Guide' (1998), the cause of contamination can either be 'general background contamination,' or 'specific ions in the background.' However, specific contaminant ions interfering with target peaks is rare as it is unlikely that contaminant peaks will produce an ion with the same mass and have the same retention times as target compounds. Therefore general contamination is usually the cause. The performance of the capillary column depends on many factors such as

sample volume, temperature program and column dimensions. Contaminants are one of the main causes of column failure.

In general, contaminants, upon entering a column, can behave in two ways. They can pass through the column (semi-volatile contaminants), or they can remain within the column (non-volatile contaminants) (Agilent Technologies, 2007). Semi-volatile contaminants can take several days to pass through a column, depending on the nature of the contaminant and the usage of the column. Such compounds cause problems by interfering with the stability of the baseline and can lead to ghost peaks. Non-volatile contaminants do not elute from the column at normal operating temperatures, and therefore build up inside the column. Such contaminants will not be evenly spread along the column; the start of the column will have a high concentration of contaminants when compared to the end of the column. This leads to interference as molecules within a sample will interact differently with the stationary phase, depending on how much contaminant they encounter. The practical outcome of this is a change in retention time and a loss of peak shape. This decreases resolution and affects the accuracy of quantitative calculations making it harder to draw comparisons with data from previous analyses.

In addition, any contaminants within the column can interact with the column stationary phase causing it to break down and degrade. The rate of column bleed is increased at high temperatures in the presence of contaminants (Agilent Technologies, 2007). Column bleed can lead to 'ghost peaks' in a chromatogram. These ghost peaks can usually be identified by their mass spectra as they are often of a high molecular weight. Excessive column bleed decreases the life of a column.

4.1.1. Atmospheric water vapour and its impact on the column

Water vapour is the dominant, and therefore most important greenhouse gas (Dessler, Zhang, & Yang, 2008; Held & Soden, 2000; Minschwaner, Dessler, & Sawaengphokhai, 2006). The source for atmospheric water vapour is at the planetary boundary layer through evaporation from oceans. Much of the water vapour is therefore found in the troposphere, closest to the source. The benefits of water vapour are apparent in the formation and destruction of ozone, and the nature of aerosols in the atmosphere (Andreae, 1997). Like carbon dioxide, it is able to absorb infrared radiation, thus contributing to the greenhouse effect, and assisting in keeping global temperatures constant. However important water vapour is within the atmosphere, it is a severe drawback in chromatography. Water vapour can act as a contaminant in gas chromatography (Kitson, 1996). Due to the polar nature of the O-H bond, it can interact with polar compounds which, when the concentrations of target compounds are in the region of ppb, can seriously affect retention times and peak shapes.

When water is allowed to enter (or at least, not excluded from) the column it interacts with both the column itself, and with compounds passing through the column causing column bleed and unfavourable interactions with the mobile phase. This is exacerbated by elevated temperatures within the column. The result of this is a very noisy baseline and distortion of peak shapes. Detecting compounds of low relative abundance within this region is made impossible by the noise created by water in the MS interacting with these species. Fehsenfeld *et al* listed many compounds commonly found in the atmosphere, whose detection could be compromised by not excluding water from the column (Fehsenfeld, Calvert, Fall, & Goldan, 1992). The compounds of primary interest in understanding atmospheric processes are VOCs such as isoprene, acetone, benzene and toluene, among

many more (see citation for a more comprehensive list of VOCs commonly found in the troposphere).

For the reasons highlighted above, it is crucial that water be excluded from the system. There is a large amount of water in tropospheric air, particularly in the warm, humid air found in the tropics, where a campaign is planned to fly the instrument over the Amazon rainforest in September 2012.

4.2. Experimental

During the BORTAS field campaign that took place in July and August of 2011, the drying of air samples prior to injection onto the column was carried out using a Nafion membrane. Figure 2 shows the structure of the Nafion monomer. As can be seen, there are 39 carbon-fluorine bonds per monomer, making it a highly polar structure. Dehydration of the sample relies on the membrane being extremely hydrophilic, attracting nearby water molecules. The structure of it is such that any water passing through will reversibly bind strongly to the fluorine through either of the two hydrogen atoms on the water molecule.

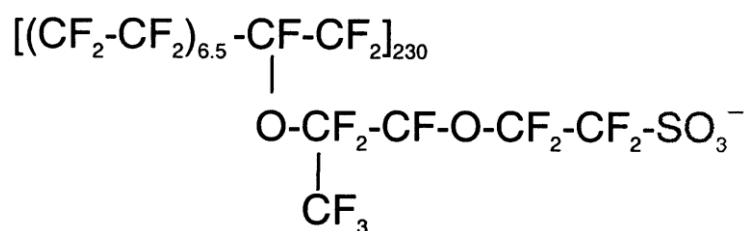


Figure 4.1: The structure of the Nafion monomer (Haubold, Vad, Jungbluth, & Hiller, 2001)

During the campaign, the air sample was passed through a piece of tubing. The interior of the tubing was coated in the Nafion membrane to remove any water vapour. The tubing

around which the membrane was bound to was porous enough to let the relatively small water molecules to pass through. Surrounding this were a large number of desiccator beads designed to remove the water and prevent it from moving back across the membrane. The water bound to the Nafion membrane, then was carried across the membrane along a concentration gradient. The relative humidity within the instrument was monitored to ensure no water vapour moved back into the sample line.

Due to time constraints, the drying device was not properly tested before the instrument was mounted onto the aircraft. After only a few chromatograms were recorded during the BORTAS field campaign, the use of the Nafion-based dryer was discontinued. There were two main reasons for this. Firstly, it was thought that the Nafion was the source of impurities that were seen in the chromatograms. These contaminants appeared to be of a semi-volatile nature and were therefore eluting from the column, causing ghost peaks and a noisy baseline. Secondly, it was thought that the polar nature of the Nafion membrane may have been removing more than just water vapour from the sample. Oxygenated VOCs (OVOCs) present in the troposphere have a polar bond and could have been removed from the sample by the polar Nafion membrane. Examples of atmospheric OVOCs include acetone, acetaldehyde, methanol, ethanol and other air-borne alcohols (Fehsenfeld *et al.*, 1992). Tests, highlighted below, were carried out to investigate whether or not this was, indeed, occurring.

4.2.1. Preliminary Results

After the Nafion membrane was excluded during the BORTAS campaign, it was evident from the data that the presence of water was having a detrimental effect on the chromatography. Figure 4.2 shows a sample chromatogram taken from the BORTAS field data. A noisy baseline can be seen across the chromatogram particularly in the region

between retention times of 0.4 and 0.9 minutes. It is in this region that acetone, isoprene and benzene would be expected to elute. However, the baseline noise makes it very hard to identify them at their atmospheric concentrations, and even harder to determine resolution and peak shapes. The noisy baseline makes the determination of the peak width at half height almost impossible to calculate, therefore, the resolution factor calculated from the software is unreliable. However, in this case, isoprene can indeed be identified. Other chromatograms from the BORTAS data show a lower baseline, but a significantly worse peak shape for isoprene, as shown in Figure 4.3.

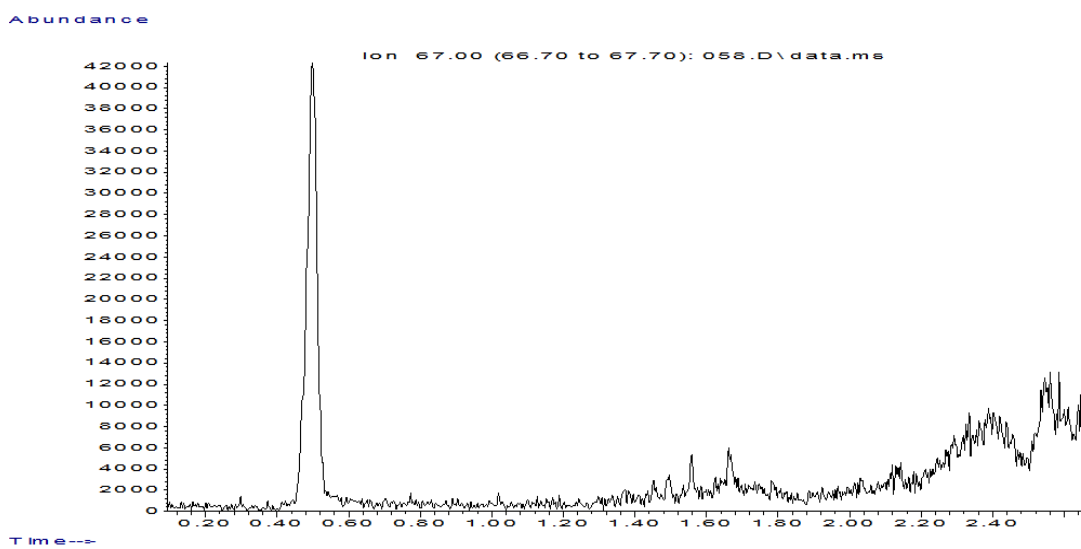
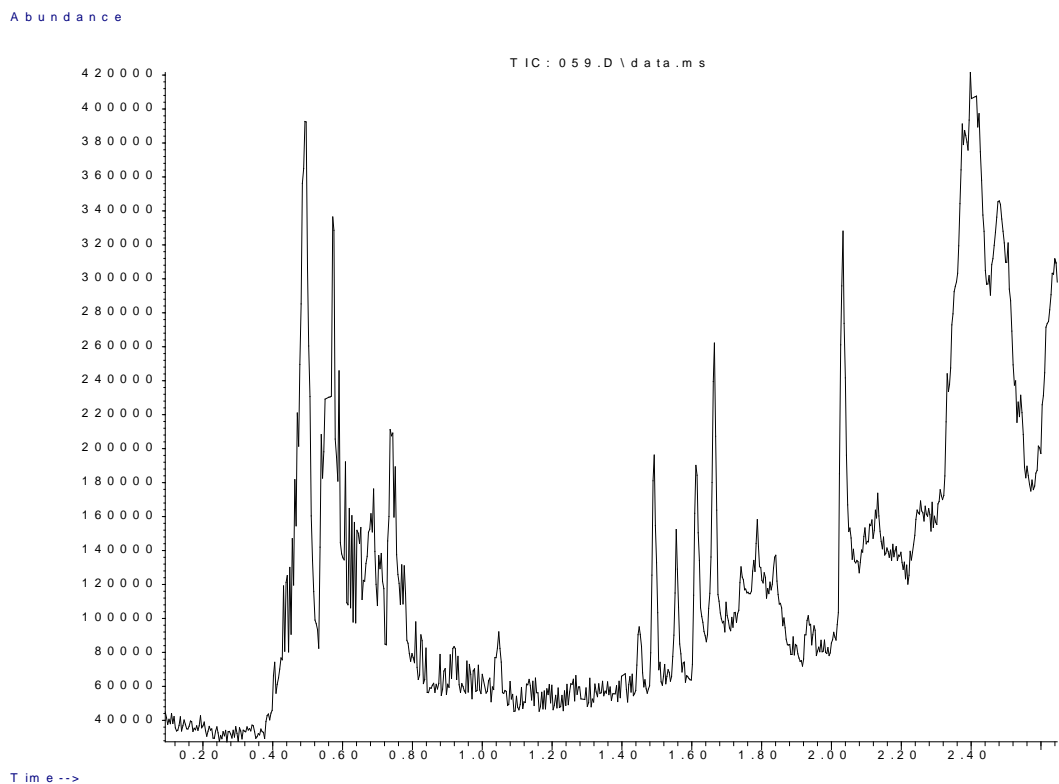


Figure 4.2: (a) Sample chromatogram from the BORTAS field campaign, showing a very noisy baseline across the entire chromatogram, but especially at retention times between 0.4 and 0.9 minutes. The noisy baseline was caused by an abundance of water on the column and (b) the extracted ion of isoprene

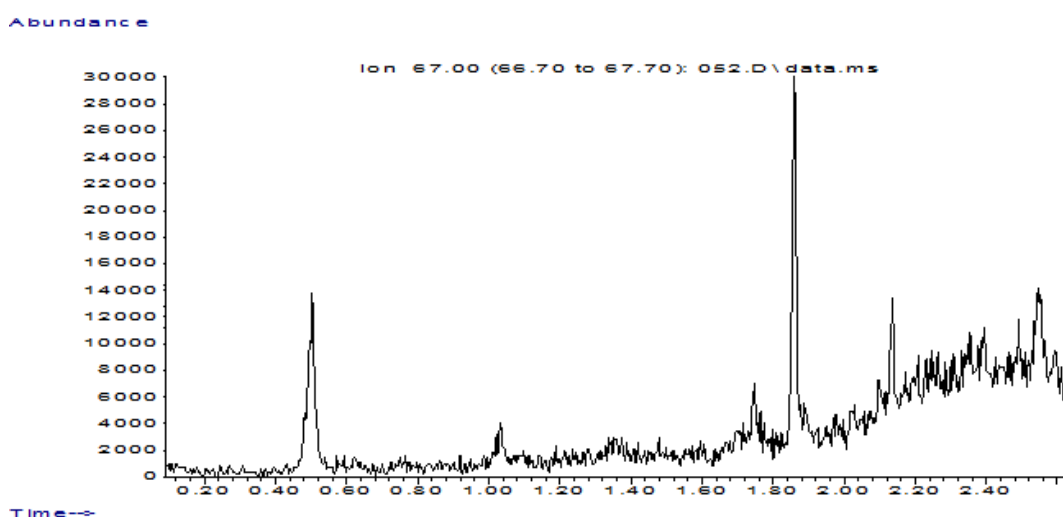
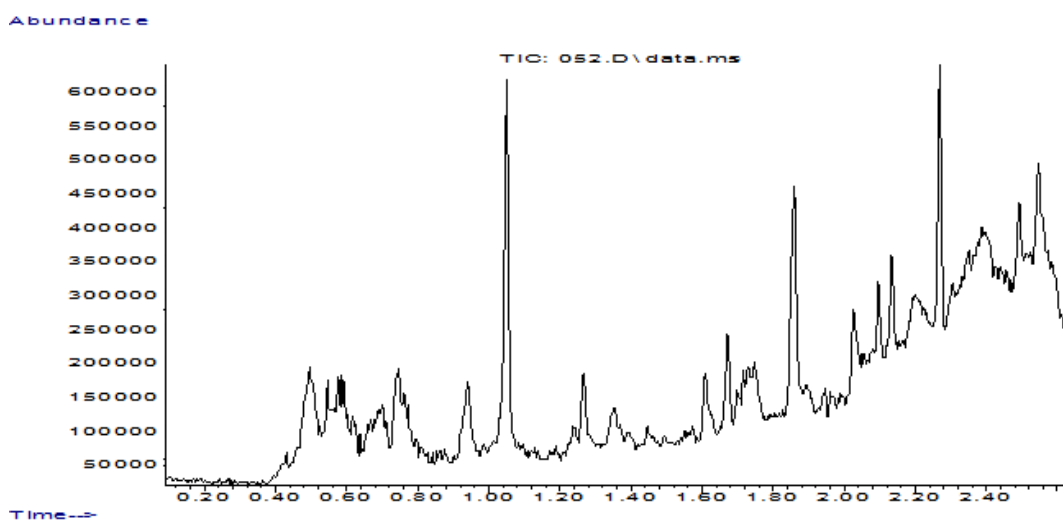


Figure 4.3: (a) sample chromatogram from the BORTAS data showing a less noisy baseline, but (b) a poor peak shape for isoprene

It was thought that the polar nature of the Nafion membrane could also have been removing polar OVOCs from the sample. If there were only trace amounts of OVOCs in an air sample, it is possible that all of these components would be removed before reaching the column, leading to inaccurate measurements of target compound concentrations. When extrapolating to global models, these errors would have a large effect on predictions. For these reasons, it was clear that a different method of removing water vapour was needed.

Alternative methods for removing water include freezing water out of the sample. However, the use of cryogenic cooling processes would not be a practical method of cooling the sample down, as the instrument will be located in a pressurized cabin, causing safety concerns for those in the cabin. Instead, a cold trap was designed using the Peltier effect to cool down a piece of glassware that the sample flowed through. The Peltier effect is one manifestation of the thermoelectric effect. A current is applied across a semiconductor, giving a change in temperature across the device. Therefore, Peltier devices can be used as a method to remove heat from an object. This is achieved by configuring the devices in such a way that the object is in good thermal contact with the cool side of the device, whilst the hot side of the device is in contact with a heat sink to remove the transferred heat.

In this case, the Peltier effect was used to cool down a glass cold finger (York glassware, UK), surrounded by a copper sheath, to improve heat conduction. This was done as copper is a much better heat conductor than glass. Therefore more uniform cooling would occur around the cold finger. Two 55.4W Peltier devices (Farnell, UK) were arranged in parallel, powered by a 12V DC supply. The configuration was such that the upper surface of the Peltier devices (in contact with the cold finger) was cooling, whilst the lower surface was heating. The lower surface was in contact with a fan cooled heat sink to dissipate the heat emitted by the lower surface of the Peltier devices. By constantly drawing heat away from the lower side of the Peltier devices through the heat sink, it was possible to cool the cold finger to well below 0°C. Figure 3 shows the set up of the cold trap.

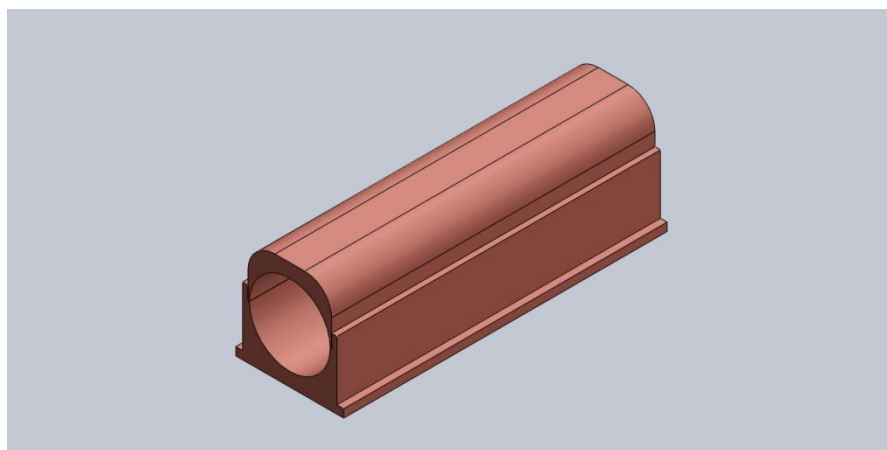
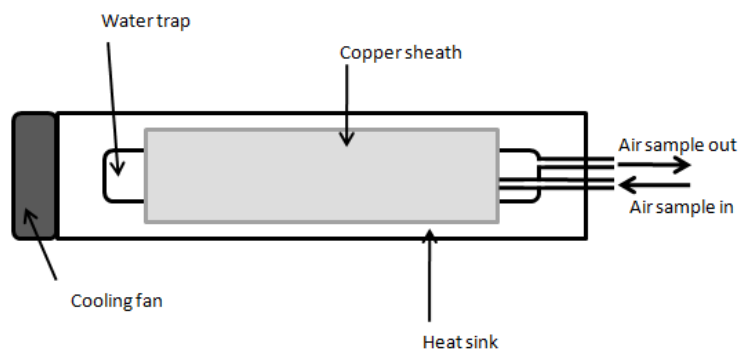
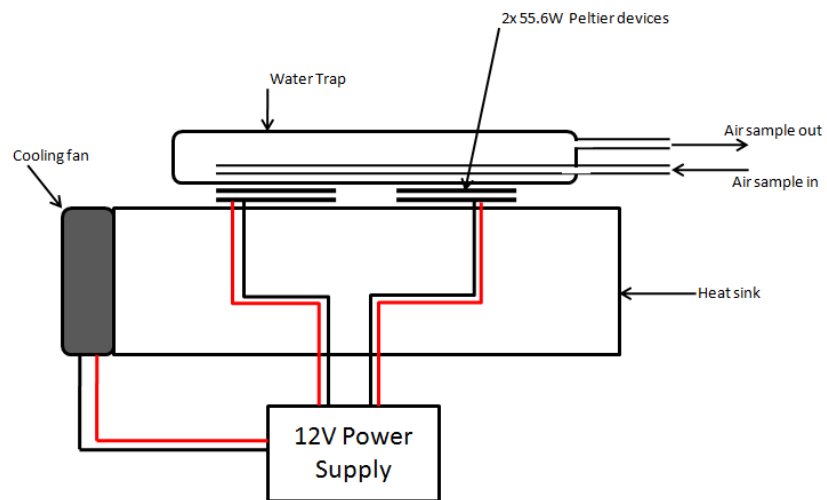


Figure 4.4: Schematic diagrams of the cold trap showing (top) the Peltier devices and power supply from a side on view, (middle) the cold trap inside the copper sheath from a bird's eye view and (bottom) a CAD image of the copper sheath

In an attempt to further increase the amount of cooling experienced by the cold trap, insulating foam was attached around the copper sheath. In order to test the validity of the cold trap, it must have been capable of reaching temperatures low enough for water vapour to freeze out of the air sample. To test this, a thermocouple temperature probe was added to the top of the copper sheath, as this was assumed to be the warmest area. It was found that, with no sample running through the instrument, the thermocouple measured the temperature at -18°C , rising to -16°C with a flow through the system.

To test the viability of the cold trap, an analysis of analyte selectivity was carried out. Several different sample types were passed through the water trap and subsequently analysed by the GC/MS. The first test to be carried out was to test the ability of the cold trap to remove water from a sample. To this end, laboratory air was used. The humidity was measured at between 55.2% and 91.7% on the days of the tests (University of York, Electronics Department Weather Station). The method of analysis was to quantify the baseline counts of the chromatograms. If this seemed fairly low, and expected compounds such as acetone, isoprene and toluene were present with an acceptable degree of resolution, the cold trap was deemed to have removed water vapour from the sample. In addition, ice was expected to build up inside the cold trap.

The second step in analysing the viability of the cold trap was to ensure the glassware or surrounding fittings were not introducing any impurities. Zero air (BOC, UK) was passed through the cold trap to detect for impurities. The zero air contained less than 1 ppm of hydrocarbons. A hydrocarbon scrubber was attached to the cylinder, removing any remaining hydrocarbons. As a final precaution, the zero air was analysed using a separate GC/FID instrument, confirming the absence of any impurities in the cylinder or scrubber. Therefore, any peaks present in the chromatogram must have been caused by an impurity

in the line. As the only variable was the inclusion/exclusion of the cold trap, any impurities must have originated from here.

The final step in analysing the cold trap was to pass a gas standard of OVOCs through the trap (NPL, UK). This was to ensure the trap was not removing any polar compounds from the sample. Table 4.1 shows the compounds included in the OVOC gas standard, along with concentrations. A fixed amount (5 μ L) of deuterated toluene was added to each sample as a method of comparison.

Table 4.1: Compounds in the OVOC gas standard used in testing the various sample drying methods.

Compound	Concentration (ppmv)
n-butane	0.57
acetaldehyde	0.53
methanol	0.55
ethanol	0.54
acetone	0.54
methyl acetate	0.54
methacrolein	0.53
1-propanol	0.54
butanal	0.52
methyl vinyl ketone	0.48
2-methyl-3-butene-2-ol	0.54
1-butanol	0.53
toluene	0.52
hexanal	0.47
benzaldehyde	0.54

4.3. Results and Discussion

As highlighted above, the first step in analysing the cold trap was to ensure it was removing water vapour from the sample in an effective enough way. This was examined by lowering the temperature of the sample to around -16°C. It was confirmed that water was indeed freezing out of the air sample in two ways. Firstly, ice crystals could be seen forming on the

inside of the glassware. Secondly, the chromatograms recorded in this experiment show a much cleaner baseline than those from the BORTAS field campaign where no sample drying was carried out. This is especially obvious when studying the region between 0.4 minutes and 0.9 minutes.

Carbon tetrachloride (CCl_4) was used as an internal standard to compare the quality of peak shapes between chromatograms from the BORTAS field campaign, and York laboratory air, where the Peltier water trap was included in the sample line. Figure 4.5 shows how the peak shapes vary. The peak from the BORTAS data is wider than that from the laboratory air, and in addition, shows the start of a split peak forming. The extracted ions shown in both chromatograms were 117 and 119 amu.

In addition, Figure 4.6 shows the peak shapes of toluene collected during BORTAS and compared to data from York laboratory air. As can be seen, the extracted ion (91) from BORTAS shows a much more distorted peak with a wider variety of retention times, whereas, where water is excluded in York laboratory air, the peak is much more concentrated, and therefore easier to quantify. Based on this evidence we conclude that the cold finger was indeed removing water from the sample, reducing the baseline noise, leading to improved resolution and compound identification.

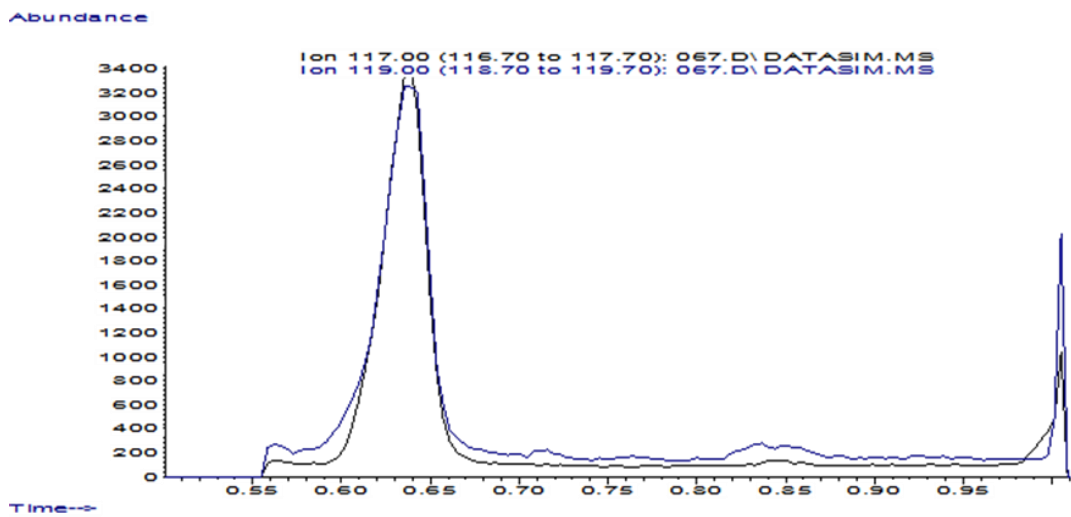
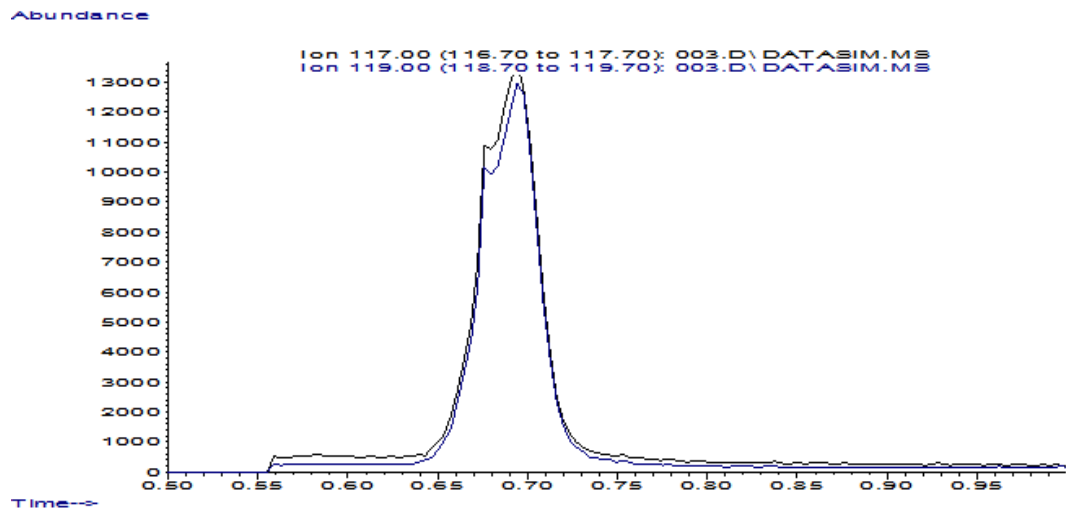


Figure 4.5: Chromatograms showing (a) a split CCl_4 peak with a less well defined peak shape from the BORTAS field campaign (b) a CCl_4 peak from laboratory air whilst using the cold trap to remove water.

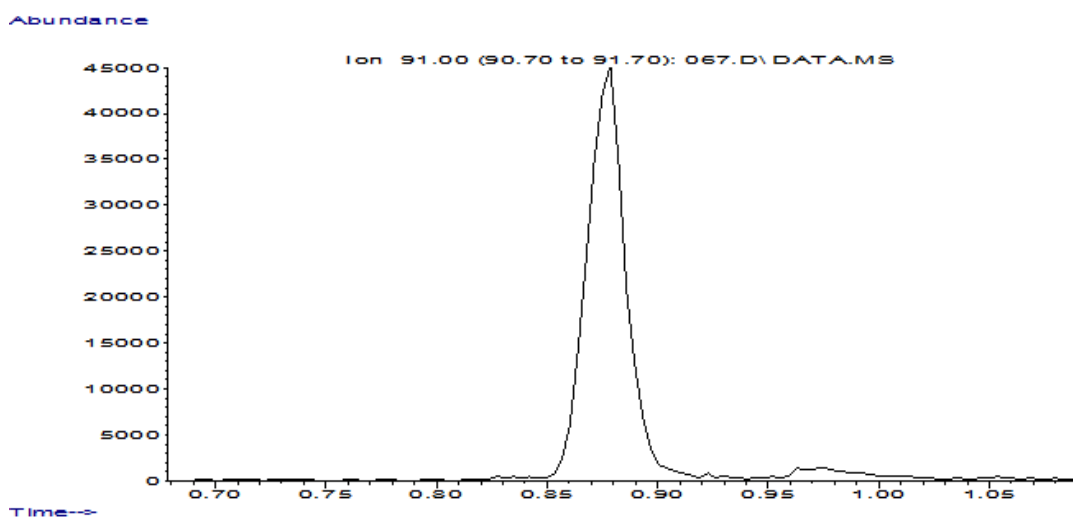
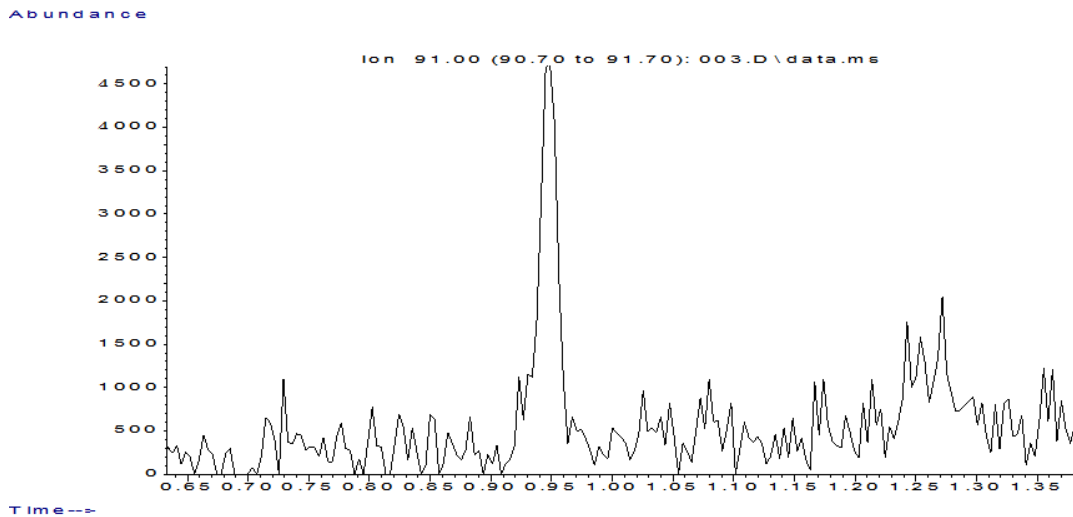


Figure 4.6: Chromatograms showing (a) toluene peak extracted from the BORTAS data, showing poor peak shape, and (b) toluene peak extracted from York laboratory air data showing a much improved peak shape

The next step in the analysis of the cold trap was to determine whether or not the cold trap was introducing any impurities to the sample. As stated, one of the reasons the use of the Nafion drying unit was removed from the sample line was that researchers on the aircraft thought it could be the source of impurities seen in the chromatograms. Therefore, it was crucial that the cold trap did not also introduce impurities. To test this, zero air was passed through the cold trap. The Zero air used contained less than 1 ppm of all hydrocarbons. A hydrocarbon trap was also fitted in the sample line so no VOCs would have adsorbed onto

the thermal desorption trap. Figure 4.7 below shows chromatograms of zero air using both drying methods. The two chromatograms have been overlaid showing the presence of an impurity in the Nafion chromatogram that is not present in the cold trap chromatogram. It is also important to note that the baseline of chromatogram taken using the cold trap is improved when compared to that of the Nafion dryer. In addition, Figure 4.8 shows the mass spectrum of the major impurity peak that is present in many of the chromatograms when Nafion is included in the sample line.

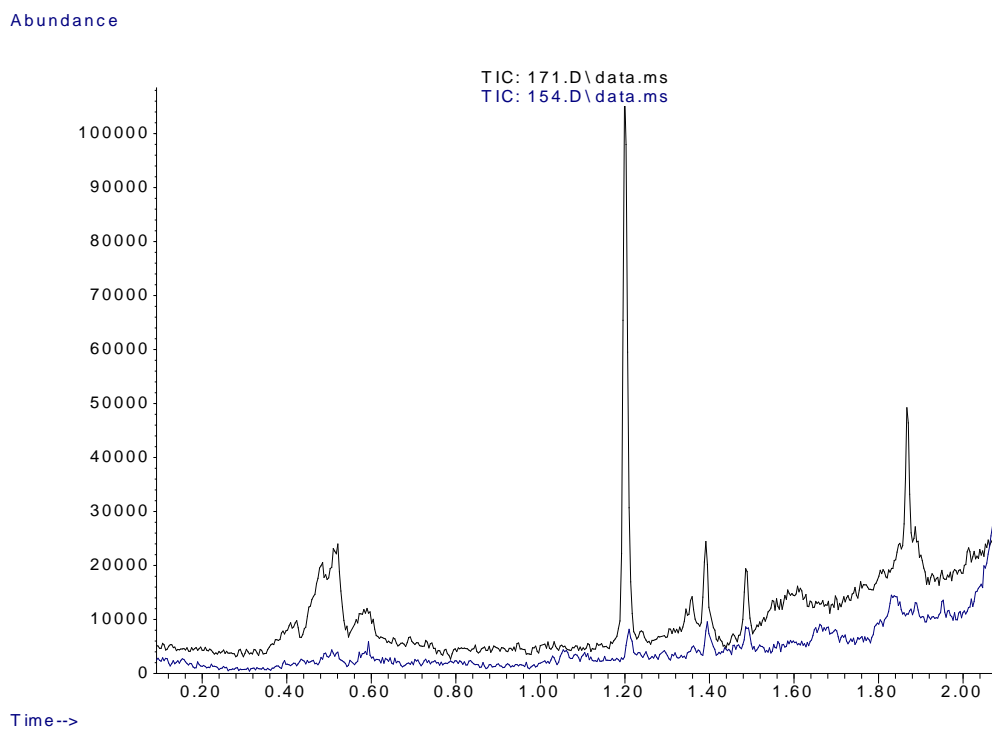


Figure 4.7: Showing the baselines of chromatograms taken when the Nafion dryer was included in the sample line (black) and when the cold trap was included in the sample line (blue).

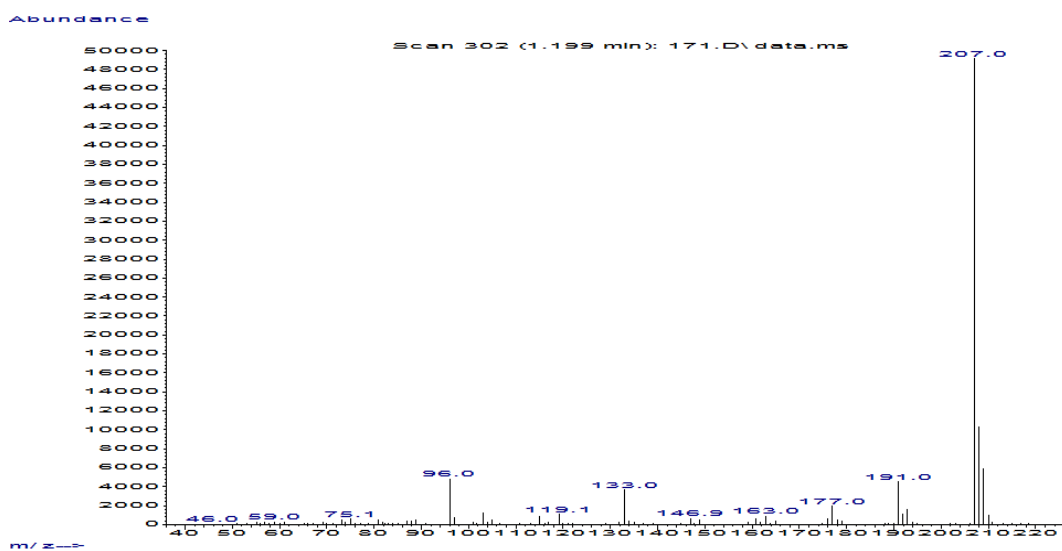


Figure 4.8: Mass spectrum of the major impurity peak when the Nafion dryer was added to the sample line

The chromatogram corresponding to the Nafion dryer (black) shows a large impurity peak at retention time 1.2 minutes. By comparison, this is absent in the chromatogram corresponding to the cold trap (blue). From this, the conclusion can be made that (a) the Nafion dryer was indeed introducing impurities to the sample whilst on the BORTAS campaign, potentially having a negative effect on data, by interfering with surrounding peaks, and (b) that the cold trap does not introduce impurities, making the cold trap the preferred method of removing water vapour from the sample.

The final step in analysing the two sample drying methods was to test their affinity with polar compounds. The OVOC gas standard was analysed using both drying methods. It should be noted that not all compounds present in the OVOC standard could be identified in the chromatogram, as the mass spectrometer was programmed to detect compounds with a molecular weight above 55 amu. This excludes lightweight VOCs such as methane, ethane and propane derivatives. Figure 6 shows the chromatograms produced with the Nafion dryer (a) and with the cold trap (b). It can be seen that the cold trap allows through many more compounds than the Nafion dryer, particularly low weight OVOCs. Polar species with a low molecular mass are present in chromatogram (b) but are absent from the sample in chromatogram (a). Chromatogram (b), where the cold trap was used, shows the following compounds: acetone, propanal, methyl acetate, methacrolein, methyl vinyl ketone, 2-methyl-3-buten-2-ol, butanol, hexanal and benzaldehyde. In contrast, chromatogram (a), where the Nafion dryer was used, shows only methacrolein, methyl vinyl ketone, hexanal and benzaldehyde. The first eluting peak on chromatogram (a) (retention time ~0.45 minutes) cannot be identified by the software. On extracting particular ions, it appears that many compounds are eluting together. However, the molecular structures of these compounds were not present in the gas standard. The conclusion drawn from this is that the C-F bonds on the Nafion membrane are reacting with polar regions on the OVOCs, causing a change in molecular structure.

In addition, the ratio of the benzaldehyde: deuterated toluene peak areas are also of interest. The benzaldehyde peak has a 16.6% lower peak area in chromatogram (a) compared to that of the benzaldehyde peak in chromatogram (b) (relative to the peak areas of the deuterated toluene). This demonstrates further that the Nafion dryer was removing compounds from the sample.

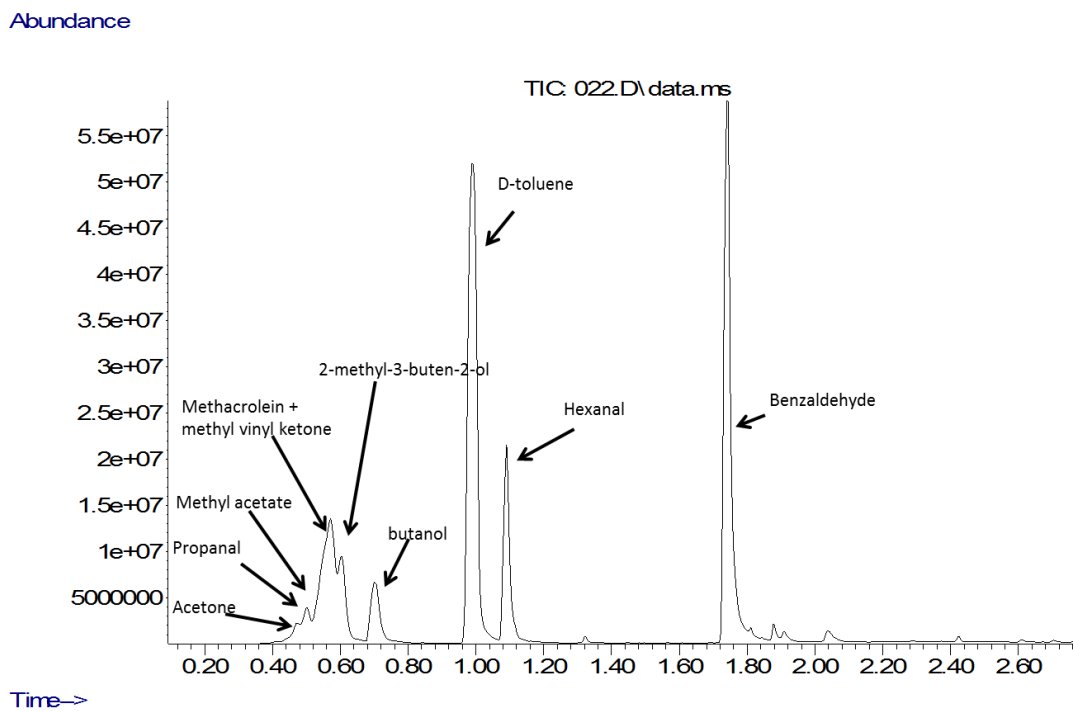
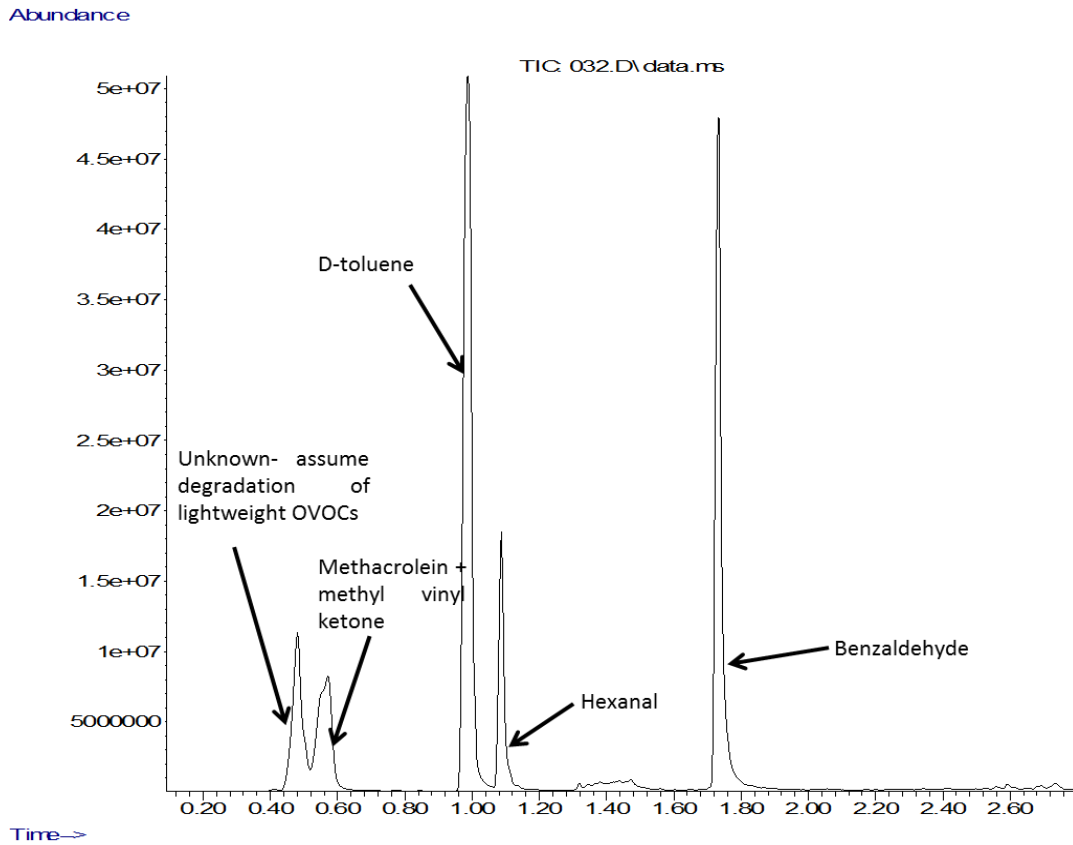


Figure 4.9: Assigned chromatograms of the OVOC standard through (a) the Nafion dryer, and (b) the cold trap. The software is capable of determining many more compounds when the cold trap is used.

4.4. Conclusion

After analysing the two sample drying methods, the results confirmed that the cold trap removes water vapour from the sample, with fewer negative consequences than the Nafion membrane in this application.

The Nafion dryer was removed from the sample line during the BORTAS field study as it was thought that it was having a detrimental effect on the quality of the chromatograms. It was thought that 1) it was adding impurities to the sample and 2) it was interacting unfavourably with polar compounds within the sample. To this end, the cold trap was constructed, using Peltier devices to freeze water vapour out of the sample. The cold trap was then analysed to ensure the problems created by the use of the Peltier devices had been averted. Firstly, the cold trap was shown to remove water vapour in an efficient manner when compared to the BORTAS data, where no sample drying occurred. This was shown by demonstrating the lower, less noisy baseline in comparison to the BORTAS data when analysing laboratory air. Secondly, the cold trap was shown to introduce fewer (if any) impurities into the sample than the Nafion dryer. Finally, an analysis of an OVOC gas standard showed that the Nafion dryer was having an adverse effect on the sample by interacting with polar compounds passing through. The cold trap eliminated this effect, and many more compounds could be seen in the chromatogram. For these reasons, the cold trap will be used as the main method of excluding water from the column and mass spectrometer for the foreseeable future.

The instrument was dispatched to Porto Velho, Brazil, with the objective of monitoring the output of forest fire plumes from the Amazon rainforest as part of the SAMBBA field campaign. The modifications to the method discussed here were implemented for the duration of the campaign. Presented below are some preliminary results to show the instruments response to monoterpenes and other VOCs (Figures 4.10 – 4.13).

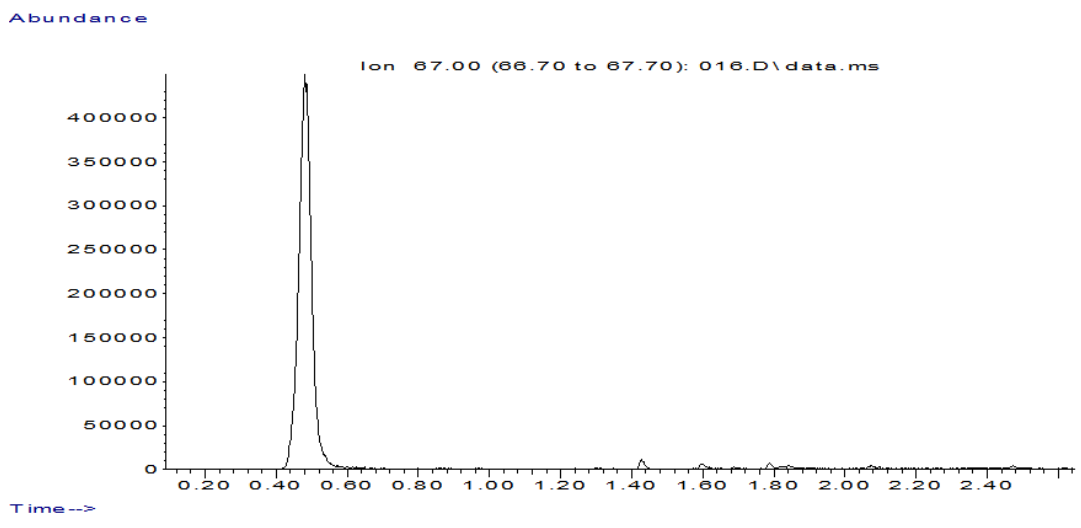


Figure 4.10: Sample chromatogram from SAMBBA, showing extracted isoprene

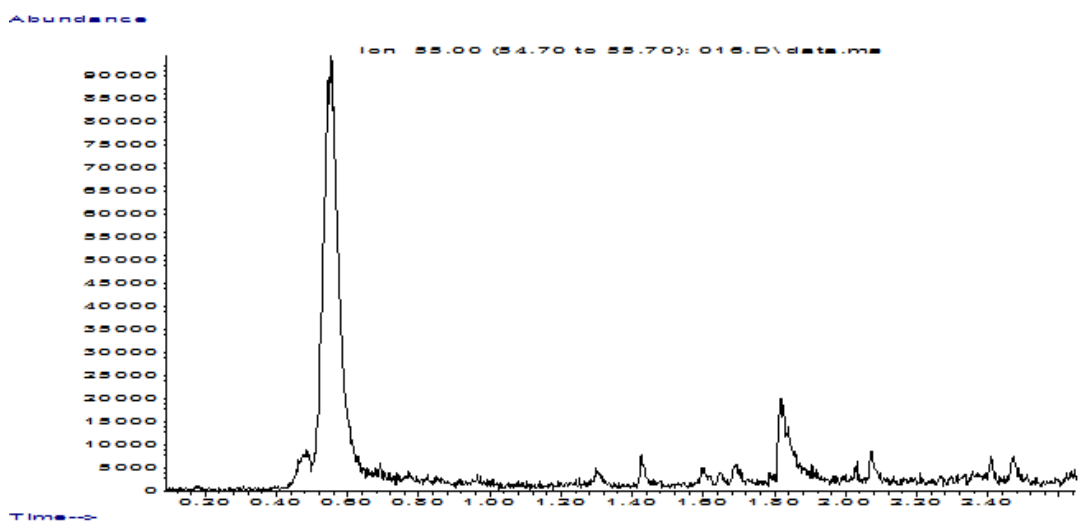


Figure 4.11: Sample chromatogram from SAMBBA, showing extracted methylvinyl ketone

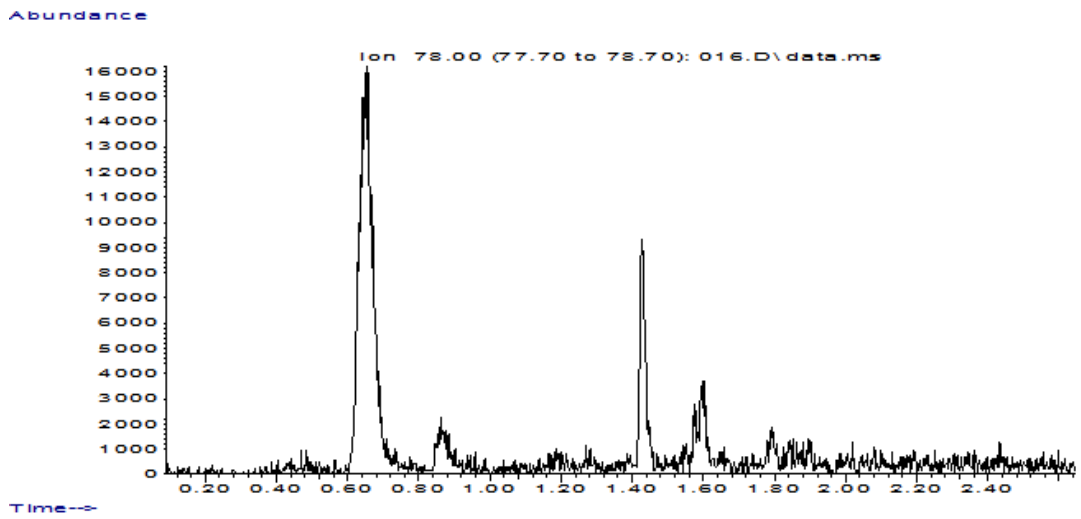


Figure 4.12: Sample chromatogram from SAMBBA, showing extracted benzene

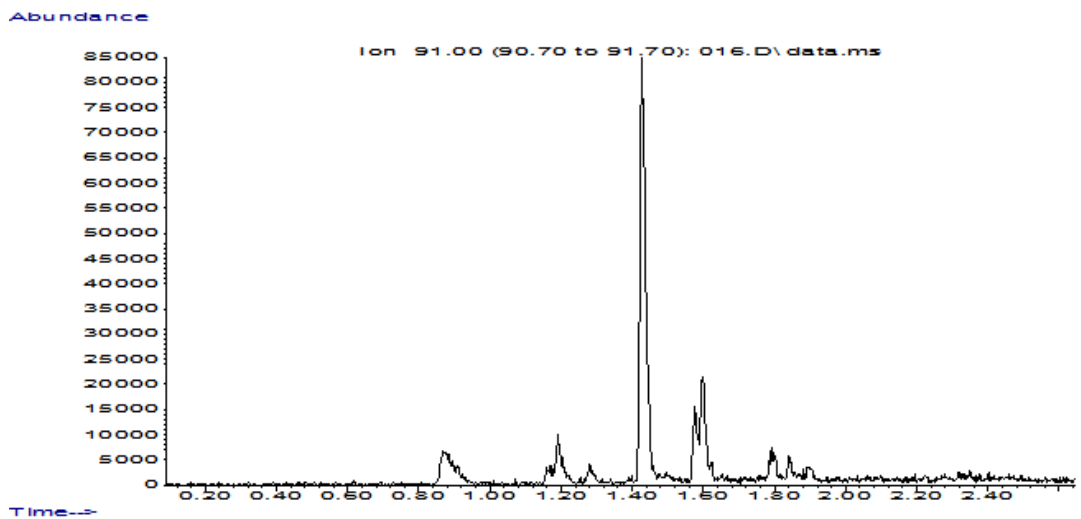


Figure 4.13: Sample chromatogram from SAMBBA, showing extracted toluene

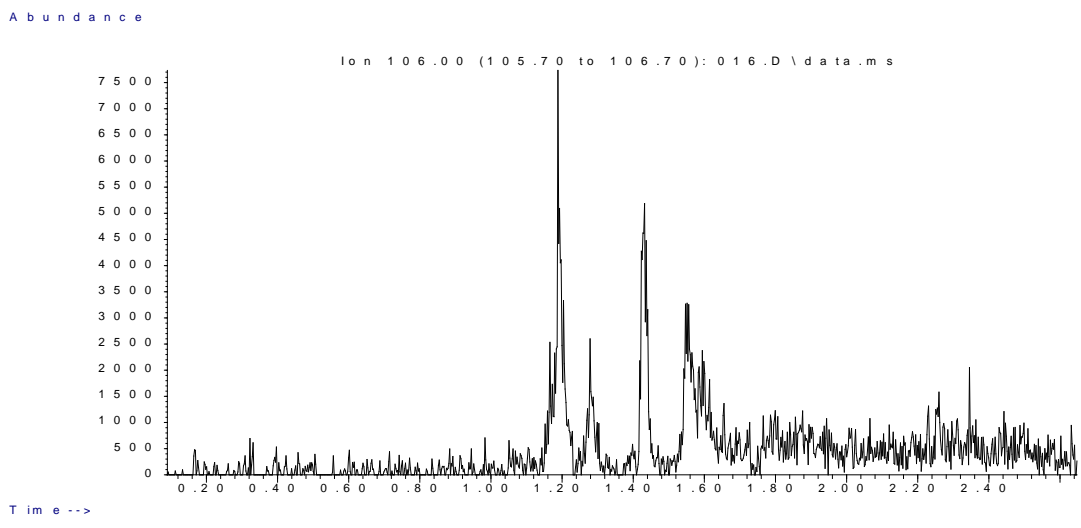


Figure 4.14: Sample chromatogram from SAMBBA, showing extracted *m-p-* and *o-* xylene

These chromatograms show that many monoterpenes are able to be identified using the instrument in this configuration, to a high degree of accuracy and speed. Figure 4.15 and Figure 4.16 show some preliminary results of how the concentrations of several compounds vary over a flight. In general, the flights moved in and out of plumes and this can be clearly seen in Figure 4.15 as isoprene concentrations increase dramatically between 15:21 and 16:33 on the day of the flight. This is match by the methylvinyl ketone and methacrolein, both of which are products of photolysis of isoprene.

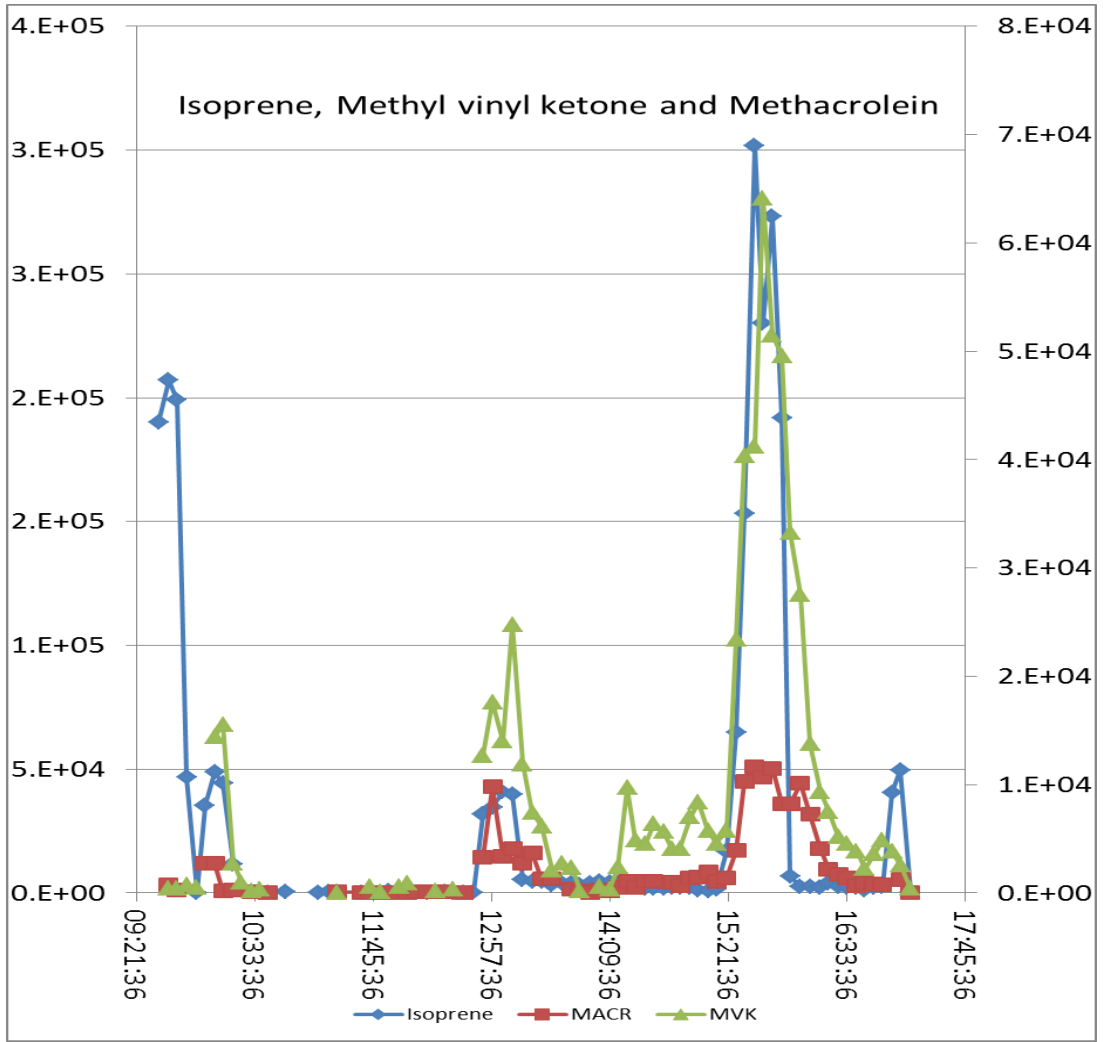


Figure 4.15: Changing concentrations of isoprene, methylvinyl ketone and methacrolein during a flight

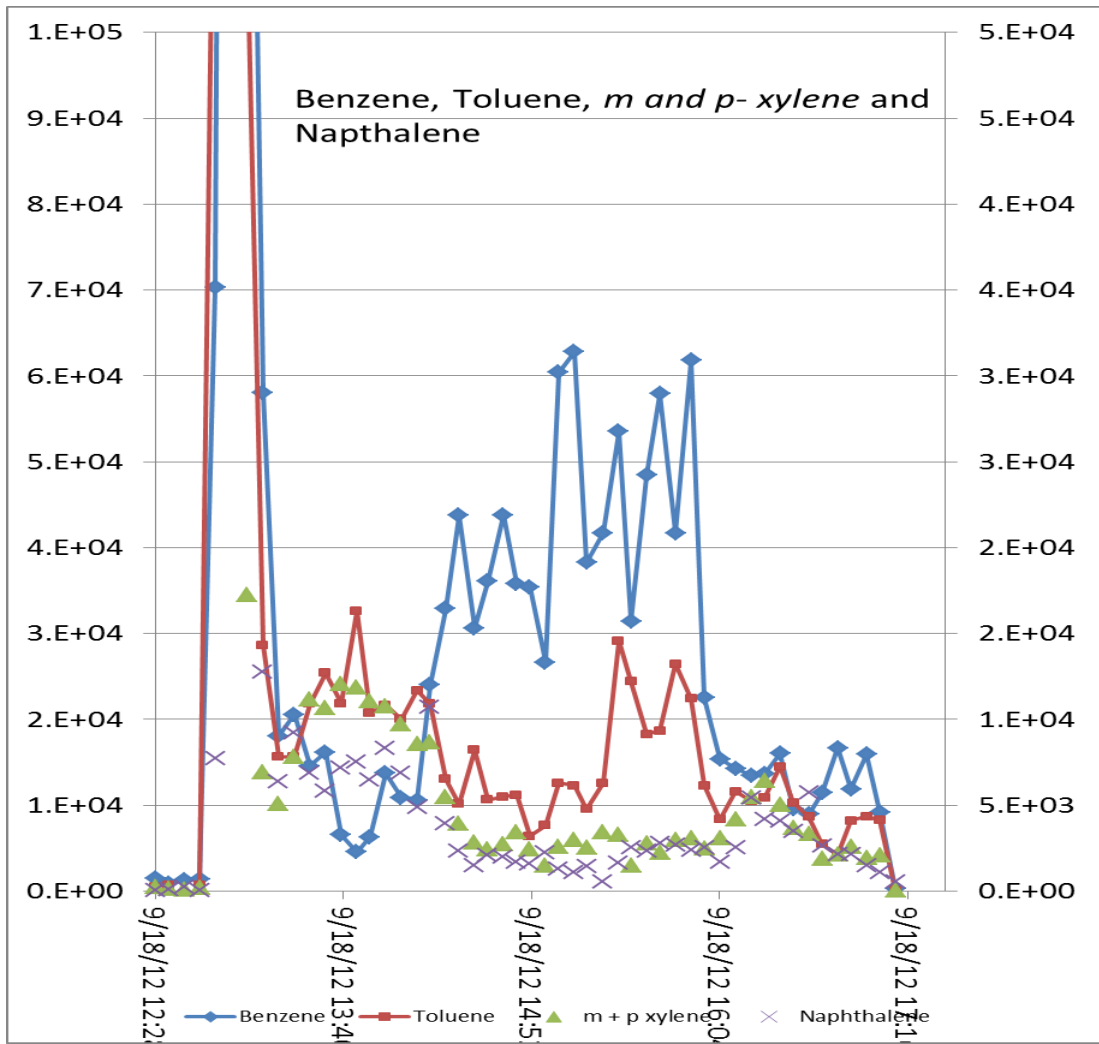


Figure 4.16: Changing concentrations of benzene, toluene, *m*- and *p*-xylene and naphthalene during a flight

CHAPTER 5. CONCLUSION

This project was undertaken in order to improve the spatial resolution of the University of York airborne GC/MS. This was done by optimising the temperature program so the GC spent less time in an idle state to enable more analyses of tropospheric VOCs per flight.

The cool down times for an Agilent 6850 GC oven were measured from and to a range of initial and final temperatures, in order to identify temperature programs that have a shorter cool down time than the currently used program (initial temperature: 40 °C, final temperature: 130 °C).

Chromatographic resolution data was also collected for all the temperature ranges. This was carried out by analysing a multi-component gas standard at all temperature ranges. From analysis of the data, it was noted that at higher initial temperatures, peaks indicating the presence of ethyl benzene and *para*- and *meta*-xylene started to coelute from the column, to the point where the analysis software could not identify the two peaks. At the highest initial temperatures, these peaks could not even be qualitatively identified manually. However, a certain degree of coelution is not always a disadvantage as it is not always necessary to have all peaks resolved to the baseline, especially if this saves on analysis time. The final temperature was seen to not have as large an effect on the cool down time as the initial temperature and an almost negligible effect on resolution. A higher final temperature enables compounds heavily retained by the column to elute, giving more information about heavier weight compounds. This can be varied based on the nature of each individual field campaign/laboratory analysis.

The resolution data and the cooling data were then compared to determine a range of temperatures at which the resolution of these two peaks was at an acceptable level, but

where the initial temperature led to a shorter cool down time. Raising the initial temperature was determined to have the largest effect on the cool down time, to the extent that an increase of 2-3 degrees can cause the cool down time to decrease by as much as ~30-40 seconds per analysis. A compromise between the two parameters was found for an initial temperature in the range of 42- 44 °C. This means that many more samples can be analysed per flight on board the BAe-146 aircraft, improving spatial resolution, and decreasing the cost-per-analysis.

In addition, from data acquired from the BORTAS field campaign, some data was lost due to water entering the traps and the GC column. Originally, a water trap using Nafion was used to remove water from samples. Laboratory tests showed that due to the high polarity of the Nafion membrane, polar compounds other than water were also being removed from samples. A new cold trap was therefore developed, using the Peltier effect to freeze water out of the incoming sample. This proved successful within the laboratory, and was used to a reasonable level of success on the SAMBBA field campaign in September 2012.

In order to further speed up the analysis time, the use of a resistively heated column will be investigated in the future and, should tests prove successful, this will be integrated into the instrument. In addition, a cryogenic liquid CO₂ cold trap will be introduced onto the head of the column to improve refocusing. These developments will be implemented for future campaigns where the instrument will be deployed on the aircraft.

The instrument was dispatched to Porto Velho, Brazil, with the objective of monitoring the output of forest fire plumes from the Amazon rainforest. The modifications to the method discussed here were implemented for the duration of the field campaign. Presented below are some preliminary results to show the instruments response to monoterpenes and other VOCs.

CHAPTER 6. APPENDIX 1

Presented here is the data acquired from experiments into the cool down times of the GC oven. The raw data has been averaged, and tabulated.

Table 6.1: Average time taken to cool down from 130 °C to a range of initial temperatures

Initial Temperature (°C)	Final Temperature (°C)	Time (Average) (s)
40	130	120.25
41	130	107.65
42	130	115.55
43	130	103.7
44	130	93.2
45	130	100.35
46	130	95.5
47	130	95.2
48	130	82.6
49	130	83.1
50	130	83.1
51	130	70.65
52	130	73.05
55	130	66.85
57	130	64.35
60	130	61.4
62	130	56.2
65	130	54.9

Table 6.2: Average time taken to cool down from 135 °C to a range of initial temperatures

Initial Temperature (°C)	Final Temperature (°C)	Time (Average) (s)
40	135	127.7
41	135	88.0
42	135	117.7
43	135	89.0
44	135	89.5
45	135	110.6
46	135	90.5
47	135	106.1
48	135	91.5
49	135	92.0
50	135	89.5
51	135	93.0
52	135	75.6
55	135	73.0
57	135	68.1
60	135	64.3
62	135	62.1
65	135	59.1

Table 6.3: Average time taken to cool down from 140 °C to a range of initial temperatures

Initial Temperature (°C)	Final Temperature (°C)	Time (Average) (s)
40	140	119.65
41	140	113.95
42	140	118.95
43	140	103.6
44	140	107.2
45	140	112.65
46	140	103.05
47	140	114.6
48	140	92.6
49	140	87.7
50	140	99.45
51	140	80.05
52	140	82.65
55	140	76.1
57	140	69.65
60	140	64.95
62	140	63.25
65	140	59.45

Table 6.4: Average time taken to cool down from 145 °C to a range of initial temperatures

Initial Temperature (°C)	Final Temperature (°C)	Time (Average) (s)
40	145	125.4
41	145	93.0
42	145	120.2
43	145	94.0
44	145	94.5
45	145	121.1
46	145	95.5
47	145	107.7
48	145	96.5
49	145	97.0
50	145	99.8
51	145	98.0
52	145	92.3
55	145	78.7
57	145	73.2
60	145	76.4
62	145	64.6
65	145	64.3

Table 6.5: Average time taken to cool down from 150 °C to a range of initial temperatures

Initial Temperature (°C)	Final Temperature (°C)	Time (Average) (s)
40	150	131.9
41	150	124.15
42	150	123.1
43	150	111.1
44	150	117.2
45	150	125.05
46	150	109.75
47	150	111.8
48	150	97.6
49	150	95.1
50	150	97.75
51	150	87.7
52	150	86.3
55	150	81.6
57	150	76.75
60	150	78.9
62	150	72
65	150	66

Table 6.6: Average time taken to cool down from 155 °C to a range of initial temperatures

Initial Temperature (°C)	Final Temperature (°C)	Time (Average) (s)
40	155	135.9
41	155	98.0
42	155	128.8
43	155	99.0
44	155	99.5
45	155	133.9
46	155	100.5
47	155	122.9
48	155	101.5
49	155	102.0
50	155	95.8
51	155	103.0
52	155	90.9
55	155	88.0
57	155	80.5
60	155	81.5
62	155	73.6
65	155	68.9

Table 6.7: Average time taken to cool down from 160 °C to a range of initial temperatures

Initial Temperature (°C)	Final Temperature (°C)	Time (Average) (s)
40	160	144.7
41	160	130.9
42	160	135.2
43	160	118.5
44	160	121.6
45	160	128.8
46	160	117.7
47	160	121.7
48	160	103.6
49	160	103.5
50	160	99.1
51	160	93.8
52	160	91.8
55	160	91.3
57	160	82.6
60	160	82.7
62	160	74.6
65	160	71.0

Table 6.8: Average time taken to cool down from 165 °C to a range of initial temperatures

Initial Temperature (°C)	Final Temperature (°C)	Time (Average) (s)
40	165	154.5
42	165	148.3
43	165	104.0
44	165	104.5
45	165	133.8
46	165	105.5
47	165	128.8
48	165	106.5
49	165	107.0
50	165	103.0
51	165	108.0
52	165	100.8
55	165	95.7
57	165	84.0
60	165	88.3
62	165	78.2
65	165	72.8

Table 6.9: Average time taken to cool down from 170 °C to a range of initial temperatures

Initial Temperature (°C)	Final Temperature (°C)	Time (Average) (s)
40	170	162.9
42	170	152.9
44	170	107.0
45	170	142.9
46	170	108.0
47	170	129.2
48	170	109.0
49	170	109.5
50	170	112.1
51	170	110.5
52	170	104.9
55	170	99.7
57	170	91.7
60	170	86.4
62	170	80.4
65	170	74.0

Table 6.10: Average time taken to cool down from 175 °C to a range of initial temperatures

Initial Temperature (°C)	Final Temperature (°C)	Time (Average) (s)
40	175	169.9
42	175	151.5
45	175	145.8
46	175	110.5
47	175	131.1
48	175	111.5
49	175	112.0
50	175	115.9
51	175	113.0
52	175	102.6
55	175	102.6
57	175	96.2
60	175	94.1
62	175	83.7
65	175	77.1

Table 6.11: Average time taken to cool down from 180 °C to a range of initial temperatures

Initial Temperature (°C)	Final Temperature (°C)	Time (Average) (s)
40	180	175.5
42	180	160.0
45	180	145.0
47	180	142.9
48	180	114.0
49	180	114.5
50	180	110.9
51	180	115.5
52	180	108.6
55	180	101.6
57	180	97.6
60	180	94.0
62	180	93.4
65	180	77.8

Table 6.12: Average time taken to cool down from 185 °C to a range of initial temperatures

Initial Temperature (°C)	Final Temperature (°C)	Time (Average) (s)
40	185	176.3
42	185	169.1
45	185	158.1
47	185	156.8
50	185	121.5
52	185	114.7
55	185	105.4
57	185	104.9
60	185	99.6
62	185	87.6
65	185	79.1

Table 6.13: Average time taken to cool down from 190 °C to a range of initial temperatures

Initial Temperature (°C)	Final Temperature (°C)	Time (Average) (s)
40	190	183.9
42	190	170.2
45	190	162.0
47	190	135.4
50	190	122.6
52	190	114.0
55	190	109.6
57	190	107.5
60	190	101.5
62	190	94.2
65	190	87.1

Table 6.14: Average time taken to cool down from 195 °C to a range of initial temperatures

Initial Temperature (°C)	Final Temperature (°C)	Time (Average) (s)
40	195	192.2
42	195	178.4
45	195	164.3
47	195	138.2
50	195	124.7
52	195	116.5
55	195	115.4
57	195	111.3
60	195	108.4
62	195	94.7
65	195	87.5

Table 6.15: Average time taken to cool down from 200 °C to a range of initial temperatures

Initial Temperature (°C)	Final Temperature (°C)	Time (Average) (s)
40	200	194.7
42	200	182.4
45	200	170.2
47	200	144.0
50	200	136.5
52	200	118.9
55	200	113.2
57	200	111.4
60	200	106.2
62	200	102.1
65	200	86.3

CHAPTER 7. APPENDIX 2

Presented here is the data acquired from experiments into the effects of a variation in initial and final temperatures on chromatographic resolution.

Table 7.1: Resolution of the ethyl benzene and o- and p-xylene peaks where the initial temperature is varied and the final temperature is 130 °C.

Initial Temperature (°C)	Final Temperature (°C)	Resolution
40	130	1.800
41	130	2.240
42	130	1.543
43	130	2.154
45	130	1.677
47	130	1.625
50	130	1.455
52	130	1.394
55	130	1.235
57	130	1.273
60	130	0.718

Table 7.2: Resolution of the ethyl benzene and o- and p-xylene peaks where the initial temperature is varied and the final temperature is 135 °C.

Initial Temperature (°C)	Final Temperature (°C)	Resolution
40	135	1.867
41	135	2.154
42	135	1.543
43	135	1.929
45	135	1.576
47	135	1.471
50	135	1.278
52	135	1.243
55	135	1.053
57	135	0.974
60	135	1.389

Table 7.3: Resolution of the ethyl benzene and o- and p-xylene peaks where the initial temperature is varied and the final temperature is 140 °C.

Initial Temperature (°C)	Final Temperature (°C)	Resolution
40	140	1.421
41	140	2.154
42	140	1.572
43	140	2.231
45	140	1.576
47	140	1.412
50	140	1.371
52	140	1.243
55	140	1.167
57	140	1.143
60	140	0.927

Table 7.4: Resolution of the ethyl benzene and o- and p-xylene peaks where the initial temperature is varied and the final temperature is 145 °C.

Initial Temperature (°C)	Final Temperature (°C)	Resolution
40	145	1.647
41	145	2.320
42	145	1.688
43	145	2.000
45	145	1.529
47	145	1.500
50	145	1.412
52	145	1.257
55	145	1.200
57	145	0.909
60	145	0.732

Table 7.5: Resolution of the ethyl benzene and o- and p-xylene peaks where the initial temperature is varied and the final temperature is 150 °C.

Initial Temperature (°C)	Final Temperature (°C)	Resolution
40	150	2.077
41	150	2.240
42	150	2.077
43	150	1.862
45	150	1.926
47	150	1.724
50	150	1.125
52	150	1.586
55	150	1.313
57	150	1.187
60	150	1.188

Table 7.6: Resolution of the ethyl benzene and o- and p-xylene peaks where the initial temperature is varied and the final temperature is 155 °C.

Initial Temperature (°C)	Final Temperature (°C)	Resolution
40	155	2.000
41	155	2.154
42	155	1.800
43	155	1.862
45	155	1.667
47	155	0.878
50	155	1.484
52	155	1.353
55	155	1.313
57	155	1.176
60	155	0.895

Table 7.7: Resolution of the ethyl benzene and o- and p-xylene peaks where the initial temperature is varied and the final temperature is 160 °C.

Initial Temperature	Final Temperature	Resolution
40	160	1.862
41	160	2.240
42	160	2.000
43	160	2.154
45	160	1.667
47	160	1.724
50	160	1.500
52	160	1.394
55	160	1.273
57	160	1.118
60	160	0.789

Table 7.8: Resolution of the ethyl benzene and o- and p-xylene peaks where the initial temperature is varied and the final temperature is 165 °C.

Initial Temperature (°C)	Final Temperature (°C)	Resolution
40	165	2.000
41	165	2.154
42	165	1.667
43	165	2.074
45	165	1.667
47	165	1.724
50	165	1.438
52	165	1.438
55	165	1.167
57	165	1.000
60	165	1.189

Table 7.9: Resolution of the ethyl benzene and o- and p-xylene peaks where the initial temperature is varied and the final temperature is 170 °C.

Initial Temperature (°C)	Final Temperature (°C)	Resolution
40	170	2.000
41	170	2.074
42	170	1.857
45	170	1.625
47	170	1.667
50	170	1.533
52	170	1.394
55	170	1.235
57	170	1.226
60	170	1.143

Table 7.10: Resolution of the ethyl benzene and o- and p-xylene peaks where the initial temperature is varied and the final temperature is 175 °C.

Initial Temperature (°C)	Final Temperature (°C)	Resolution
40	175	2.000
41	175	1.697
42	175	2.000
45	175	1.667
47	175	1.667
50	175	1.533
52	175	1.294
55	175	1.235
57	175	1.187
60	175	2.654

Table 7.11: Resolution of the ethyl benzene and o- and p-xylene peaks where the initial temperature is varied and the final temperature is 180 °C.

Initial Temperature (°C)	Final Temperature (°C)	Resolution
40	180	2.000
41	180	2.333
42	180	1.926
45	180	1.733
47	180	1.667
50	180	1.437
52	180	1.333
55	180	1.250
57	180	3.692
60	180	3.264

Table 7.12: Resolution of the ethyl benzene and o- and p-xylene peaks where the initial temperature is varied and the final temperature is 185 °C.

Initial Temperature (°C)	Final Temperature (°C)	Resolution
40	185	1.929
41	185	2.000
42	185	1.929
45	185	1.667
47	185	1.625
50	185	1.455
52	185	1.333
55	185	1.200
57	185	1.176
60	185	1.032

Table 7.13: Resolution of the ethyl benzene and o- and p-xylene peaks where the initial temperature is varied and the final temperature is 190 °C.

Initial Temperature (°C)	Final Temperature (°C)	Resolution
40	190	1.933
41	190	2.000
42	190	1.647
45	190	1.588
47	190	1.444
50	190	1.333
52	190	1.211
55	190	1.000
57	190	0.727
60	190	2.459

Table 7.14: Resolution of the ethyl benzene and o- and p-xylene peaks where the initial temperature is varied and the final temperature is 195 °C.

Initial Temperature (°C)	Final Temperature (°C)	Resolution
40	195	1.750
41	195	2.154
42	195	1.697
45	195	1.543
47	195	1.486
50	195	1.263
52	195	1.150
55	195	0.565
57	195	0.976
60	195	2.542

Table 7.15: Resolution of the ethyl benzene and o- and p-xylene peaks where the initial temperature is varied and the final temperature is 200 °C.

Initial Temperature (°C)	Final Temperature (°C)	Resolution
40	200	1.813
41	200	1.647
42	200	1.871
45	200	1.444
47	200	1.444
50	200	1.389
52	200	1.231
55	200	0.800
57	200	0.780
60	200	2.552

LIST OF ABBREVIATIONS

amu	Atomic Mass Units
	Boreal forest fires on Tropospheric oxidants over the Atlantic using Aircraft
BORTAS	and Satellites
CFC	Chloro Fluoro Carbon
d.f.	film thickness
ECD	Electron capture Detector
EPC	Electronic pressure controller
FID	flame ionisation detector
GC	gas chromatography
GC/MS	Gas Chromatography/Mass Spectrometry
HCFC	Hydro Chloro Fluoro Carbon
HETP	Height Equivalent of theoretical plates
HFC	Hydro Fluoro Carbon
i.d.	internal diameter
m/z	mass to charge ratio
MS	mass spectrometry
ng	nanograms
PID	photoionisation detector
PMD	Photomultiplier Detector
ppb	parts per billion
ppm	parts per million
ppt	parts per trillion
PTFE	Polytetrafluoroethylene
PTR	Proton transfer reaction
SAMBBA	South American Biomass Burning Analysis
SOA	Secondary Organic Aerosol
TDU	Thermal Desorption Unit
TOF	Time of Flight
UPS	Uninterrupted Power Supply
VOCs	Volatile Organic Compounds

REFERENCES

- Abraham, M. H., Poole, C. F., & Poole, S. K. (1999). *Classification of stationary phases and other materials by gas chromatography*. *Journal of Chromatography A* (Vol. 842, pp. 79–114). doi:10.1016/S0021-9673(98)00930-3
- Agilent Technologies. (2007). How can I make my GC column last longer, 1–4.
- Andreae, M. O. (1997). Atmospheric Aerosols: Biogeochemical Sources and Role in Atmospheric Chemistry. *Science*, 276(5315), 1052–1058. doi:10.1126/science.276.5315.1052
- Atkinson, R. (2000). Atmospheric chemistry of VOCs and NOx. *Atmospheric Environment*, 34(12-14), 2063–2101. doi:10.1016/S1352-2310(99)00460-4
- Barletta, B., Meinardi, S., Simpson, I. J., Khwaja, H. a, Blake, D. R., & Rowland, F. S. (2002). Mixing ratios of volatile organic compounds (VOCs) in the atmosphere of Karachi, Pakistan. *Atmospheric Environment*, 36(21), 3429–3443. doi:10.1016/S1352-2310(02)00302-3
- Bartle, K., & Myers, P. (2002). Gas Chromatography. *Trends in Analytical Chemistry*, 21(5), 547. Retrieved from <http://www.ncbi.nlm.nih.gov/pubmed/22545724>
- Blumberg, L. M., & Klee, M. S. (2001). Quantitative comparison of performance of isothermal and temperature-programmed gas chromatography. *Journal of chromatography. A*, 933(1-2), 13–26. Retrieved from <http://www.ncbi.nlm.nih.gov/pubmed/11758743>
- Brown, R. H., & Purnell, C. J. (1979). Collection and analysis of trace organic vapour pollutants in ambient atmospheres; The performance of a TENAX-GC adsorbent tube. *Journal of Chromatography*, 178, 79–90.
- Crutzen, P. (1971). Ozone production rates in an oxygen-hydrogen-nitrogen oxide atmosphere. *Journal of Geophysical Research*, 76. Retrieved from <http://www.agu.org/pubs/crossref/1971/JC076i030p07311.shtml>
- Dandeneau, R. D., & Zerenner, E. H. (1979). An Investigation of Glasses for Capillary Chromatography, 2(June).
- Darnall, K., & Lloyd, A. (1976). Reactivity scale for atmospheric hydrocarbons based on reaction with hydroxyl radical. *Environmental Science & ...*. Retrieved from <http://pubs.acs.org/doi/abs/10.1021/es60118a008>
- Davies, N. W. (1990). Gas chromatographic retention indices of monoterpenes and sesquiterpenes on methyl silicone and carbowax 20M phases. *Journal of chromatography*, 503(1), 1–24. Retrieved from <http://cat.inist.fr/?aModele=afficheN&cpsid=19281088>

- Dessler, a. E., Zhang, Z., & Yang, P. (2008). Water-vapor climate feedback inferred from climate fluctuations, 2003–2008. *Geophysical Research Letters*, 35(20), 10–13. doi:10.1029/2008GL035333
- Desty, D. ., Haresnape, J. ., & Whyman, B. H. . (1960). Construction of Long Lengths of Coiled Glass Capillary. *Analytical Chemistry*, 32, 302–304.
- Dewulf, J., & Van Langenhove, H. (1999). Hydrocarbons in the atmosphere. *Environmental and Ecological Chemistry*, II. Retrieved from <http://www.springerlink.com/index/J47J550876618256.pdf>
- Fehsenfeld, F., Calvert, J., Fall, R., & Goldan, P. (1992). Emissions of volatile organic compounds from vegetation and the implications for atmospheric chemistry. *Global Biogeochemical*, 6(4), 389–430. Retrieved from <http://www.agu.org/pubs/crossref/1992.../92GB02125.shtml>
- German, a. L., Pfaffenberger, C. D., Thenot, J. P., Horning, M. G., & Horning, E. C. (1973). High resolution gas chromatography with thermostable glass open tubular capillary columns. *Analytical Chemistry*, 45(6), 930–935. doi:10.1021/ac60328a032
- Golay, M. J., & Desty, D. . (1958). Gas Chromatography. *Academic Press, New York*, 6.
- Graham, B. (2002). Water-soluble organic compounds in biomass burning aerosols over Amazonia1. Characterization by NMR and GC-MS. *Journal of Geophysical Research*, 107(D20). doi:10.1029/2001JD000336
- Graham, B. (2003). Organic compounds present in the natural Amazonian aerosol: Characterization by gas chromatography–mass spectrometry. *Journal of Geophysical Research*, 108(D24), 1–13. doi:10.1029/2003JD003990
- Guenther, A., Hewitt, C., & Erickson, D. (1995). A global model of natural volatile organic compound emissions. *Journal of geophysical ...*, 100(94), 8873–8892. Retrieved from <http://www.agu.org/pubs/crossref/1995/94JD02950.shtml>
- Hallquist, M. (2009). The formation, properties and impact of secondary organic aerosol: current and emerging issues. *Atmospheric Chemistry and Physics*, 9(November 2008), 5155–5236. Retrieved from <http://authors.library.caltech.edu/15129/>
- Harley, J., Nel, W., & Pretorius, V. (1958). Flame ionization detector for gas chromatography. *Nature*, 181, 177. Retrieved from <http://adsabs.harvard.edu/abs/1958Natur.181..760M>
- Haubold, H., Vad, T., Jungbluth, H., & Hiller, P. (2001). Nano structure of NAFION : a SAXS study. *Electrochimica Acta*, 46, 1559–1563.
- Held, I., & Soden, B. (2000). Water Vapor Feedback and Global Warming 1. *Annual Review of Energy and the Environment*, 25, 441–75. Retrieved from <http://www.annualreviews.org/doi/pdf/10.1146/annurev.energy.25.1.441>
- James, A., & Martin, A. J. P. (1952). Gas-liquid partition chromatography: the separation and micro-estimation of volatile fatty acids from formic acid to dodecanoic acid.

Biochemical Journal, 50, 679–690. Retrieved from <http://www.ncbi.nlm.nih.gov/pmc/articles/PMC1197726/>

- Karl, T., Apel, E., Hodzic, a., Riemer, D. D., Blake, D. R., & Wiedinmyer, C. (2009). Emissions of volatile organic compounds inferred from airborne flux measurements over a megacity. *Atmospheric Chemistry and Physics*, 9(1), 271–285. doi:10.5194/acp-9-271-2009
- Kormann, R., Fischer, H., De Reus, M., Lawrence, M., Brühl, C., Von Kuhlmann, R., Holzinger, R., et al. (2003). Formaldehyde over the eastern Mediterranean during MINOS: Comparison of airborne in-situ measurements with 3D-model results. *Atmospheric Chemistry and Physics Discussions*, 3(2), 1303–1331. doi:10.5194/acpd-3-1303-2003
- Krupa, S. V, & Manning, W. J. (1988). Atmospheric ozone: formation and effects on vegetation. *Environmental pollution (Barking, Essex: 1987)*, 50(1-2), 101–37. Retrieved from <http://www.ncbi.nlm.nih.gov/pubmed/15092655>
- Lee, J., Lewis, a, Monks, P., Jacob, M., Hamilton, J., Hopkins, J., Watson, N., et al. (2006). Ozone photochemistry and elevated isoprene during the UK heatwave of august 2003. *Atmospheric Environment*, 40(39), 7598–7613. doi:10.1016/j.atmosenv.2006.06.057
- Lipsky, S., & Landowne, R. (1960). Gas Chromatography-Biochemical Applications. *Annual Review of Biochemistry*. Retrieved from <http://www.annualreviews.org/doi/pdf/10.1146/annurev.bi.29.070160.003245>
- MacLeod, G., & Ames, J. M. (1986). Comparative assessment of the artefact background on thermal desorption of tenax GC and tenax TA. *Journal of Chromatography A*, 355, 393–398. doi:10.1016/S0021-9673(01)97343-1
- Marvin, M. (1998). GC/MS A Practical Users Guide. Retrieved from <http://scholar.google.com/scholar?hl=en&btnG=Search&q=intitle:GC+/+MS+A+Practical+User+?+s+Guide#4>
- Matisová, E., & Dömötöröová, M. (2003). Fast gas chromatography and its use in trace analysis. *Journal of chromatography. A*, 1000(1-2), 199–221. Retrieved from <http://www.ncbi.nlm.nih.gov/pubmed/12877172>
- McWilliam, I., & Dewar, R. (1958). Flame ionization detector for gas chromatography. *Nature*, 181, 760. Retrieved from <http://adsabs.harvard.edu/abs/1958Natur.181..760M>
- Minschwaner, K., Dessler, A. E., & Sawaengphokhai, P. (2006). Multimodel Analysis of the Water Vapor Feedback in the Tropical Upper Troposphere. *Journal of Climate*, 19(20), 5455–5464. doi:10.1175/JCLI3882.1
- Molina, M., & Rowland, F. (1974). Stratospheric sink for chlorofluoromethanes: chlorine atom-catalysed destruction of ozone. *Nature*. Retrieved from <http://faculty.rmu.edu/~short/envs4450/references/Molina-and-Rowland-1974.pdf>
- Montzka, S., Butler, J., & Myers, R. (1996). Decline in the tropospheric abundance of halogen from halocarbons: Implications for stratospheric ozone depletion. *Science*.

Retrieved

from

http://www.osti.gov/energycitations/product.biblio.jsp?osti_id=263039

- O'Doherty, S. (2004). Rapid growth of hydrofluorocarbon 134a and hydrochlorofluorocarbons 141b, 142b, and 22 from Advanced Global Atmospheric Gases Experiment (AGAGE) observations at Cape Grim, Tasmania, and Mace Head, Ireland. *Journal of Geophysical Research*, 109(D6), 1–16. doi:10.1029/2003JD004277
- Parliament Council of the European Union. (2006). DIRECTIVE 2006/40/EC OF THE EUROPEAN PARLIAMENT AND OF THE COUNCIL of 17 May 2006 relating to emissions from air-conditioning systems in motor vehicles and amending Council Directive 70/156/EEC, (L 161/12), 1–7.
- Poole, C. F., Li, Q., Kiridena, W., & Koziol, W. W. (2000). Selectivity equivalence of poly(ethylene glycol) stationary phases for gas chromatography. *Journal of chromatography. A*, 898(2), 211–26. Retrieved from <http://www.ncbi.nlm.nih.gov/pubmed/11117419>
- Ras, M. R., Marcé, R. M., & Borrull, F. (2009). Volatile organic compounds in air at urban and industrial areas in the Tarragona region by thermal desorption and gas chromatography-mass spectrometry. *Environmental monitoring and assessment*, 161(1-4), 389–402. doi:10.1007/s10661-009-0755-6
- Ray, N. H. (1954). Gas chromatography. I. The separation and estimation of volatile organic compounds by gas-liquid partition chromatography. *Journal of Applied Chemistry*, 4(1), 21–25. doi:10.1002/jctb.5010040106
- Ribes, A., Carrera, G., Gallego, E., Roca, X., Berenguer, M. a J., & Guardino, X. (2007). Development and validation of a method for air-quality and nuisance odors monitoring of volatile organic compounds using multi-sorbent adsorption and gas chromatography/mass spectrometry thermal desorption system. *Journal of chromatography. A*, 1140(1-2), 44–55. doi:10.1016/j.chroma.2006.11.062
- Seco, R., Peñuelas, J., Filella, I., Llusà, J., Molowny-Horas, R., Schallhart, S., Metzger, a., et al. (2011). Contrasting winter and summer VOC mixing ratios at a forest site in the Western Mediterranean Basin: the effect of local biogenic emissions. *Atmospheric Chemistry and Physics*, 11(24), 13161–13179. doi:10.5194/acp-11-13161-2011
- Simmons, M., & Snyder, L. (1958). Two-stage gas-liquid chromatography. *Analytical Chemistry*, 32–35. Retrieved from <http://pubs.acs.org/doi/abs/10.1021/ac60133a007>
- Smolková-Keulemansová, E. (2000). A few milestones on the journey of chromatography. ... *Resolution Chromatography*, (23), 497–501. Retrieved from [http://onlinelibrary.wiley.com/doi/10.1002/1521-4168\(20000801\)23:7/8%3C497::AID-JHRC497%3E3.0.CO;2-S/abstract](http://onlinelibrary.wiley.com/doi/10.1002/1521-4168(20000801)23:7/8%3C497::AID-JHRC497%3E3.0.CO;2-S/abstract)
- Wang, Z., Fingas, M., & Sergy, G. (1995). Chemical characterization of crude oil residues from an Arctic beach by GC/MS and GC/FID. *Environmental science & technology*, 29(10), 2622–2631. Retrieved from <http://pubs.acs.org/doi/abs/10.1021/es00010a025>

WHO. (2000). Air Quality Guidelines, (91).

Yassaa, N., & Williams, J. (2005). Analysis of enantiomeric and non-enantiomeric monoterpenes in plant emissions using portable dynamic air sampling/solid-phase microextraction (PDAS-SPME) and chiral gas chromatography/mass spectrometry. *Atmospheric Environment*, 39(27), 4875–4884. doi:10.1016/j.atmosenv.2005.04.034

Yokelson, R. J., Karl, T., Artaxo, P., Blake, D. R., Christian, T. J., Griffith, D. W. T., Guenther, a., et al. (2007). The Tropical Forest and fire emissions experiment: overview and airborne fire emission factor measurements. *Atmospheric Chemistry and Physics Discussions*, 7(3), 6903–6958. doi:10.5194/acpd-7-6903-2007